Institute of Active Polymers, Helmholtz-Zentrum Hereon

Modulation of mesenchymal stem cell behavior by temperature and mechanical strain stimulation

Inaugural-Dissertation
to obtain the academic degree
Doctor rerum naturalium (Dr. rer. nat.)
submitted to the Department of Biology, Chemistry, Pharmacy
of Freie Universität Berlin

by
Zijun Deng

09. 2021

Declaration

The work in this thesis was performed in the Institute of Active Polymers, Helmholtz-Zentrum Hereon in Teltow during the period of 04/11/2015 - 31/10/2021 under the supervision of Prof. Dr. Andreas Lendlein and Prof. Dr. Nan Ma.

The thesis was submitted to the Department of Biology, Chemistry and Pharmacy of Freie Universität Berlin. Therefore, I declare that the presented research work here is original and didn't been submitted as a thesis or a part of the thesis for another degree or university. The writing of the thesis is finished by myself. Any help and contribution from others in my research work have been acknowledged.

_____

Signature, Date and place

1st Reviewer: Prof. Dr. Andreas Lendlein
(Universität Potsdam and Freie Universität Berlin)
2nd Reviewer: Prof. Dr. Nan Ma
(Universität Potsdam and Freie Universität Berlin)

Date of Defense: 30.09.2021

Acknowledgements

First of all, I would express my sincere gratitude to my supervisors Prof. Andreas Lendlein and Prof. Nan Ma, who have supported my research work these years. They provided me the opportunity to study in the institute and helped me grow up in scientific training. Their comments and discussions give me more chances to perform better in the research work. Their specific instruction encouraged me to finish the publication and thesis successfully.

I would like to thank Dr. Weiwei Wang and Dr. Xun Xu, who helped me a lot in the experiments and manuscripts. They gave lots of suggestions and concerns from the beginning of my study here. Their patience and caring attitude guide me to work efficiently.

I want to acknowledge Dr. Karl Kratz, who gave me lots of support and suggestion about the polymer materials and manuscript. Thanks for the help from Dr. Oliver E. C. Gould, who helped revise the manuscript and draw schematic cartoons using blender software. Many thanks to Dr. Yi Jiang and Yue Liu for their kindly help in polymer materials research and suggestions. Thanks for the help from Dr. Tian Liu, who helped to check the statistical analysis in my manuscript.

Many thanks to Dr. Zhengdong Li, Dr. Jie Zou, Xianlei Sun, Yan Nie, Wing-tai Tung, Thanga Bhuvanesh Vijaya Bhaskar, and Anja Müller-Heyn. Their kindness and friendliness make me study and living happily in the lab. The friendship among us gives me a lot of encouragement to finish the study. They helped me to adapt the living and research in Germany. Their suggestions with multidisciplinary knowledge helped me learned more and solved many problems during my experiments.

I also would like to thanks Nicole Schneider, Daniela Radzik, Patrick Budach and Dr. Maria Balk, who synthesized and prepared the polymer samples. The same sincere thanks to Dr. Yi Jiang, Dr. Tobias Rudolph and Dr. Liudmila Lysyakova, who helped to characterize the shape changes and surface roughness of the polymer samples.

Also, I should thank all of the staff in the office who paid lots of attention and effort to process the meeting, reagent purchase, manuscripts, and publication work. Many

thanks to other students and researchers from the institute who provided their suggestions and concerns about my studies.

Finally, I would like to express my deepest gratitude to my family for their love, understanding, and support. Primarily, my parents have a profound influence on me, and their work attitude keeps me always working hard in different workplaces. With the company of my wife and son, I can finish my studies here.

Foreword

The cumulative thesis includes the following publications in the appendix I, II, and III:

Appendix I

Zijun Deng, Weiwei Wang, Xun Xu, Oliver E C Gould, Karl Kratz, Nan Ma, Andreas Lendlein. Polymeric sheet actuators with programmable bioinstructivity. *Proc Natl Acad Sci U S A*. 2020; 117:1895-901. **DOI**: https://doi.org/10.1073/pnas.1910668117

Appendix II

Zijun Deng, Weiwei Wang, Xun Xu, Nan Ma, Andreas Lendlein. Modulation of Mesenchymal Stem Cell Migration using Programmable Polymer Sheet Actuators. *MRS Advances*. 2020; 5(46-47), 2381-2390. **DOI**: https://doi.org/10.1557/adv.2020.235

Appendix III

Zijun Deng, Jie Zou, Weiwei Wang, Yan Nie, Wing-Tai Tung, Nan Ma, Andreas Lendlein. Dedifferentiation of mature adipocytes with periodic exposure to cold. *Clin Hemorheol Microcirc*. 2019; 71:415-24. **DOI**: https://doi.org/10.3233/CH-199005

Contents

Abstract

Different physical cues are known to affect mesenchymal stem cell (MSC) behavior, indicating a complex relationship between the cell and its microenvironment. Mechanical strain and temperature changes are examples of cues that are relevant in vitro and in vivo. However, the combined effects of multiple physical cues on MSCs remained unclear. Traditional mechanical devices used in cell research have limitations on the integration of various factors and high-throughput applications. The requirement of new biomaterials to integrate the multiple external stimuli was arising to figure out the complex cellular mechanisms.

The thermoresponsive mechanical strain was investigated to achieve the aim of using active biomaterials to study the combined effects on human MSCs. Poly (ε-caprolactone)-butyl acrylate (PCL-BA) copolymer sheet actuators were programmed so that the reversible shape change could be controlled by temperature changes between 37 °C and 10 °C. A thermochamber was used to culture the human adipose-derived stem cells (ADSCs) on the shape-memory polymer sheet actuators. 50 × 50 μm grids were created on the underside of the actuator sheets to observe the shape change of polymer and cells. Cell morphology, orientation, and migration were observed and recorded using time-lapse microscopy. The dual stimuli of temperature change and mechanical strain were translated into intracellular signals, such as calcium oscillation and nuclei translocation of the mechanical sensors, which were characterized using chemical reagents and immunostaining. Further, epigenetic histone modification of hADSCs was analyzed using chromatin immunoprecipitation quantitative real-time PCR (ChIP-qPCR). Finally, adipogenesis and osteogenesis of the hADSCs were studied to evaluate MSC differentiation capacity with the combined physical cues. The effect of temperature changes on adipocyte dedifferentiation was demonstrated by quantifying lipid accumulation in mature adipocytes. The expression of lipid accumulation-related genes and cell proliferation capacity were analyzed to investigate the dedifferentiation properties.

In this work, the PCL-BA shape-memory polymer actuator elongated more than 10% at 10 °C, and contracted when returned to 37 °C. The mechanical strain was generated with the polymer actuator's elongation, which modified the cell morphology and

increased cell migration. The periodic temperature change and mechanical strain induced calcium influx into cells; meanwhile, the mechanical strain promoted nuclei translocation of the YAP and RUNX2. The dual stimuli further increased the epigenetic acetylation of histone H3 lysine 9 (H3K9ac) and enhanced the expression level of osteogenesis-related genes and proteins. In addition, the dual stimuli of temperature change and mechanical strain induced the focal adhesion activation by regulation of integrin and myosin light chain (MLC) phosphorylation. As a result, cytoskeleton organization and focal adhesion activation were reduced by pretreatment of the MSCs with temperature changes but enhanced with mechanical strain changes. Temperature change alone decreased the cell migration velocity on SMPA substrate, while temperature change and mechanical strain combined increased cell migration velocity. Further, the cyclic temperature change (10 - 37 °C) decreased intracellular lipid of mature adipocytes and increased free fatty acids (FFA) outside. Simultaneously, mature adipocyte marker FABP4 was significantly down-regulated, while the brown adipocyte-related genes UCP1, PGC-1α, and PRDM16 were up-regulated. Ki67 represents the proliferation marker that was increased after the treatment of temperature change. The transformation of mature adipocytes and increasing proliferation capacity indicates the promotion of adipocyte dedifferentiation.

The shape-memory polymer actuator sheet is an active biomaterial that can generate mechanical strain with simple temperature control. This artificial muscle allows the combined influence of multiple physical cues on stem cells to be studied. We found the combinative effects of the interplay of mechanical and temperature stimuli on MSC behavior and lineage commitment change, instead of the typical single effect on MSCs. We also established the adipocyte dedifferentiation with periodic temperature changes, which might be used to generate alternative stem cell sources and improve the MSC-based cell therapy in regenerative medicine.

Abbreviations and symbols

ADSCs	adipose-derived stem cells
AIBN	azobisisobutyronitrile
ALP	alkaline phosphatase
ARS	alizarin red S
CFSE	carboxyfluorescein succinimidyl ester
ChIP	chromatin immunoprecipitation
DMEM	dulbecco's dodified eagle medium
DFAT cells	dedifferentiated fat cells
ECM	extracellular matrix
ER	endoplasmic reticulum
FABP4	fatty acid binding protein 4
FAK	focal adhesion kinase
FFA	free fatty acids
H3K9ac	acetylation of histone H3 lysine 9
H3K27me3	Trimethylation of histone H3 lysine 27
HDAC1	histone deacetylase 1
MHC	major histocompatibility complex
MSCs	mesenchymal stem cells
MYC	MYC proto-oncogene, bHLH transcription factor
Oct4	octamer-binding transcription factor 4
OCN	osteocalcin

ORO	oil red O
PCR	polymerase chain reaction
PGC-1α	peroxisome proliferator-activated receptor gamma coactivator 1-alpha
PPARγ	Peroxisome proliferator-activated receptor gamma (PPARgamma)
PCL-BA	AB co polymer network with poly (ε-caprolactone) and poly (n-butyl acrylate) segments
PCL-DIEMA	Poly (ε-caprolactone) - diisocyanatoethyl dimethacrylate
PI	propidium iodide
PRDM16	PR domain containing 16
RUNX2	runt-related transcription factor 2
SVF	stromal vascular fraction
SOX2	SRY (sex determining region Y) -box transcription factor 2
SMPA	shape-memory polymer actuator
TAZ	transcriptional coactivator with PDZ-binding motif
TCP	tissue culture plate
TRP	transient receptor potential
UCP1	uncoupling protein 1
YAP	yes-associated protein
2APB	2-aminoethoxydiphenyl borate
ΔT	periodic temperature change
$\Delta \varepsilon$	periodic change in mechanical strain

1. Introduction

1.1 Mesenchymal stem cells

Mesenchymal stem cells (MSCs) can be initially isolated from various adult tissues, exhibit excellent self-renewal capacity, and have the potential to be differentiated towards mesodermal, ectodermal, and endodermal lineages (1-3). The clinical application of adult tissue-specific MSCs obviates several concerns regarding the ethical considerations and the risk of genetic modifications (4, 5). Moreover, because MSCs can be isolated from patients and lack major histocompatibility complex (MHC) II, they do not elicit a robust immune response after cell transplantation (6). The weak immune response in MSC therapy has even allowed the allogeneic transplantation without immunosuppression treatment in MSCs therapy (7, 8). The above advantages suggest the outstanding potential of MSCs for clinical applications, such as tissue regeneration and engineering. Meanwhile, MSCs have a homing capacity migrate into injured tissues to help repair and regenerate the tissues by differentiation and secretion function (9, 10). Therefore, a better understanding of MSCs should facilitate substantial advancements in clinical MSC therapy (Fig. 1).

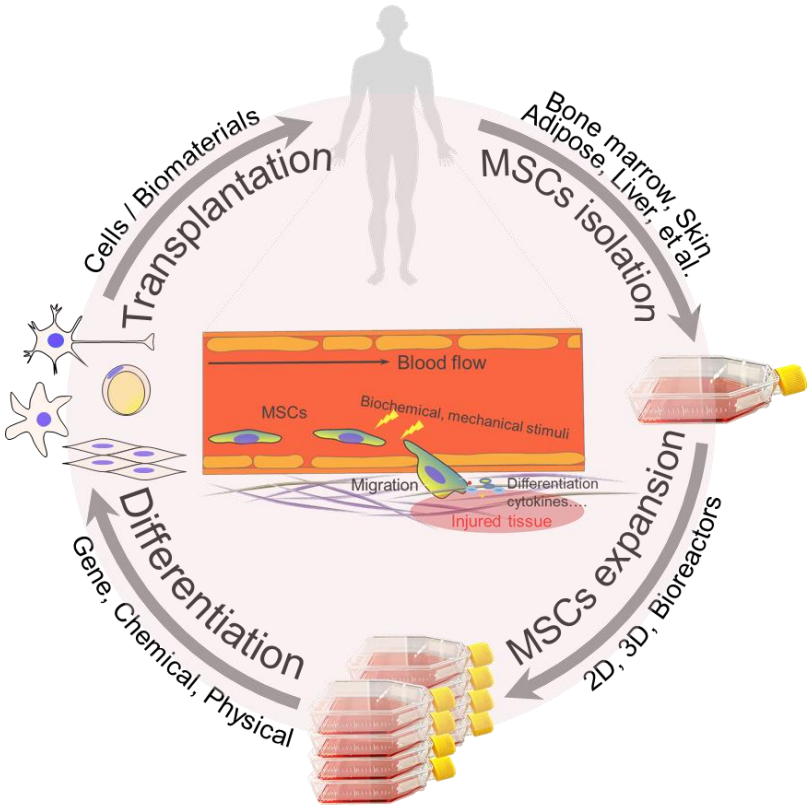

Figure 1. The schematic illustrations demonstrate the applications of MSCs both in vitro and in vivo.

Most human adult tissues contain MSCs, such as the bone marrow (11), adipose tissue (12), dental pulp (13), skin (14), brain (15), muscle tissue (16), peripheral blood (17), placenta (18), and umbilical cord tissue and blood (19, 20). MSCs isolated from the bone marrow, peripheral blood, and adipose tissue are most widely studied because they are easy to harvest from human tissues. Specifically, the bone marrow and blood are renewable, and the adipose tissue is usually considered non-essential, and they are generally abundant throughout life.

1.1.1 Adipose-derived stem cells

Adipocyte precursors were isolated for the first time from human adipose tissue in 1976 (21). They are a constituent of the stromal vascular fraction (SVF) separated from the adipose tissue after centrifugation. In 2001, the cells in the SVF were characterized with MSC markers and certified to possess multilineage differentiation potential and termed adipose-derived stem cells (ADSCs) (12). Compared to other tissue isolated MSCs, ADSCs have shown more advantages in regenerative medicine (22-26): (1) the adipose tissue is easier to harvest with minimally invasive surgery procedures, (2) the adipose tissue is abundant in the human body throughout the lifetime and is feasible for autologous MSCs based cellular therapy, (3) the weak immunogenicity of ADSCs facilitates allogeneic stem cell transplantation, (4) ADSCs can secrete a large number of cytokines to improve the survival of the transplanted cells and suppress the inflammatory response, (5) ADSCs show more genomic stability in long-term cultivation, which slows down cellular senescence during in vitro cultivation.

Furthermore, adipose tissue is distributed around most organs, and the closely localized ADSCs may contribute to tissue repair in vivo. Compared to other sources of MSCs, the adipose tissue that developed under the skin may show a significant response to frequent tissue movements and temperature changes. Therefore, it is worth investigating the influence of physical cues in the microenvironment on ADSCs. The results may further enhance our understanding and improve the methods used in regenerative medicine.

1.1.2 Adipocyte dedifferentiation

ADSCs constitute a relatively small proportion of the cell population in the adipose tissue, whereas mature adipocytes contribute more than 50% of the adipose tissue (27). From 1986, studies have found that the primary culture of mature adipocytes obtained using the ceiling culture method can generate a cell type with proliferation and differentiation properties (28-30). This transition from a differentiated cell type to a less differentiated state is defined as dedifferentiation (31). Mature adipocytes show the ability to dedifferentiate into fibroblast-like cells with robust proliferation capacity and multilineage differentiation potential (32-34), is known as dedifferentiated fat (DFAT) cells (Fig. 2).

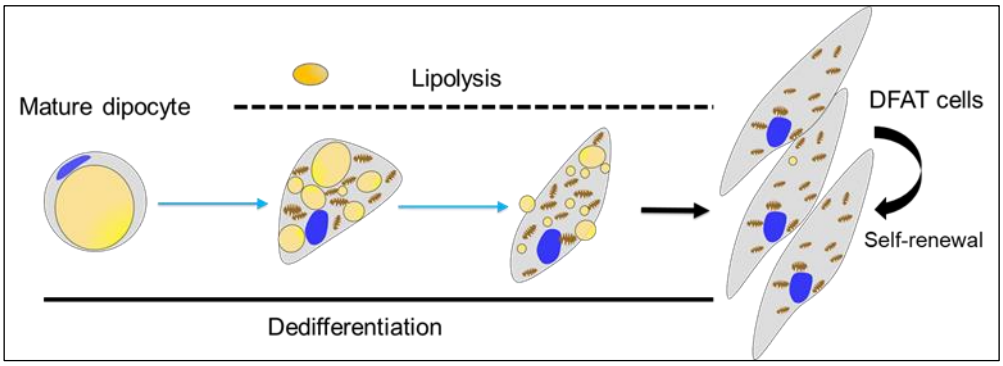

Figure 2. The schematic illustrations demonstrate the dedifferentiation process of mature adipocytes into DFAT cells.

DFAT cells were regarded as a new source of stem cells because of the expression of pluripotency markers, such as Oct4, SOX2, c-MYC, and Nanog (35, 36). In addition, DFAT cells differentiate into any of the three germ layers after cell transplantation in immune-deficient mice without the risk of developing tumors (32). Although DFAT cells can be generated from mature adipocytes using the ceiling culture method without any additional biochemical or genetic intervention, the dedifferentiation efficiency is relatively low hampering clinical applications. Therefore, improvements in the dedifferentiation method of DFAT cells are necessary to explore their applications in clinical regenerative medicine.

Therefore, adipose tissue-derived ADSCs and DFAT cells show many advantages among MSCs. Investigating the effects and mechanisms of physical cues on their

growth and behavior will further improve our understanding of MSCs to meet various clinical application requirements.

1.2 Physical cues affecting stem cell behavior

Various factors can influence the behavior of stem cells and determine their fate. Stem cells interact with adjacent cells in their specific niche, consisting of various soluble macromolecules and extracellular matrix (ECM) components. They are influenced not only by their interactions with various biochemical components in the microenvironment but also by physical and mechanical properties (37, 38). Recently, several physical cues such as stiffness, stretch force, shear stress, and 3D topography of culture substrates have been proposed as essential regulators of stem cell behavior (Fig.3) (39-41).

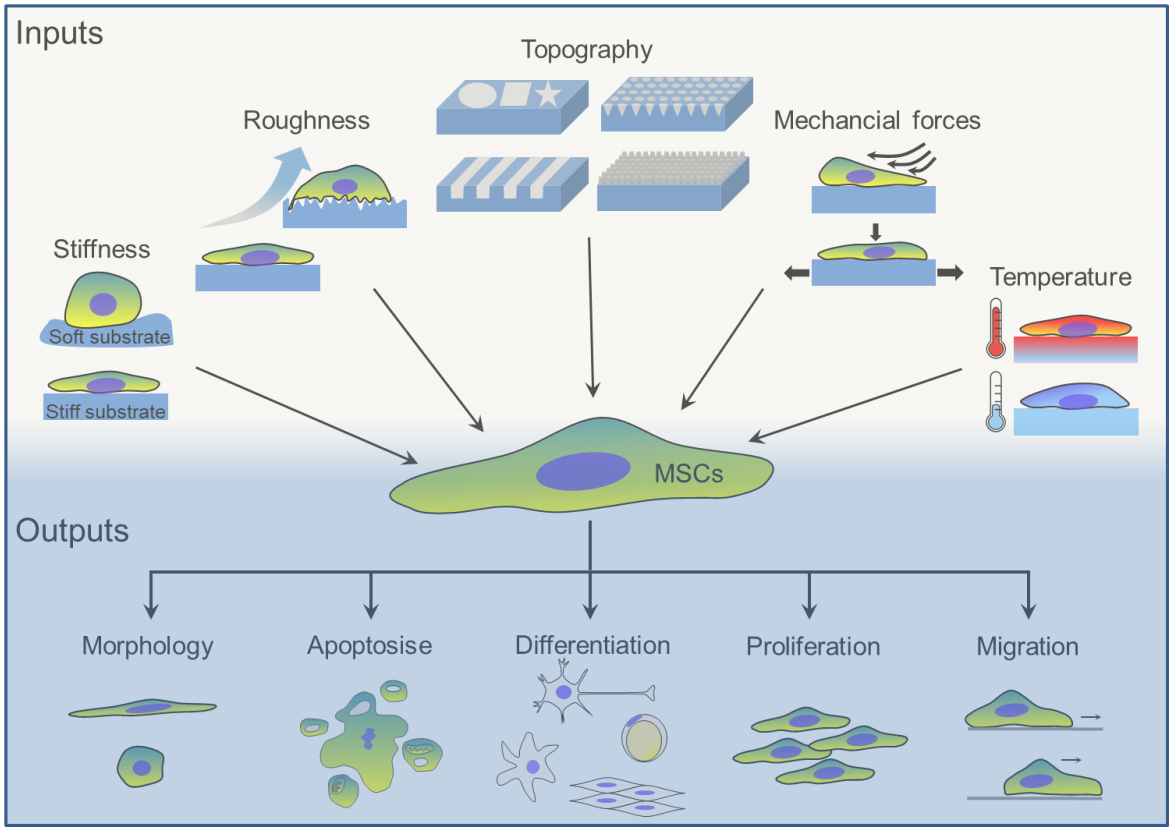

Figure 3. Schematic illustration generalizes the input information from cell culture substrates with different physical cues modulate MSC behavior, and especially direct the MSC differentiation fate.

1.2.1 Surface properties of cell culture substrate

From the blood cells within a fluid microenvironment to the bone cells within the hardest microenvironment with highest Young's modulus up to 1 GPa, various cells were surrounded by different physical cues in human body (42). The different physical stiffness of the cell microenvironment directs the fate of MSCs and the development of distinct tissues. For example, the brain and fat tissue are soft with lower Young's modulus around 1 KPa, then the mimicked soft substrates favor the differentiation of MSCs into neuronal cells and adipocytes in vitro, whereas stiff substrates mimic the bone microenvironment promoted osteogenic differentiation in vitro (43). Moreover, compared to stiff substrates, soft substrates were found to maintain the pluripotency or multipotent properties of stem cells and ensure a higher proliferation rate (44-46) and faster migration speed of MSCs (47).

In addition to the inherent properties of the substrate surface, the artificial topography of the cell adhesion surface at the nano or micro-scale can modulate MSC behavior, orientation, migration, and differentiation (48). For example, the micro-scale roughness and pattern alter cell migration, cytokine secretion, and osteogenic differentiation of MSCs (49-51). Increasing surface roughness from nano-scale to micro-scale promotes osteogenic differentiation (52, 53). Although it is not clear how stem cells sense topography structures, the modulation of focal adhesion and cytoskeleton by topography plays essential role in MSCs (54, 55).

1.2.2 Mechanical strain

Mechanical force, such as shear stress, stretch, and compression, changes the morphology of MSCs and controls their differentiation fate. Shear stress induces higher cell contractility and further enhances the osteogenic differentiation of MSCs (56, 57). It was found that the application of compressive force on MSCs promoted chondrogenic differentiation in vitro and in vivo (58-60). This is considered to be helpful to repair knee articular cartilage, which has a similar physical microenvironment. Similarly, the stretch force on MSCs leads to changes in the cell shape and promotion of myogenic and osteogenic differentiation (61-64). Mechanical forces also promote cell migration through the altered cytoskeleton and focal adhesion formation (9, 65-68).

1.2.3 Temperature changes as physical cue

Environmental temperature of cell cultivation is another critical and common physical parameter. However, this factor is usually ignored because the human body is thermostatic. Typically, in vitro cell culture experiments cannot avoid slight changes in the cell culture temperature. It is known that MSCs can tolerate higher temperatures (up to 48 °C) with no severe effect on cell metabolism (69). Under low temperatures (32 °C), oxidative stress is decreased and improves long-term cultivation and differentiation (70, 71). Some thermal-sensitive ion channels are activated to modulate cell behavior during cold stress (as low as 4 °C) (72). In vivo studies have confirmed that cold exposure can induce lipid metabolism (73, 74). Meanwhile, in vitro studies have found that cold exposure can promote browning adipogenic and osteogenic differentiation of MSCs (75, 76). Because most adipose tissues under the skin store excess energy by lipids, a better understanding of the effect of cell culture temperature on adipocytes in vitro may provide helpful insights.

Although the modulation of MSC behavior by many physical cues has been well studied, little is known about the effect of multiple simultaneous physical cues or input signals. Because MSCs receive numerous inputs from their complex microenvironment in vivo, research integrating multiple inputs on MSC behavior changes in vitro could reveal critical regulatory pathways during tissue development and disease.

1.3 Signal transduction from physical cues to cell response

Physical cues of the MSCs microenvironment modulate cell behavior and drive particular stem cell differentiation fate via the regulation of certain mechanotransduction factors in the cells to transfer extracellular signals to gene and protein expression. Different kinds of sensing molecules on the cell membrane respond to stimulation, such as integrin, ion channels, tyrosine kinase receptors, and G-protein coupled receptors (37).

Cell adhesion molecules on the cell membrane, such as integrin and cadherin, are the initial receptors that receive the input information from the outside microenvironment.

The cell attachment and migration on ECM and biomaterial substrates are dominated by integrins transmitting extracellular information to intracellular cytoskeletal filaments, such as actin, myosin, and microtubules (37). The nuclear transcription factors, Yes-associated protein (YAP), and transcriptional coactivator with PDZ-binding motif (TAZ) can transmit the information further into the cell nuclei and regulate related gene expression (77). For instance, stiff substrates can enormously enhance YAP/TAZ activity in cell nuclei to control the stem cell geometry and differentiation fate (78). Runt-related transcription factor 2 (RUNX2) and peroxisome proliferator-activated receptor gamma (PPARγ) are transcription factors that function in balance to induce the differentiation of the stem cells into osteoblast or adipocyte (79). Meanwhile, the YAP/TAZ activation on stiff substrates can activate RUNX2 and represses PPARγ-related gene expression (41, 80). Compared to stiff substrates that induce osteogenic differentiation, soft substrates lead to adipogenic differentiation (81). Moreover, the application of mechanical strain to cells can induce YAP nuclear translocation (82), which can promote osteogenic differentiation of MSCs by the modulation of nuclei architecture (83) and ion channels (84).

Calcium plays an essential role in almost all kinds of cells, with level changes in the cytoplasm and nuclei regulating the expression of specific genes and the activity of various proteins (85). For example, mechanical strain (84), shear stress (86), and electrical stimulation (87) were applied to stimulate calcium oscillation in MSCs to facilitate osteogenic and chondrogenic differentiation. Many ion channels on the cell membrane can sense the physical microenvironment and regulate the influx and outflow of Ca^{2+} via the intracellular calcium pool in the endoplasmic reticulum (ER) can further amplify the effects (88). Many series of transient receptor potential (TRP) channels are expressed in MSCs (89), and they play an essential role in calcium regulation with different activities (90). For example, TRPM7 is a mechanical stimulation-dependent channel (84, 90), and some TRP channels, such as TRPV3, TRPV4, TRPC5, TRPM4, TRPM5, TRPM8, and TRPA1, exhibit regional temperatures dependent activity (91-93). Mechanical membrane tension-activated Piezo1 and Piezo2 channels have been identified since 2010, regulating calcium transport through the cell membrane and further modulating cell behavior (94).

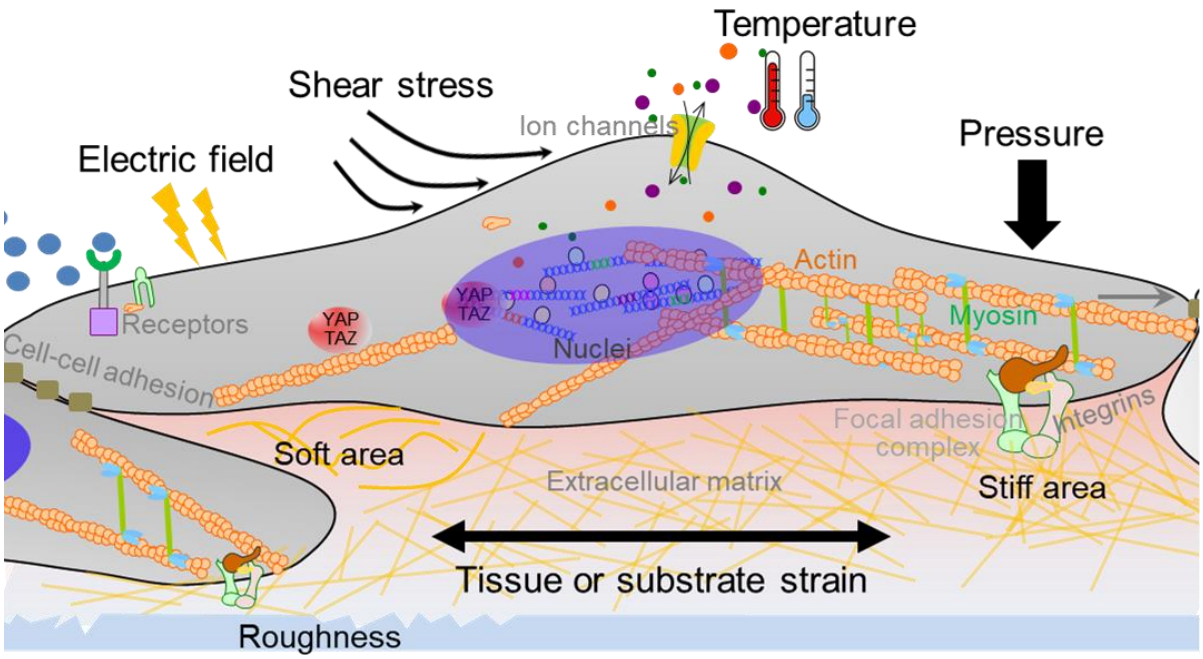

Figure 4. MSCs sense various stimuli from the microenvironment and translate the inputs to intracellular signaling pathway.

Similar to the complex and multiple-input information from the cell microenvironment, intracellular signal transduction pathways rely on molecular networks that process the input information and regulate protein activity to precisely control cell behavior (Fig. 4). Although many multiplex signaling pathways have been thoroughly investigated, complicated regulatory pathways have only begun to be explored. Because previous experimental approaches only focus on the single input information and follow induced cellular behavior, and signal tracking follows a string from one upstream molecule to the following downstream molecule, understanding of the interconnections of the numerous molecular networks remains poor. Therefore, new research approaches should combine multiple-input information and demonstrate the interactive signaling pathway synthetically. Only in this way may MSCs behavior modulation become more precise and closer to clinical applications.

1.4 Polymeric substrate design for MSC cultivation

The strategies used in the design of multifunctional biomaterials for MSC cultivation and differentiation include the following routes (37): (1) biofunctionalization of the

substrate with adhesion molecules, e.g. by coating with a mixture of functional biomolecules and nanoparticles; (2) chemical modifications of the surface chemistry and chemical cross-linking of the polymer substrate; (3) modeling and reconfiguring the interface's topography by positioning ligands or creating piles patterning, microgrooves, roughness, and defined geometric topologies; (4) mechanical culture chambers with shear stress, stretch, and compression force. Most biomaterials used as substrates for MSC cultivation are based on these strategies and are improved from monolayer cell culture to tissue engineering.

Artificial materials with different biophysical and biochemical properties and function used as cell culture substrates can lead to significant cell microenvironment changes, leading to various specific responses in MSCs. Because the stimulation can be triggered at different levels in a controlled manner, the corresponding changes in cell behavior and related molecular pathways can be clearly investigated. This outside-in strategy helps understand MSC behavior through various stimulations out of cells, which improves practical applications by specially designed biomaterials (95, 96).

Advances in biomaterials and molecular cell biology have allowed the incorporation of more complex and quantifiable signals that recreate the MSCs microenvironment gradually. The influences of various physical cues mentioned above on MSCs have been well studied independently. However, few studies report how the interplay of multiple stimulations acting together can affect cell behavior. Although we may expect them to share similar signaling pathways, the cumulative impact on the behavior of MSCs may turn out to be different. Conversely, multiple physical cues can be designed and used to alter the behavior of MSCs depending on the demand of regenerative applications. Therefore, changing or recovering the microenvironment using new biomaterials with multiple quantifiable properties could lead to a more effective and controlled change in MSC behavior.

2. Motivation, Hypothesis and Strategy

2.1 Motivation

Firstly, the behaviour changes influenced by many single physical cues have been well studied. However, the native microenvironment in vivo includes multiple physical cues but not a single cue, how the cells sense different cues simultaneously and subsequently change their behavior is little known. For example, changes in temperature and mechanical strain are controllable physical cues, and the effects of their independent changes on MSC behavior have been widely studied. While, few studies explored the combined effects of temperature and mechanical strain. Therefore, developing a method to study MSCs by varying combined physical cues would provide important information about these cells.

Secondly, the methods used in modulating MSC behavior by mechanical strain usually involve expensive mechanical instruments based on motor-driven mechanical principles, and these methods are accessible but unsuitable for high-thought cell cultivation. While, mechanical strain generated by shape-memory biomaterial actuator may achieve similar effects on cells. In addition, most studies have demonstrated that temperature can control polymer properties dynamically. Therefore, a biomaterial actuator with thermoresponsive mechanical stratin changes may mimic multiple physical cues in one system, and will be an excellent tool for studying the combined effects of mechanical strain and temperature changes on MSC behavior (Fig. 5).

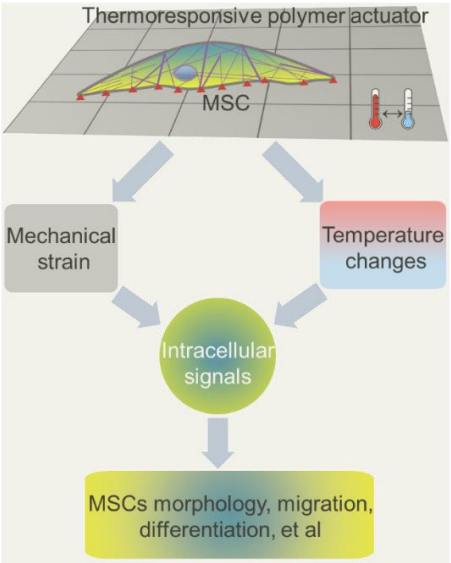

Figure 5. Schematic illustration describes the dual combined stimuli of mechanical strain and temperature changes. MSCs were cultured on the polymer sheet actuator and stimulated by mechanical strain and temperature changes. The molecular sensor of mechanical and thermal changes transforms the physical cues to intracellular signals and further regulates MSC behavior.

White adipose tissue can loose fat and become browning after exposure to cold in vivo. Most studies have confirmed that the mature adipocytes can loose lipids and be dedifferentiated into stem cell-like DFAT cells in vitro. Since the mature adipocytes abounded in tissues and the dedifferentiation method using a natural process without any gene modification, this stem cell source can provide a large number of cells in clinical application. However, the previous dedifferentiation methods produce DFAT cells with low efficiency and have little advancement on the dedifferentiation process, which obstructed the clinical application of DFAT cells currently. Because the DFAT cells show more advantages in regenerative medicine than the MSCs extracted from bone marrow and adipose tissue, a new efficient approach based on temperature changes may potentially improve the method for adipocyte dedifferentiation (Fig. 6).

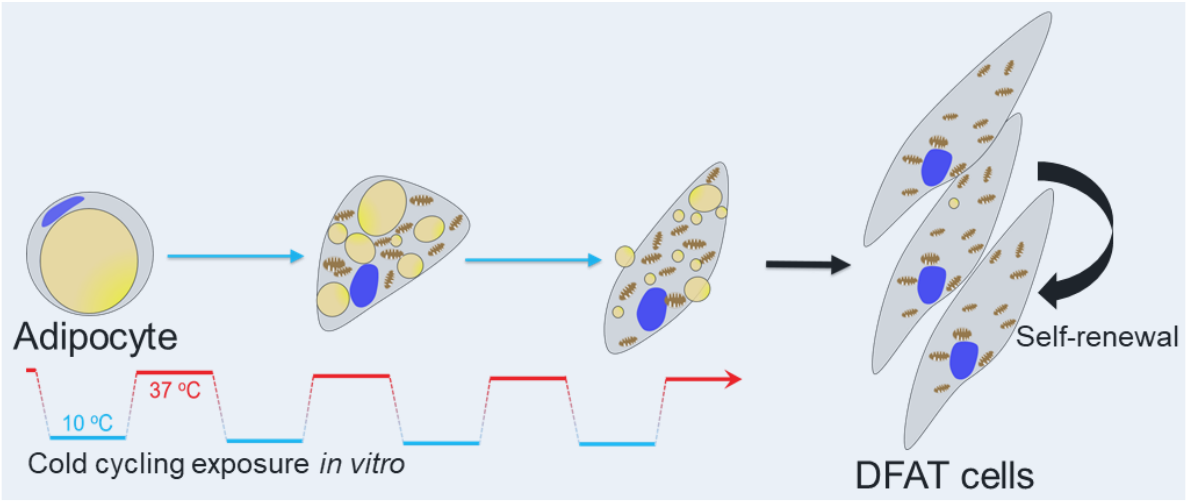

Figure 6. Schematic illustration describing the approach of the periodic temperature changes used in the dedifferentiation of mature adipocytes into DFAT cells. The periodic cooling/heating promotes lipids decreasing and increasing of dedifferentiation process.

2.2 Hypothesis

With appropriate design, a shape-memory polymer actuator sheet as active substrate can combine mechanical and temperature cues and exert their influence on MSCs. The mechanical strain could be achieved simply using temperature controllable shape-memory polymer actuator material self-sufficiently.

The mechanical strain and temperature change can induce mechanical and thermal sensitive sensors to regulate intracellular molecules' dynamic activation in MSCs. Mechanical strain applied on the cell membrane should influence the focal adhesion formation and regulate cell morphology and migration, leading to the mechanical strain being transferred into the intracellular cytoskeleton and controlling downstream signaling pathways that regulate gene expression differentiation.

The dedifferentiation process of mature adipocytes relies on the depletion of intracellular lipids, whereas the low temperature can promote energy consumption and further decrease the intracellular lipids. Therefore, periodic temperature changes may accelerate the dedifferentiation process, which can be developed as a new method to generate sufficient DFAT cells to meet clinical application requirements.

2.3 Strategy

AB co polymer network with poly(ε-caprolactone) and poly(n-butyl acrylate) segments (PCL-BA) showed the reversible shape-memory effect after the initial programming process, and no external force is needed to the material during subsequent multicyclic experiments (97-99). The PCL-BA sheet can be elongated at a low temperature and recovered at a higher temperature. These free-standing reversible memory properties avoid network anisotropy of the polymer sheet compar with external force derived material deformation (99), which could stimulate different cells by the same level of mechanical strain. The environmental temperature can control the elongation level, and the reversible property makes the integration of periodic temperature change and mechanical strain possible.

The PCL-BA sheet was synthesized with a crossline pattern on one side of the substrate with 50 × 50 µm grids. The grids on the transparent sheet can be elongated with the shape change, enabling us to quantify the elongation level under the microscope, while the top surface is smooth and biocompatible for cell cultivation. The PCL-BA sheet can be programmed to exhibit an actuator capability, and the programmable shape-memory polymer actuator (SMPA) sheets were used to explore the effect of temperature change and mechanical strain on MSCs. The hold temperature was defined at 37 °C, whereas the elongation temperature was set at 10 °C. The elongation and recovery process was started once the temperature changed. A faster elongation and recovery speed could be achieved over a range of 37 °C to 10 °C gradually (Fig. 7).

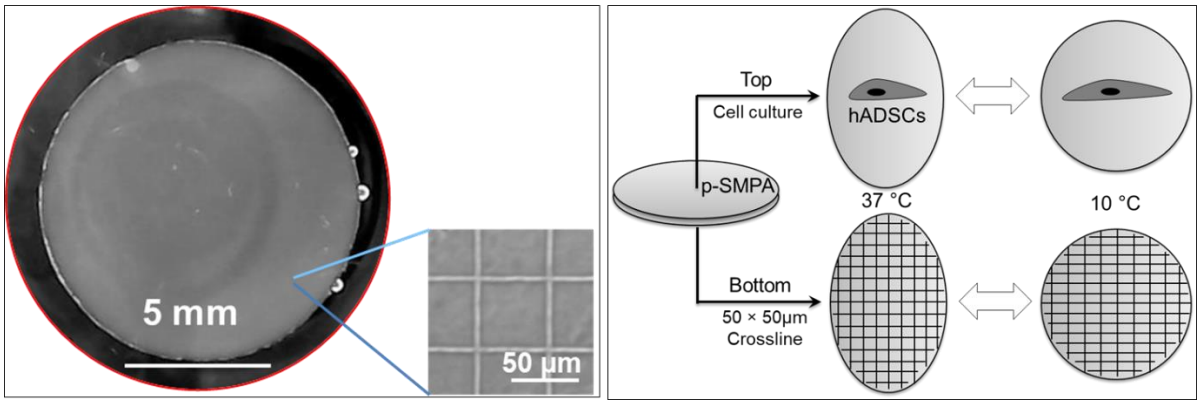

Figure 7. Overview of the polymer sheet (scale bar = 5 mm) and bottom grids (scale bar = 50 µm) (Left panel). Schematic illustration describes the cell culture on the top side and the patterned grids on the bottom side of the p-SMPA sheet with temperature change between 37 °C and 10 °C (Right panel).

The environmental temperature was tuned between 37 °C and 10 °C using electronic temperature control. The thermochamber (Instec, Colorado, USA) with standard tissue culture plates and dishes could be used for both controlling the temperature and cell culture (Fig. 8). For comparison, the traditional mechanical instrument (MCB1, CellScale, Ontario, Canada) can be used to generate the same periodic elongation of the SMPA sheet without any temperature change, which would provide a constant temperature control group for mechanical strain effects on MSCs.

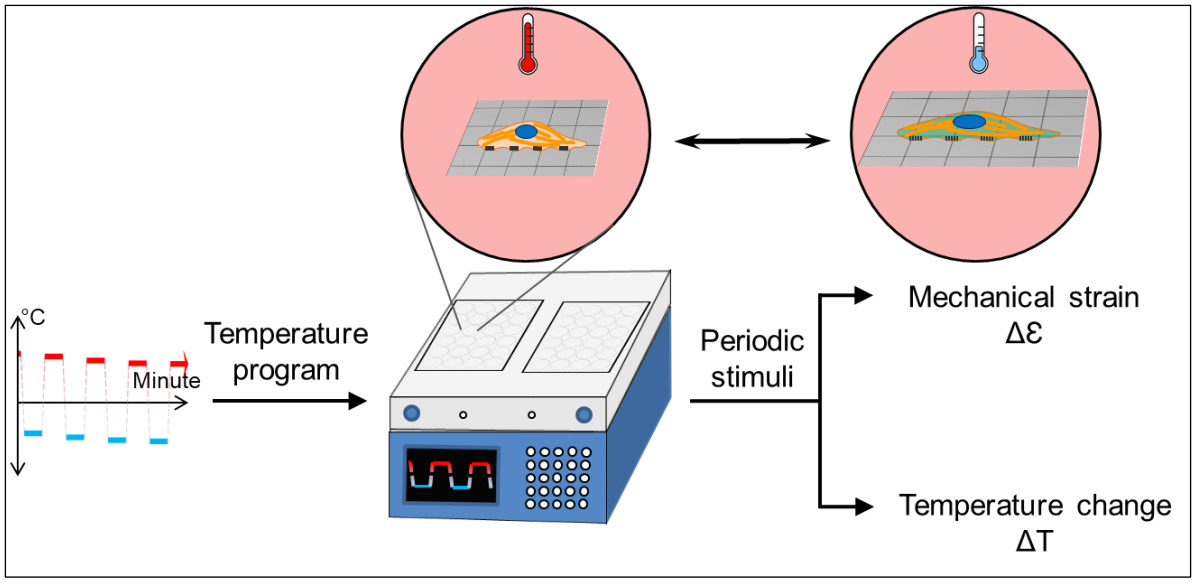

Figure 8. Schematic illustration describes the strategy flow of combined mechanical and temperature cues. With the temperature control program's input, the cells cultured on the material can receive dual outputs (temperature change, ΔT; mechanical force, Δε).

Human ADSCs were mainly used in the work, and cells adhered to the SMPA sheet directly. Live imaging with a time-lapse microscope was used to monitor the morphology and migration of human ADSCs and the cyclic shape change of SMPA sheets. Live imaging was also used to track intracellular calcium levels through ion channel activation. Immunostaining was used to indicate expression and cytoplasm/nuclei translocation of mechanical sensor YAP in response to the mechanical force on cells. Finally, ADSCs adipogenic and osteogenic differentiation were detected to thoroughly investigate the influence of the combined physical cues on ADSCs. Regarding adipocyte dedifferentiation, mature adipocytes were obtained by differentiation of ADSCs on the SMPA sheet in advance. The amount of lipid in the adipocytes was quantified after periodic temperature changes. The related gene expression and proliferation property were detected to evaluate the effect of periodic temperature changes on adipocyte dedifferentiation.

3. Organization of the thesis

This cumulative thesis mainly includes 10 sections to describe the effect of periodic temperature change and mechanical strain on MSC behavior.

Abstract: A brief synopsis of the research work

Introduction: Research background of the thesis

Motivation, Hypothesis and Strategy: Explanation of the scientific challenges, goals, and strategies of the thesis

Organization of the thesis: The organizational structure of the thesis content

Publication I: Polymeric sheet actuators with programmable bioinstructivity. *Proc Natl Acad Sci U S A*. 2020;117:1895-901. https://doi.org/10.1073/pnas.1910668117. This work presents that the interplay of periodic temperature change and mechanical strain promotes osteogenic differentiation via calcium influx and YAP activation to regulate histone modification. (Appendix I)

Publication II: Modulation of mesenchymal stem cell migration using programmable polymer sheet actuators. *MRS Advances*. 2020; 5(46-47), 2381-2390. https://doi.org/10.1557/adv.2020.235. This work presents that the mechanical strain promotes hADSC migration via focal adhesion activation, while the periodic temperature change exhibits a reverse effect. (Appendix II)

Publication III: Dedifferentiation of mature adipocytes with periodic exposure to cold. *Clinical Hemorheology and Microcirculation*. 2019;71:415-24. https://doi.org/10.3233/CH-199005. This work presents that periodic temperature change increases lipolysis and further promotes adipocyte dedifferentiation. (Appendix III)

Discussion: Discussion and comparison of the main results in the thesis

Summary and Outlook: Summary of the research work and further prospects

Kurzzusammenfassung: a brief summary of the thesis work in German

4. Publications

4. 1 Polymeric sheet actuators with programmable bioinstructivity

Zijun Deng [#], Weiwei Wang [#], Xun Xu [#], Oliver E C Gould, Karl Kratz, Nan Ma*, Andreas Lendlein*

# Authors contributed equally to this work

* Corresponding authors

Proc Natl Acad Sci U S A. 2020;117:1895-901.

DOI: https://doi.org/10.1073/pnas.1910668117

4. 1. 1 Contribution to the publication

- Literature study

  1> Modulation of mesenchymal stem cell differentiation by biomaterials.

  2> Signaling transduction of thermal and mechanical strain, such as integrin, YAP/TAZ, thermal ion channels.

- Study design with discussion and advice from co-authors

  1> Establish the competitive differentiation of hADSC adipogenesis and osteogenesis to evaluate the fate decision.

  2> Adjustment of the temperature control system and phase contrast and confocal microscopes for hADSCs cultivation and live imaging.

  3> Define the methods to measure the polymer shape and cell morphology change with temperature change between 37 °C and 10 °C using an inverted phase contrast microscope and confocal microscope respectively.

- Experimental work

  1> hADSCs cultivation, passaging and differentiation.

2> Measuring the shape change of PCL-BA polymeric actuator sheets and cells using the inverted phase contrast microscope and confocal microscope respectively.

3> Calcium labeling and imaging of hADSCs on glass and polymer using a confocal microscope.

4> Adjustment and measurement of sheet stretching and cell behavior on the sheet using a mechanical instrument at constant 37 °C.

5> Staining and imaging for the intracellular localization of YAP, RUNX2, p-HDAC1.

6> Chromatin immunoprecipitation and detection of histone H3K9 acetylation and related gene expression in hADSCs.

7> Detection of adipogenic and osteogenic markers including FABP4, ALP, Osteocalcin at gene and protein levels.

8> Staining and imaging for analysis of cell orientation, proliferation, viability.

- Contribution to analysis and interpretation of experimental data

  1> Microscopic image-based analysis of the shape changes of polymeric sheet actuators and cells, cell orientation, Ki67 positive cells, calcium influx level, and nuclear translocation of YAP and RUNX2.

  2> Quantitative analysis of histone H3K9ac level at osteogenic associated gene promoters.

  3> Comparison of adipogenesis and osteogenesis by protein and gene expression.

- Manuscript

  1> Providing a preliminary report about the experiments (methods, legends, and results).

  2> Contributing to the manuscript based on the outline, which was created in discussions with the co-authors, especially by revised versions of methods, legends, results.

Declaration of shared first co-author contributions

This publication comprises three co-authors with shared first co-authorship. Zijun Deng's contribution is focused on cell culture, measurement of the microscopic shape change of polymeric actuators, analysis of the cell orientation, proliferation and

mechanosensor protein nuclear translocation, evaluation of the histone modification, calcium influx, osteogenic differentiation and the expression of differentiation markers. Dr. Weiwei Wang and Dr. Xun Xu contributed especially the design of thermochamber, initial thermal cycle setup, time-lapse tracking of the actuator and cell shape change, macroscale polymeric actuator shape change, viability and cytotoxicity analysis, Integrin activation, ECM components production. All three shared first co-authors contributed to writing of the manuscript.

4. 1. 2 Summary of the publication

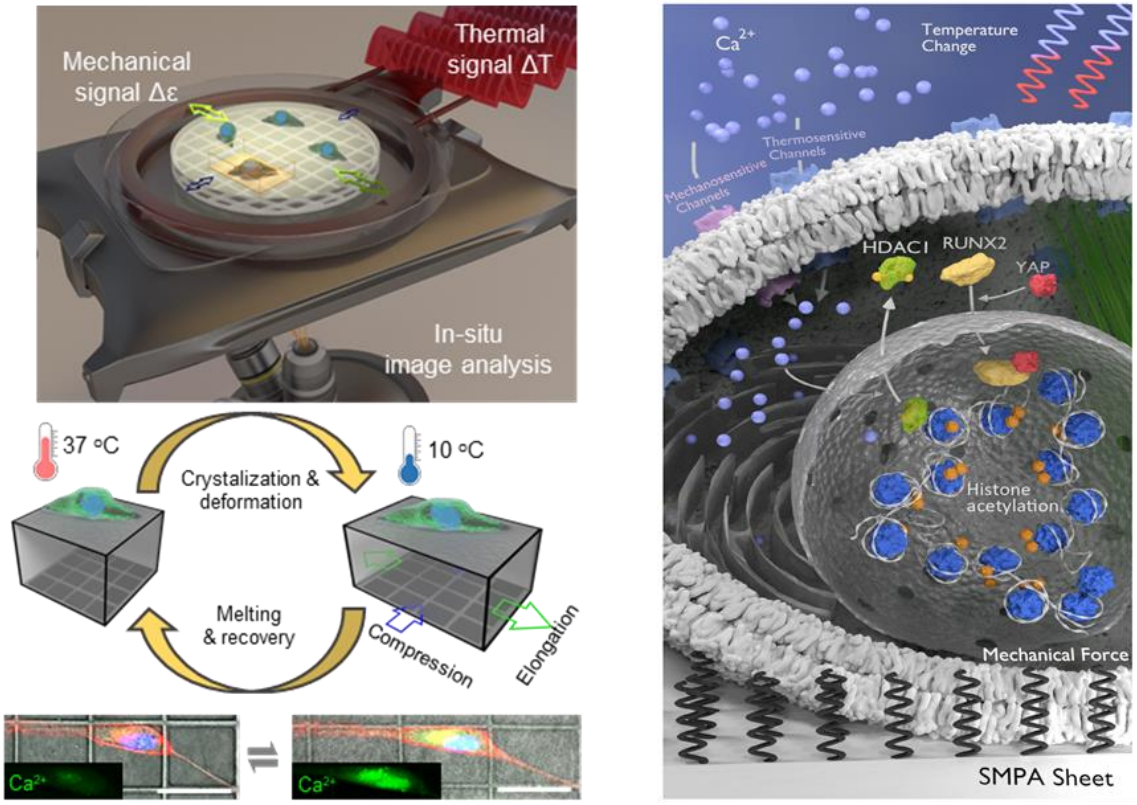

Reprinted from Proc Natl Acad Sci U S A, 117. Zijun Deng, Weiwei Wang, Xun Xu, Oliver E C Gould, Karl Kratz, Nan Ma, Andreas Lendlein. Polymeric sheet actuators with programmable bioinstructivity, 415-424. Copyright (2019), with permission from the National Academy of Sciences.

In this study, the programmable SMPA sheet showed thermoresponsive mechanical strain. Elongation of the SMPA sheet was induced by cold (10 °C) exposure, and the stretching was recovered by warm (37 °C) exposure. The shape change of the SMPA sheet interplay both mechanical strain and cold stress on hADSCs. Both temperature and mechanical changes induced calcium influx into cells and subsequently increased

histone H3K9 acetylation to promote osteogenesis. The mechanical strain activates YAP and RUNX2 by nuclei localization, which promoted osteogenesis. The dual effects of temperature and the mechanical strain showed integrated cooperation on the osteogenesis of hADSCs. This system demonstrated the interplay of multiple physical cues on MSCs and provided a culture and differentiation platform to modulate MSC behavior.

4. 1. 3 Full text of the publication (Appendix I)

4.2 Modulation of mesenchymal stem cell migration using programmable polymer sheet actuators

Zijun Deng, Weiwei Wang, Xun Xu, Nan Ma*, Andreas Lendlein*

* Corresponding authors

MRS Advances. 2020; 5(46-47), 2381-2390.

DOI: https://doi.org/10.1557/adv.2020.235

4. 2. 1 Contribution to the publication

- Literature study
  1> Determining factors for stem cell migration, such as focal adhesion and cytoskeleton.
  2> Recent reports about the Influence of mechanical properties and temperature on cell migration and related signaling pathways.
- Study design with discussion and advice from co-authors
  1> Determination of cell migration by live imaging after cell cultivation on different substrates.
  2> Defining focal adhesion formation-related mechanism.
- Experimental work
  1> Preparation of polymer substrates and hADSCs cultivation.
  2> Measurement of cell migration using a time-lapse microscope.
  3> Immunostaining of migration-related integrin β1, myosin, F-actin, and β-tubulin.
- Contribution to analysis and interpretation of experimental data
  1> Tracking the cell migration and velocity calculation using ImageJ software based on the time-lapse recording movies.
  2> Imaging analysis and comparison of protein expression for integrin β1, myosin, F-actin, and β-tubulin.
- Manuscript

1> Providing first draft of the manuscript according to outline discussion with co-authors.

2> Revision of the manuscript according to comments from co-authors and reviewers.

4. 2. 2 Summary of the publication

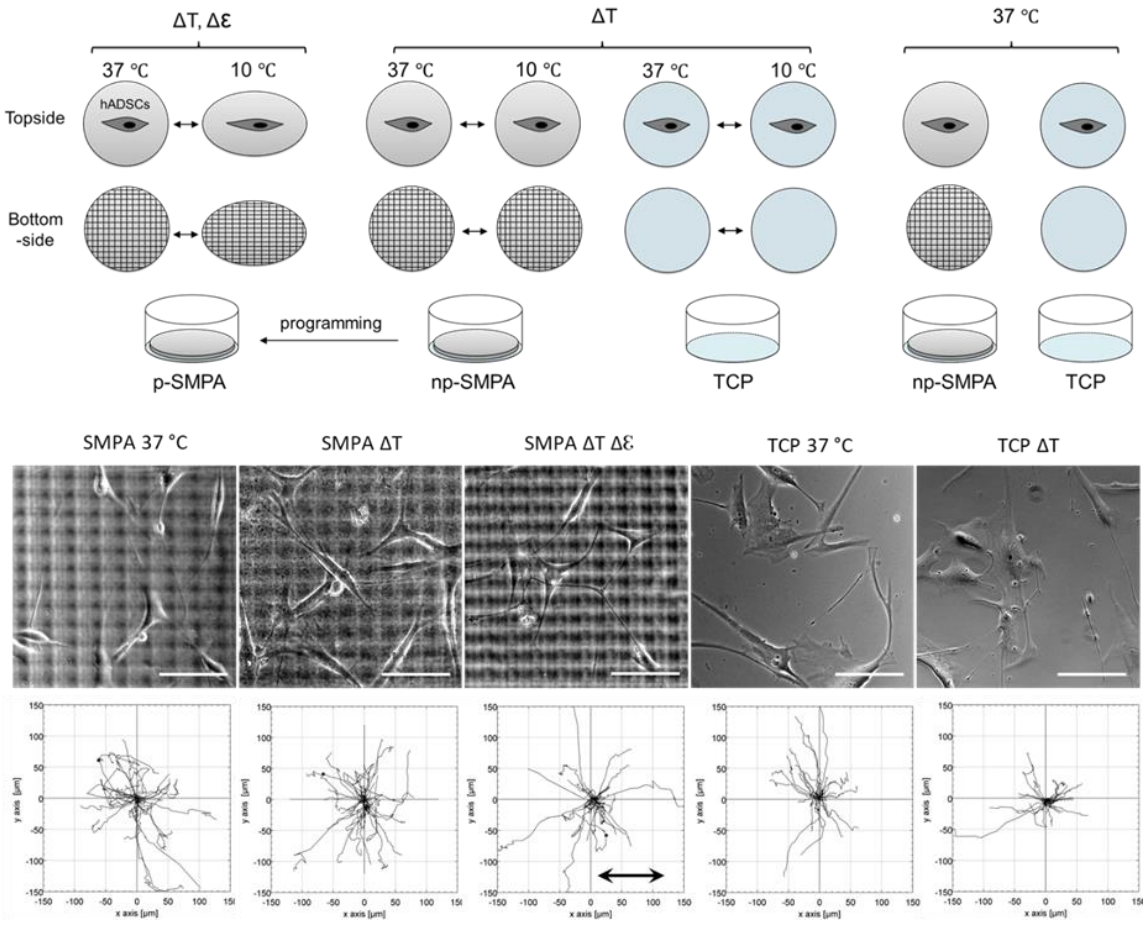

Reprinted by permission from Springer Nature: Springer Nature, MRS Advances, 5(46-47), Modulation of Mesenchymal Stem Cell Migration using Programmable Polymer Sheet Actuators, 2381-2390. Zijun Deng, Weiwei Wang, Xun Xu, Nan Ma, Andreas Lendlein. Copyright (2020).

This work investigated the effect of temperature and mechanical strain on hADSC migration using temperature-responsive polymer sheets. The mechanical strain significantly enhanced cell migration capacity by promoting focal adhesion activation, while the temperature changes slightly reduced the migration capacity. The interplay of dual stimuli suggested a novel insight for MSC homing modulation.

4. 2. 3 Full text of the publication (Appendix II)

4.3 Dedifferentiation of mature adipocytes with periodic exposure to cold

Zijun Deng, Jie Zou, Weiwei Wang, Yan Nie, Wing-Tai Tung, Nan Ma*, Andreas Lendlein*

* Corresponding authors

Clinical Hemorheology and Microcirculation. 2019;71:415-24.

DOI: https://doi.org/10.3233/CH-199005

4. 3. 1 Contribution to the publication

- Literature study
  1> The method for adipocyte dedifferentiation and mechanism about lipolysis and lipid metabolism.
  2> *In vivo* and *in vitro* studies about the influence of temperature on adipocytes.
- Study design with discussion and advice from co-authors
  1> Dedifferentiation promotion using low temperature.
  2> Methods for cultivation of mature adipocytes and detection of intracellular lipids.
- Experimental work
  1> Differentiation of hADSCs into mature adipocytes at 37 °C on TCP substrate.
  2> Evaluation of lipids change in adipocytes by staining and microscope imaging.
  3> Evaluation of the expression level of adipocyte dedifferentiation-related genes and proteins including FABP4, Leptin, PPAR γ , C/EBPα, UCP1, PGC-1α, PRDM16, and Ki67.
- Contribution to analysis and interpretation of experimental data
  1> Quantitative analysis of the amount of lipids in adipocytes with periodic temperature changes.
  2> Comparison of expression level of adipogenic and thermogenic genes between constent 37 °C and periodic low temperature.

3> Analysis of fluorescence images and comparison of protein expression including Perilpin-1, FABP4, and Ki67.

- Manuscript

1> Providing first draft of the manuscript according to outline discussion with co-authors.

3> Revision of the manuscript according to comments from co-authors and reviewers.

4. 3. 2 Summary of the publication

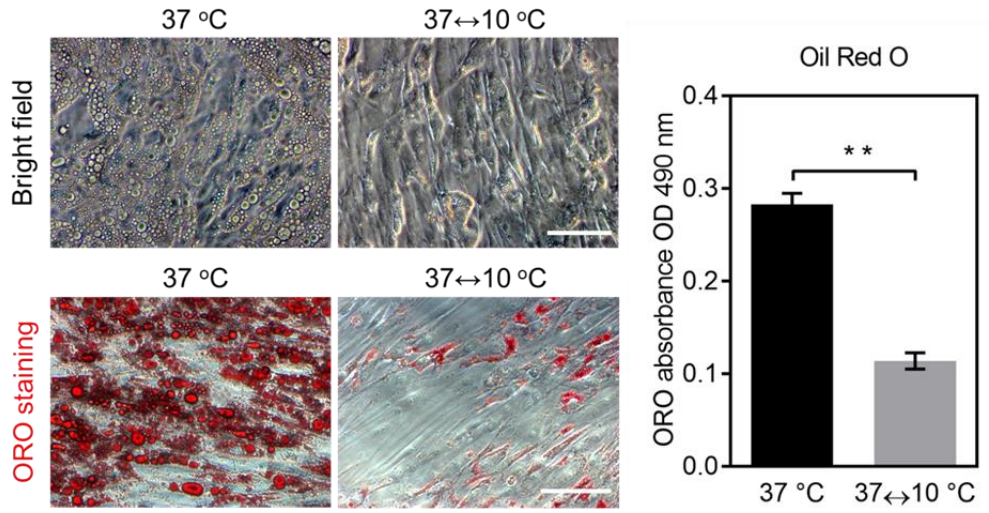

Reprinted from Clin Hemorheol Microcirc, 71, Zijun Deng, Jie Zou, Weiwei Wang, Yan Nie, Wing-Tai Tung, Nan Ma, Andreas Lendlein, Dedifferentiation of mature adipocytes with periodic exposure to cold, 415-424. Copyright (2019), with permission from IOS Press.

In this publication, we demonstrated the promotion effort of periodic temperature changes on adipocyte dedifferentiation. Compared with 37 °C, adipocytes lost most of the intracellular lipids after periodic temperature changes (37 ↔10 °C) for one week *in vitro*. The temperature changes significantly down-regulated the adipogenic genes (FABP4 and Leptin) and up-regulated the thermogenesis genes (UCP1, PGC-1, and PRDM16). Consequently, the protein (FABP4) expression of mature adipocyte was decreased, followed by the increase of the cell proliferation marker Ki67. This publication provides a simple approach to induce lipolysis by periodic temperature changes and further improves the dedifferentiation method of mature adipocytes to generate stem cells.

4. 3. 3 Full text of the publication (Appendix III)

5. Discussion

The properties associated with the self-renewal, migration, secretion, and differentiation of MSCs play essential roles in tissue repair in vivo and profoundly impact regenerative medicine in clinical studies (9, 100). Comprehensive mimic of the cellular native microenvironment in vitro can bring a clear research and better understanding of the cell modulation. The physical cues provided by the MSC microenvironment can influence their behaviors directly. In Publication I, we developed a new system that can combine two different physical signals (thermal and mechanical strain) to control MSC behavior and provided a new strategy to study the influence of multiple physical cues on MSCs. In Publication II, the combined effects of mechanical strain and temperature change on MSCs migration were evaluated. Based on this system and previous studies, we examined the influence of periodic temperature changes on mature adipocyte dedifferentiation in Publication III.

Compared to previous independent studies on single physical cues (101-103), the interplay among different essential factors in the cellular microenvironment has attracted more attention (104). In Publication I and II, we integrated two different physical cues in one system to study the complex interplay of the two factors on MSCs' microenvironment. In our study, using the SMPA sheet, more than 10% elongation could be achieved even after 21-day temperature treatment cycles, changing between 37 °C and 10 °C (Publication I, Fig. S1). In most studies, the mechanical stretch of around 10% is sufficient to influence cell behavior (Table 1). Meanwhile, the periodic temperature between 37 °C and 10 °C had almost no impact on cell survival or apoptosis (Publication I, Fig. S4), but it decreased cell proliferation (Publication I, Fig. S3). Various thermosensitive ion channels were activated by reducing the temperature from 60 °C to 0 °C, and most of them can induce calcium influx (105). Although the environmental temperature changes widely, the human body's temperature is maintained at around 37 °C mainly. Violent temperature change caused severe calcium oscillation, which typically has a substantial impact on intracellular signaling. Therefore, we used a low frequency (1 cycle per hour) of stretch force on MSCs

compared with other studies (Table 1), which enable the MSCs and polymer to fully recovered from the extreme calcium event and shape changes.

Table 1: Example of studies about mechanic strain level.

Cell source	Mechanic strain	Duration	Highlights	Ref.
Calvarial osteoblasts	8% elongation	2 cycles/min 24h, 48h and 96h	Increased expression of anti-apoptosis and autophagy-related genes	(106)
Amniotic epithelial cells	5% elongation	30 cycles/min 2, 6, 12 and 24 h	Induced osteoblastic differentiation	(107)
C3H10T1/2 MSCs	6% elongation	60 cycles/min 12 hours	cytoskeleton reorganization, osteogenic differentiation	(108)
Osteoblast like MG-63 cells	12% elongation	6 cycles/min 1, 4, 8, 12 and 24 h	Increased expression of osteogenesis genes	(109)
Intraoral MSCs	10% elongation	30 cycles/min 7 days, 14 days	Increased expression of osteogenesis genes, higher calcium deposition	(110)
MC3T3-E1 cells	5%, 10% and 15% elongation	6 cycles/min 24h	Induced osteoblastic differentiation	(111)
Bone marrow MSCs	10% elongation	60 cycles/min for 4h, 7 days	Induced osteoblastic differentiation	(112)
Epidermal keratinocytes	10% elongation	6 cycles/min 12h	Epigenetic accumulation of H3K27me3	(113)

We also restricted the investigation to the temperature range from 37 °C to 10 °C in

our system, which is sufficient for the thermally controlled polymer actuator and ensured the cell response in this temperature range. Indeed, further studies over a broader range of temperatures may generate a different strain level and frequency for cell cultivation.

As early as 1892, Julius Wolff hypothesized that mechanical force increases bone remodeling (114-116). Indeed, numerous studies have confirmed that mechanical stimulation, such as compression and stretching forces, can affect cell behavior and guide stem cell differentiation. Initially, research into the mechanical influence on cell behavior was performed using various artificial mechanical devices. With advances in further investigation, the methods become more precise, resulting in the accumulation of large volumes of experimental data that revealed the relationship between mechanical forces and cell behaviors and the mechanisms involved (Tables 1). However, the methods heavily relied on advances in machine control technology. Moreover, these traditional mechanical devices involve complicated operations that limit their widespread use. Although these devices are commercially available, customizing the complex designs for specific samples or experiments each time is difficult owing to their complex mechanical principles. The most commonly used cell stretch instruments are commercially available (for example, STREX Inc. (106, 107), Flexcell® International Corporation (108-113), and CellScale Inc. (117, 118)), and silicon or polydimethylsiloxane (PDMS) films were used as the cell culture substrate for stretching. Some investigations used a customized manufactured instrument that involved a more complicated mechanical control connection (119-123). Overall, these mechanical devices are expensive for research purposes and are also not suitable for high-throughput experiments and applications in clinical studies.

Advances in chemical composition, polymerization, crosslinking, and technology transforming different chemical structures and molecular functionalities have led to many innovative biomaterials and considerably improved cell research strategies (124-126). Recently, various innovative biomaterials with specific properties such as nano- and microscale topography and roughness (49, 127-129), controllable stiffness, and elasticity (130-136) have been applied to cell biology. These studies have shown substantial influence of these properties on cell behavior and genome modification. However, active biomaterials showed dynamic mechanical strain on cell culture self-

sufficiently. Considering the requirement of high-throughput cell experiments and applications, our innovative method can achieve these goals using temperature-controlled PCL-BA polymer with shape-memory actuator capability (98). The temperature control is more accessible than mechanical control, and the temperature changing system can be integrated with the cell culture system by setting the temperature of the culture environment and medium. Moreover, the polymer can be easily cut out as a film and adapted for different cell culture systems. They can also be synthesized as various 3D models for tissue engineering. Therefore, our solution and studies in the thesis provide new insights into the next generation design for combinatorial regulation of biochemical and physical signals for stem cell research and application.

MSCs attachment and migration rely on the dynamic changing of focal adhesion and stress fibers and are sensitive to the substrates' composition and chemical characteristics. For the outside-in signaling pathway, external forces drive integrin activation on new binding sites to recruit other components, such as talin, FAK, vinculin, myosin, and actin, to mature new focal adhesion binding sites and cytoskeletal fibers. Meanwhile, with myosin's intracellular contractile force, the integrin can also be activated at the new binding sites to drive cell migration, known as inside-out signaling (137).

Therefore, we investigated integrin activation and cell migration with the external influence of temperature change and mechanical strain in Publication I, the polymer substrate's dual stimulation. The elongation rate of the polymer sheet was about six times that of cell migration velocity. The elongated morphology and activated integrin of MSCs confirmed that the mechanical strain generated by the polymer sheet shape change could stimulate focal adhesion formation (138). The following mechanotransduction was related to stress fibers and YAP, transforming the external physical cues into nuclei to regulate gene expression. For instance, various studies of outside-in mechanotransduction focused on YAP signaling, such as stiffness (77, 139, 140), shear and microfluidic stress (57, 141), micro-and nano-patterning (142, 143), and stretch strain (144-146), which influences stem cell behavior, proliferation, and differentiation (147).

Publication II examined the inside-out signaling effect on MSCs migration after the same treatment combined with temperature change and mechanical strain. Based on the study in Publication I, we confirmed that both the temperature and mechanical strain could influence intracellular signaling and epigenetic modification. The physical cues could alter genome modification and leave the training marks or memories in the MSCs. We found that mechanical strain wrote a memory to the cells after removal of the stimulation, and this memory still promoted cell migration by the high levels of integrin and myosin activation. Our results verified various outside-in studies that showed increased cell migration caused by physical cues, such as mechanical stretch (68, 148, 149), shear stress (67, 150), and matrix stiffness (151-154). Thus, the studies in this thesis used active polymeric actuator to apply the physical cues on MSCs to study their differentiation and identified the related mechanism involved at both outside-in and inside-out levels.

In Publication III, we demonstrated the influence of periodic temperature change on adipocytes, aiming to improve the method of adipocyte dedifferentiation. Although the adipocyte dedifferentiation into DFAT cells has shown great potential in the optimization of stem cell sources for clinical regenerative medicine (155), a highly effective method used for adipocyte dedifferentiation in vitro still needs to be developed. The original method for adipocyte dedifferentiation is the ceiling culture method that has been in use since 1986 (28). Then, some minor advancements of the dedifferentiation method were developed based on the original ceiling culture (34, 156, 157). In 2015, Birgit Huber and Petra J. Kluger compared different culture medium compositions in adipocyte dedifferentiation using hydrogel encapsulation. They found that low percentage of fetal calf serum and insulin supplements (Adipocyte Nutrition Medium supplemented with 3% fetal calf serum, 8 µg/mL d-biotin, 0.5 µg/mL human insulin, and 400 ng/mL dexamethasone) could decelerate the mature adipocyte dedifferentiation in vitro whereas increasing of fetal calf serum promoted dedifferentiation (158). In 2010 and 2016, Wnt3a and Wnt5a were found to promote lipolysis and adipocyte dedifferentiation (159, 160). In 2016, an in vivo study reported that the adipocyte-specific activation of Notch signaling (Ad/N1ICD) could lead to adipocyte dedifferentiation and tumorigenic transformation, while the rosiglitazone (a synthetic Pparγ ligand) rescued the dedifferentiation and promoted adipogenesis (161). The indirect evidence in these studies still provided some clues (increasing

lipolysis and inhibition of adipogenesis) that may improve the adipocyte dedifferentiation in vitro.

Compared with the studies mentioned above, periodic temperature changes could increase lipolysis and inhibit adipogenesis significantly. The temperature control is easy handling and can be developed as a standard operation instead of various chemical treatments and genetic modifications that rely on different laboratory experimental conditions. The effect of the periodic temperature on adipocyte dedifferentiation in vitro is shown in Publication III. Further studies may provide an innovative method to achieve efficient dedifferentiation of mature adipocyte and promote the clinical application of DFAT cells.

6. Summary and Outlook

In this study, an active polymeric biomaterial was applied as dynamic cell culture substrate. A shape-memory polymer actuator sheet showed temperature controlled reversible shape changes that generated mechanical strain. The SMPA sheet was elongated gradually when the temperature was decreased to 10 °C and recovered when the temperature changed back to 37 °C. The dynamic mechanical strain of the SMPA sheet maintained more than 10% elongation for three weeks at a frequency of 1 cycle per hour. Human ADSCs cultured on the SMPA sheet were stretched by the mechanical strain correspondingly. This system achieved the mechanical strain effect on cell level.

The SMPA sheet were used as a cell culture substrate, which modulated MSC behaviour by integrating temperature change and mechanical strain. To verify the combined effects on MSCs, two different cell responsive pathways were studied using this system. With the combined effects of temperature and mechanical strain, human ADSCs were cyclic stretched for a period. YAP-mediated signaling transduction from focal adhesion to osteogenic gene expression highly depends on the mechanical strain effect. The dual stimuli of temperature change and mechanical strain both induced calcium oscillation in cells. The YAP and calcium mediated signaling further altered the epigenetic histone acetylation on H3K9 and promoted osteogenesis. This study explained how the temperature and mechanical strain influenced MSC behavior simultaneously in an outside-in signaling way and provided new insight into integrating multiple physical cues to demonstrate the behavioral modulation of MSCs in a complex microenvironment. On the other hand, after pretraining of temperature change and mechanical strain, the cell migration was evaluated in regular cultivation to examine the combined effects. Temperature change reduced integrin activation and cell migration, while mechanical strain reversed this effect. The pretraining of the dual stimuli altered cytoskeleton organization and focal adhesion activation independently, and the altered signaling keep on regulating cell migration velocity after withdrawing the stimuli. These studies confirmed that the SMPA sheet could transduce the mechanical effect to cells, not only by modulation of cell behavior directly but also by post regulation of cell behavior via the pretraining altered signal molecules.

Since the temperature change inhibited adipogenic differentiation of hADSCs, and to extend the application of temperature change and solve the low efficiency of adipocyte dedifferentiation, the study examined the effect of temperature change (10 - 37 °C) on mature adipocytes cultured on TCP. We achieved the promotion of lipolysis and dedifferentiation of mature adipocytes in vitro by treatment of periodic temperature changes. The down-regulation of mature adipocyte markers and up-regulation of brown adipocyte markers confirmed the cell transformation, and the increasing proliferation marker suggested the processing of adipocyte dedifferentiation. This study introduced a novel method to promote adipocyte dedifferentiation in vitro and gave an example to extend the potential application of temperature change. Moreover, this novel method can be used widely to induce adipocyte dedifferentiation, which is desired to develop an alternative stem cell source.

The thesis provides an example to demonstrate the feasibility of the concept, and further studies can extend the approach to other physical cues for various applications. In addition, the native microenvironment of cells and pathological tissues is more complex than a single physical or biochemical factor. This work studied the interplay effects of temperature and mechanical strain on MSCs initially. Further, the interplay of multiple factors should be gradually incorporated into the experiments to reveal the native complex mechanisms of development and regeneration. The application of active biomaterials and a better understanding of MSC behavior modulation will promote the application of MSCs based cell therapy and help find important regulators for tissue repair and regeneration.

7. Kurzzusammenfassung

In dieser Studie wurde eine Shape-memory Polymer-Aktuatorfolie als dynamisches Zellkultursubstrat eingesetzt. Die SMPA-Folie verlängerte sich allmählich, wenn die Temperatur auf 10 °C gesenkt wurde, und sie kontrahierte wieder, wenn man die Temperatur wieder auf 37 °C erhöhte. Die dynamische mechanische Dehnung der SMPA-Folie hielt drei Wochen lang einer Dehnung von mehr als 10%, bei einer Frequenz von 1 Zyklus pro Stunde, stand. Auf der SMPA-Folie kultivierte humane ADSCs wurden durch die mechanische Belastung entsprechend gedehnt. Dieses System erzielte einen mechanischen Dehnungseffekt auf Zellebene und ersetzte die mechanischen Geräte, die bislang in der Zellforschung für solche Zwecke verwendet werden.

Die SMPA-Folie dient als Zellkultursubstrat, wodurch sowohl Temperaturänderungen als auch mechanische Belastungen integriert werden können und die Kultivierung und Verhaltensmodulation von MSCs beeinflusst werden. Um die kombinierten Wirkungen auf MSCs zu verifizieren, wurden zwei verschiedene Zellantworten unter Verwendung dieses Systems untersucht. Mit den kombinierten Effekten von Temperatur und mechanischer Belastung wurden humane ADSCs über einen Zeitraum von 3 Wochen zyklisch gedehnt. Die YAP-vermittelte Signaltransduktion von der fokalen Adhäsion zur osteogenen Genexpression hängt stark vom mechanischen Belastungseffekt ab. Die kombinierten Reize der Temperaturänderung und der mechanischen Belastung induzierten beide eine Calciumionen Konzentration Oszillation in den Zellen. Das YAP- und Calcium-vermittelte Signal veränderte die epigenetische Histonacetylierung an H3K9 weiter und förderte die Osteogenese. Diese Studie erklärt, wie die Temperatur und die mechanische Belastung das MSC-Verhalten gleichzeitig von außen nach innen beeinflussten, und lieferte neue Erkenntnisse zur Integration mehrerer physikalischer Prozesse, um die Verhaltensmodulation von MSCs in einer komplexen Mikroumgebung zu zeigen. Des Weiteren wurden die Zellen, nach Vorbehandlung mit Temperaturänderung und mechanischer Belastung, auf Zellmigration unter normalen Kultivierungsbedingungen bewertet, um die kombinierten Effekte zu untersuchen. Die Temperaturänderung verringerte die Integrinaktivierung und Zellmigration, während die mechanische Belastung diesen Effekt umkehrte. Die Vorbehandlung der Zellen mit den dualen Stimuli veränderte,

unabhängig voneinander, die Organisation des Zytoskeletts und die Aktivierung der fokalen Adhäsion und die veränderte Signalübertragung reguliert die Zellmigrationsgeschwindigkeit nach Beendigung der Stimulation weiter. Diese Studien bestätigten, dass die SMPA-Folie die mechanische Wirkung auf Zellen übertragen kann, nicht nur durch direkte Modulation des Zellverhaltens, sondern auch durch die spätere Regulierung des Zellverhaltens über veränderter Signalmoleküle.

Da die Temperaturänderung die adipogene Differenzierung von hADSCs inhibierte, und um die Anwendung der Temperaturänderung zu erweitern und die geringe Effizienz der Adipozyten-Dedifferenzierung zu lösen, untersuchte die Studie die Auswirkung der Temperaturänderung (10 - 37 °C) auf reife Adipozyten, die auf TCP kultiviert wurden. Wir haben die Förderung der Lipolyse und Dedifferenzierung reifer Adipozyten in vitro durch eine Behandlung mit der zyklischen Temperaturänderungen erreicht. Die Herunterregulierung reifer Adipozytenmarker und die Hochregulierung brauner Adipozytenmarker bestätigten die Zelltransformation, und die Zunahme der Proliferationsmarker deutete auf die voranschreitende Adipozyten-Dedifferenzierung hin. Diese Studie führte eine neuartige Methode ein, um die Effizienz der Adipozyten-Dedifferenzierung in vitro zu verbessern, und zeigte somit ein Beispiel für mögliche weitere Anwendungen von Temperaturänderungen auf. Darüber hinaus kann diese Verbesserung in großem Umfang genutzt werden, um die Dedifferenzierung von Adipozyten zu induzieren, was erwünscht ist, um eine alternative Stammzellquelle zu entwickeln.

Den Studien zufolge, könnten polymer-basierte, aktive Biomaterialien mit Formänderungseigenschaften dazu beitragen, das Konstruktionsprinzip von Bioreaktoren Zu erneuern und effizientere Methoden zu entwickeln. Die Arbeit bietet ein einfaches Beispiel, um die Machbarkeit des Konzepts zu demonstrieren, und weitere Studien können den Ansatz auf andere physikalische Hinweise für verschiedene Anwendungen ausweiten. Darüber hinaus ist die native Mikroumgebung von Zellen und verletzten Geweben komplexer als ein einzelner physikalischer oder biochemischer Faktor. In dieser Arbeit wurden zunächst die Wechselwirkungen von Temperatur und mechanischer Belastung auf MSCs untersucht. Darüber hinaus sollte das Zusammenspiel mehrerer Faktoren schrittweise in die Experimente einbezogen werden, um die nativen komplexen Mechanismen der Entwicklung und Regeneration

aufzudecken. Die Anwendung aktive Biomaterialien und ein besseres Verständnis der MSC-Verhaltensmodulation werden die Anwendung der MSC-basierten Zelltherapie fördern und dazu beitragen, wichtige Regulatoren für die Reparatur und Regeneration von Gewebe zu finden.

8. References

1. Pittenger MF*, et al.* (1999) Multilineage potential of adult human mesenchymal stem cells. *Science* 284(5411):143-147.
2. Jiang Y*, et al.* (2002) Pluripotency of mesenchymal stem cells derived from adult marrow. *Nature* 418(6893):41-49.
3. Mishra VK*, et al.* (2020) Identifying the Therapeutic Significance of Mesenchymal Stem Cells. *Cells* 9(5):1145.
4. Volarevic V*, et al.* (2018) Ethical and Safety Issues of Stem Cell-Based Therapy. *Int J Med Sci* 15(1):36-45.
5. Wang Y, Tang Z, & Gu P (2020) Stem/progenitor cell-based transplantation for retinal degeneration: a review of clinical trials. *Cell Death Dis* 11(9):793.
6. Jacobs SA*, et al.* (2013) Human multipotent adult progenitor cells are nonimmunogenic and exert potent immunomodulatory effects on alloreactive T-cell responses. *Cell Transplant* 22(10):1915-1928.
7. Wang M, Yuan Q, & Xie L (2018) Mesenchymal Stem Cell-Based Immunomodulation: Properties and Clinical Application. *Stem Cells Int* 2018:3057624.
8. Gao F*, et al.* (2016) Mesenchymal stem cells and immunomodulation: current status and future prospects. *Cell Death Dis* 7:e2062.
9. Fu X*, et al.* (2019) Mesenchymal Stem Cell Migration and Tissue Repair. *Cells* 8(8):784.
10. Pittenger MF*, et al.* (2019) Mesenchymal stem cell perspective: cell biology to clinical progress. *NPJ Regen Med* 4:22.
11. Haynesworth SE, Goshima J, Goldberg VM, & Caplan AI (1992) Characterization of cells with osteogenic potential from human marrow. *Bone* 13(1):81-88.
12. Zuk PA*, et al.* (2001) Multilineage cells from human adipose tissue: implications for cell-based therapies. *Tissue Eng* 7(2):211-228.
13. Gronthos S, Mankani M, Brahim J, Robey PG, & Shi S (2000) Postnatal human dental pulp stem cells (DPSCs) in vitro and in vivo. *Proc Natl Acad Sci U S A* 97(25):13625-13630.
14. Toma JG, McKenzie IA, Bagli D, & Miller FD (2005) Isolation and characterization of multipotent skin-derived precursors from human skin. *Stem Cells* 23(6):727-737.
15. Paul G*, et al.* (2012) The adult human brain harbors multipotent perivascular mesenchymal stem cells. *PLoS One* 7(4):e35577.
16. Jackson WM, Nesti LJ, & Tuan RS (2010) Potential therapeutic applications of muscle-derived mesenchymal stem and progenitor cells. *Expert Opin Biol Ther* 10(4):505-517.
17. Tondreau T*, et al.* (2005) Mesenchymal stem cells derived from CD133-positive cells in mobilized peripheral blood and cord blood: proliferation, Oct4 expression, and plasticity. *Stem Cells* 23(8):1105-1112.
18. In 't Anker PS*, et al.* (2004) Isolation of mesenchymal stem cells of fetal or maternal origin from human placenta. *Stem Cells* 22(7):1338-1345.
19. Sarugaser R, Lickorish D, Baksh D, Hosseini MM, & Davies JE (2005) Human umbilical cord perivascular (HUCPV) cells: a source of mesenchymal progenitors. *Stem Cells* 23(2):220-229.

20. Bieback K, Kern S, Kluter H, & Eichler H (2004) Critical parameters for the isolation of mesenchymal stem cells from umbilical cord blood. *Stem Cells* 22(4):625-634.
21. Van RL, Bayliss CE, & Roncari DA (1976) Cytological and enzymological characterization of adult human adipocyte precursors in culture. *J Clin Invest* 58(3):699-704.
22. Puissant B*, et al.* (2005) Immunomodulatory effect of human adipose tissue-derived adult stem cells: comparison with bone marrow mesenchymal stem cells. *Br J Haematol* 129(1):118-129.
23. Meliga E, Strem BM, Duckers HJ, & Serruys PW (2007) Adipose-derived cells. *Cell Transplant* 16(9):963-970.
24. Mehrabani D, Mehrabani G, Zare S, & Manafi A (2013) Adipose-Derived Stem Cells (ADSC) and Aesthetic Surgery: A Mini Review. *World J Plast Surg* 2(2):65-70.
25. Harasymiak-Krzyzanowska I*, et al.* (2013) Adipose tissue-derived stem cells show considerable promise for regenerative medicine applications. *Cell Mol Biol Lett* 18(4):479-493.
26. Meza-Zepeda LA*, et al.* (2008) High-resolution analysis of genetic stability of human adipose tissue stem cells cultured to senescence. *J Cell Mol Med* 12(2):553-563.
27. Bourgeois C*, et al.* (2019) Specific Biological Features of Adipose Tissue, and Their Impact on HIV Persistence. *Front Microbiol* 10:2837.
28. Sugihara H, Yonemitsu N, Miyabara S, & Yun K (1986) Primary cultures of unilocular fat cells: characteristics of growth in vitro and changes in differentiation properties. *Differentiation* 31(1):42-49.
29. Sugihara H, Yonemitsu N, Miyabara S, & Toda S (1987) Proliferation of unilocular fat cells in the primary culture. *J Lipid Res* 28(9):1038-1045.
30. Sugihara H*, et al.* (1989) A simple culture method of fat cells from mature fat tissue fragments. *J Lipid Res* 30(12):1987-1995.
31. Cai S, Fu XB, & Sheng ZY (2007) Dedifferentiation: A new approach in stem cell research. *Bioscience* 57(8):655-662.
32. Jumabay M*, et al.* (2014) Pluripotent stem cells derived from mouse and human white mature adipocytes. *Stem Cells Transl Med* 3(2):161-171.
33. Lessard J*, et al.* (2015) Characterization of dedifferentiating human mature adipocytes from the visceral and subcutaneous fat compartments: fibroblast-activation protein alpha and dipeptidyl peptidase 4 as major components of matrix remodeling. *PLoS One* 10(3):e0122065.
34. Matsumoto T*, et al.* (2008) Mature adipocyte-derived dedifferentiated fat cells exhibit multilineage potential. *J Cell Physiol* 215(1):210-222.
35. Shah M, George RL, Evancho-Chapman MM, & Zhang G (2016) Current challenges in dedifferentiated fat cells research. *Organogenesis* 12(3):119-127.
36. Duarte MS*, et al.* (2017) Triennial growth and development symposium : Dedifferentiated fat cells: Potential and perspectives for their use in clinical and animal science purpose. *J Anim Sci* 95(5):2255-2260.
37. Crowder SW, Leonardo V, Whittaker T, Papathanasiou P, & Stevens MM (2016) Material Cues as Potent Regulators of Epigenetics and Stem Cell Function. *Cell Stem Cell* 18(1):39-52.
38. Watt FM & Huck WT (2013) Role of the extracellular matrix in regulating stem cell fate. *Nat Rev Mol Cell Biol* 14(8):467-473.

39. Lee DA, Knight MM, Campbell JJ, & Bader DL (2011) Stem cell mechanobiology. *J Cell Biochem* 112(1):1-9.
40. Wozniak MA & Chen CS (2009) Mechanotransduction in development: a growing role for contractility. *Nat Rev Mol Cell Biol* 10(1):34-43.
41. Yang C, Tibbitt MW, Basta L, & Anseth KS (2014) Mechanical memory and dosing influence stem cell fate. *Nat Mater* 13(6):645-652.
42. Barnes JM, Przybyla L, & Weaver VM (2017) Tissue mechanics regulate brain development, homeostasis and disease. *J Cell Sci* 130(1):71-82.
43. Engler AJ, Sen S, Sweeney HL, & Discher DE (2006) Matrix elasticity directs stem cell lineage specification. *Cell* 126(4):677-689.
44. Gerardo H*, et al.* (2019) Soft culture substrates favor stem-like cellular phenotype and facilitate reprogramming of human mesenchymal stem/stromal cells (hMSCs) through mechanotransduction. *Sci Rep* 9(1):9086.
45. Kureel SK*, et al.* (2019) Soft substrate maintains proliferative and adipogenic differentiation potential of human mesenchymal stem cells on long-term expansion by delaying senescence. *Biol Open* 8(4):bio039453.
46. Chowdhury F*, et al.* (2010) Soft substrates promote homogeneous self-renewal of embryonic stem cells via downregulating cell-matrix tractions. *PLoS One* 5(12):e15655.
47. Saxena N*, et al.* (2018) Matrix elasticity regulates mesenchymal stem cell chemotaxis. *J Cell Sci* 131(7):jcs211391.
48. Yim EK, Darling EM, Kulangara K, Guilak F, & Leong KW (2010) Nanotopography-induced changes in focal adhesions, cytoskeletal organization, and mechanical properties of human mesenchymal stem cells. *Biomaterials* 31(6):1299-1306.
49. Li Z*, et al.* (2017) Integrin beta1 activation by micro-scale curvature promotes pro-angiogenic secretion of human mesenchymal stem cells. *J Mater Chem B* 5(35):7415-7425.
50. Li Z*, et al.* (2017) Modulation of the mesenchymal stem cell migration capacity via preconditioning with topographic microstructure. *Clin Hemorheol Microcirc* 67(3-4):267-278.
51. Xu X*, et al.* (2014) Controlling major cellular processes of human mesenchymal stem cells using microwell structures. *Adv Healthc Mater* 3(12):1991-2003.
52. Yamazaki M, Kojima H, & Miyoshi H (2020) Morphology and differentiation of human mesenchymal stem cells cultured on a nanoscale structured substrate. *Electr Commun Jpn* 103(9):23-28.
53. Zhu L, Luo D, & Liu Y (2020) Effect of the nano/microscale structure of biomaterial scaffolds on bone regeneration. *Int J Oral Sci* 12(1):6.
54. Higuchi A, Ling QD, Chang Y, Hsu ST, & Umezawa A (2013) Physical cues of biomaterials guide stem cell differentiation fate. *Chem Rev* 113(5):3297-3328.
55. Kshitiz, Afzal J, Chang H, Goyal R, & Levchenko A (2016) Mechanics of Microenvironment as Instructive Cues Guiding Stem Cell Behavior. *Curr Stem Cell Rep* 2(1):62-72.
56. Sonam S, Sathe SR, Yim EK, Sheetz MP, & Lim CT (2016) Cell contractility arising from topography and shear flow determines human mesenchymal stem cell fate. *Sci Rep* 6:20415.
57. Kim KM*, et al.* (2014) Shear stress induced by an interstitial level of slow flow increases the osteogenic differentiation of mesenchymal stem cells through TAZ activation. *PLoS One* 9(3):e92427.

58. Luo L, Thorpe SD, Buckley CT, & Kelly DJ (2015) The effects of dynamic compression on the development of cartilage grafts engineered using bone marrow and infrapatellar fat pad derived stem cells. *Biomed Mater* 10(5):055011.
59. Carroll SF, Buckley CT, & Kelly DJ (2017) Cyclic Tensile Strain Can Play a Role in Directing both Intramembranous and Endochondral Ossification of Mesenchymal Stem Cells. *Front Bioeng Biotechnol* 5:73.
60. Campbell JJ, Lee DA, & Bader DL (2006) Dynamic compressive strain influences chondrogenic gene expression in human mesenchymal stem cells. *Biorheology* 43(3,4):455-470.
61. Walters B*, et al.* (2017) Engineering the geometrical shape of mesenchymal stromal cells through defined cyclic stretch regimens. *Sci Rep* 7(1):6640.
62. Chen X*, et al.* (2018) Mechanical stretch induces antioxidant responses and osteogenic differentiation in human mesenchymal stem cells through activation of the AMPK-SIRT1 signaling pathway. *Free Radic Biol Med* 126:187-201.
63. Rothdiener M*, et al.* (2016) Stretching human mesenchymal stromal cells on stiffness-customized collagen type I generates a smooth muscle marker profile without growth factor addition. *Sci Rep* 6:35840.
64. Deng Z*, et al.* (2020) Polymeric sheet actuators with programmable bioinstructivity. *Proc Natl Acad Sci U S A* 117(4):1895-1901.
65. Gao XH*, et al.* (2014) Regulation of cell migration and osteogenic differentiation in mesenchymal stem cells under extremely low fluidic shear stress. *Biomicrofluidics* 8(5):e052008.
66. Riehl BD, Lee JS, Ha L, & Lim JY (2015) Fluid-flow-induced mesenchymal stem cell migration: role of focal adhesion kinase and RhoA kinase sensors. *J R Soc Interface* 12(104):20141351.
67. Yuan L, Sakamoto N, Song G, & Sato M (2013) Low-level shear stress induces human mesenchymal stem cell migration through the SDF-1/CXCR4 axis via MAPK signaling pathways. *Stem Cells Dev* 22(17):2384-2393.
68. Zhou SB, Wang J, Chiang CA, Sheng LL, & Li QF (2013) Mechanical stretch upregulates SDF-1alpha in skin tissue and induces migration of circulating bone marrow-derived stem cells into the expanded skin. *Stem Cells* 31(12):2703-2713.
69. Reissis Y, Garcia-Gareta E, Korda M, Blunn GW, & Hua J (2013) The effect of temperature on the viability of human mesenchymal stem cells. *Stem Cell Res Ther* 4(6):139.
70. Stolzing A & Scutt A (2006) Effect of reduced culture temperature on antioxidant defences of mesenchymal stem cells. *Free Radic Biol Med* 41(2):326-338.
71. Tirza G*, et al.* (2020) Reduced culture temperature attenuates oxidative stress and inflammatory response facilitating expansion and differentiation of adipose-derived stem cells. *Stem Cell Res Ther* 11(1):35.
72. Wang XP*, et al.* (2017) TRPM8 in the negative regulation of TNFalpha expression during cold stress. *Sci Rep* 7:45155.
73. Barbatelli G*, et al.* (2010) The emergence of cold-induced brown adipocytes in mouse white fat depots is determined predominantly by white to brown adipocyte transdifferentiation. *Am J Physiol Endocrinol Metab* 298(6):E1244-1253.
74. Lynes MD*, et al.* (2018) Cold-Activated Lipid Dynamics in Adipose Tissue Highlights a Role for Cardiolipin in Thermogenic Metabolism. *Cell Rep* 24(3):781-790.
75. Nie Y, Yan Z, Yan W, Xia Q, & Zhang Y (2015) Cold exposure stimulates lipid metabolism, induces inflammatory response in the adipose tissue of mice and

promotes the osteogenic differentiation of BMMSCs via the p38 MAPK pathway in vitro. *Int J Clin Exp Pathol* 8(9):10875-10886.
76. Velickovic K*, et al.* (2018) Low temperature exposure induces browning of bone marrow stem cell derived adipocytes in vitro. *Sci Rep* 8(1):4974.
77. Dupont S*, et al.* (2011) Role of YAP/TAZ in mechanotransduction. *Nature* 474(7350):179-183.
78. Asaoka Y, Nishina H, & Furutani-Seiki M (2017) YAP is essential for 3D organogenesis withstanding gravity. *Dev Growth Differ* 59(1):52-58.
79. Chen Q*, et al.* (2016) Fate decision of mesenchymal stem cells: adipocytes or osteoblasts? *Cell Death Differ* 23(7):1128-1139.
80. Hong JH*, et al.* (2005) TAZ, a transcriptional modulator of mesenchymal stem cell differentiation. *Science* 309(5737):1074-1078.
81. Piccolo S, Dupont S, & Cordenonsi M (2014) The biology of YAP/TAZ: hippo signaling and beyond. *Physiol Rev* 94(4):1287-1312.
82. Codelia VA, Sun G, & Irvine KD (2014) Regulation of YAP by mechanical strain through Jnk and Hippo signaling. *Curr Biol* 24(17):2012-2017.
83. Heo SJ*, et al.* (2016) Differentiation alters stem cell nuclear architecture, mechanics, and mechano-sensitivity. *Elife* 5: e18207.
84. Xiao E*, et al.* (2015) Brief reports: TRPM7 Senses mechanical stimulation inducing osteogenesis in human bone marrow mesenchymal stem cells. *Stem Cells* 33(2):615-621.
85. Dolmetsch RE, Xu K, & Lewis RS (1998) Calcium oscillations increase the efficiency and specificity of gene expression. *Nature* 392(6679):933-936.
86. Liu YS*, et al.* (2015) Mechanosensitive TRPM7 mediates shear stress and modulates osteogenic differentiation of mesenchymal stromal cells through Osterix pathway. *Sci Rep* 5:16522.
87. Kwon HJ, Lee GS, & Chun H (2016) Electrical stimulation drives chondrogenesis of mesenchymal stem cells in the absence of exogenous growth factors. *Sci Rep* 6:39302.
88. Pinto MC*, et al.* (2016) Studying complex system: calcium oscillations as attractor of cell differentiation. *Integr Biol (Camb)* 8(2):130-148.
89. Goralczyk A*, et al.* (2017) TRP channels in brown and white adipogenesis from human progenitors: new therapeutic targets and the caveats associated with the common antibiotic, streptomycin. *FASEB J* 31(8):3251-3266.
90. Zheng J (2013) Molecular mechanism of TRP channels. *Compr Physiol* 3(1):221-242.
91. McKemy DD, Neuhausser WM, & Julius D (2002) Identification of a cold receptor reveals a general role for TRP channels in thermosensation. *Nature* 416(6876):52-58.
92. Peier AM*, et al.* (2002) A TRP channel that senses cold stimuli and menthol. *Cell* 108(5):705-715.
93. Tansey EA & Johnson CD (2015) Recent advances in thermoregulation. *Adv Physiol Educ* 39(3):139-148.
94. Wu J, Lewis AH, & Grandl J (2017) Touch, Tension, and Transduction - The Function and Regulation of Piezo Ion Channels. *Trends Biochem Sci* 42(1):57-71.
95. Tibbitt MW, Rodell CB, Burdick JA, & Anseth KS (2015) Progress in material design for biomedical applications. *Proc Natl Acad Sci U S A* 112(47):14444-14451.

96. Rahmati M, Silva EA, Reseland JE, C AH, & Haugen HJ (2020) Biological responses to physicochemical properties of biomaterial surface. *Chem Soc Rev* 49(15):5178-5224.
97. Behl M, Kratz K, Zotzmann J, Nochel U, & Lendlein A (2013) Reversible bidirectional shape-memory polymers. *Adv Mater* 25(32):4466-4469.
98. Behl M, Kratz K, Noechel U, Sauter T, & Lendlein A (2013) Temperature-memory polymer actuators. *Proc Natl Acad Sci U S A* 110(31):12555-12559.
99. Lendlein A & Gould OEC (2019) Reprogrammable recovery and actuation behaviour of shape-memory polymers. *Nat Rev Mater* 4(2):116-133.
100. Hu C & Li L (2018) Preconditioning influences mesenchymal stem cell properties in vitro and in vivo. *J Cell Mol Med* 22(3):1428-1442.
101. Moghaddam MM, Bonakdar S, Shariatpanahi MR, Shokrgozar MA, & Faghihi S (2019) The Effect of Physical Cues on the Stem Cell Differentiation. *Curr Stem Cell Res Ther* 14(3):268-277.
102. Kshitiz*, et al.* (2012) Control of stem cell fate and function by engineering physical microenvironments. *Integr Biol (Camb)* 4(9):1008-1018.
103. Lutolf MP, Gilbert PM, & Blau HM (2009) Designing materials to direct stem-cell fate. *Nature* 462(7272):433-441.
104. Lee J*, et al.* (2020) Combinatorial screening of biochemical and physical signals for phenotypic regulation of stem cell-based cartilage tissue engineering. *Sci Adv* 6(21):eaaz5913.
105. Lamas JA, Rueda-Ruzafa L, & Herrera-Perez S (2019) Ion Channels and Thermosensitivity: TRP, TREK, or Both? *Int J Mol Sci* 20(10):2371.
106. Inaba N, Kuroshima S, Uto Y, Sasaki M, & Sawase T (2017) Cyclic mechanical stretch contributes to network development of osteocyte-like cells with morphological change and autophagy promotion but without preferential cell alignment in rat. *Biochem Biophys Rep* 11:191-197.
107. Luan F*, et al.* (2018) Differentiation of human amniotic epithelial cells into osteoblasts is induced by mechanical stretch via the Wnt/betacatenin signalling pathway. *Mol Med Rep* 18(6):5717-5725.
108. Song Y*, et al.* (2018) Cyclic mechanical stretch enhances BMP9-induced osteogenic differentiation of mesenchymal stem cells. *Int Orthop* 42(4):947-955.
109. Gao J*, et al.* (2016) Cyclic stretch promotes osteogenesis-related gene expression in osteoblast-like cells through a cofilin-associated mechanism. *Mol Med Rep* 14(1):218-224.
110. Lohberger B*, et al.* (2014) Effect of cyclic mechanical stimulation on the expression of osteogenesis genes in human intraoral mesenchymal stromal and progenitor cells. *Biomed Res Int* 2014:189516.
111. Zeng Z, Yin X, Zhang X, Jing D, & Feng X (2015) Cyclic stretch enhances bone morphogenetic protein-2-induced osteoblastic differentiation through the inhibition of Hey1. *Int J Mol Med* 36(5):1273-1281.
112. He YB*, et al.* (2019) Mechanical Stretch Promotes the Osteogenic Differentiation of Bone Mesenchymal Stem Cells Induced by Erythropoietin. *Stem Cells Int* 2019:1839627.
113. Le HQ*, et al.* (2016) Mechanical regulation of transcription controls Polycomb-mediated gene silencing during lineage commitment. *Nat Cell Biol* 18(8):864-875.
114. Frost HM (1994) Wolff's Law and bone's structural adaptations to mechanical usage: an overview for clinicians. *Angle Orthod* 64(3):175-188.
115. Ruff C, Holt B, & Trinkaus E (2006) Who's afraid of the big bad Wolff?: "Wolff's law" and bone functional adaptation. *Am J Phys Anthropol* 129(4):484-498.

116. Goetzke R, Sechi A, De Laporte L, Neuss S, & Wagner W (2018) Why the impact of mechanical stimuli on stem cells remains a challenge. *Cell Mol Life Sci* 75(18):3297-3312.
117. Chen K*, et al.* (2018) Role of boundary conditions in determining cell alignment in response to stretch. *Proc Natl Acad Sci U S A* 115(5):986-991.
118. Kumar D, Cain SA, & Bosworth LA (2019) Effect of Topography and Physical Stimulus on hMSC Phenotype Using a 3D In Vitro Model. *Nanomaterials (Basel)* 9(4):522.
119. Rapalo G*, et al.* (2015) Live Cell Imaging during Mechanical Stretch. *J Vis Exp* (102):e52737.
120. Roche SM, Gumucio JP, Brooks SV, Mendias CL, & Claflin DR (2015) Measurement of Maximum Isometric Force Generated by Permeabilized Skeletal Muscle Fibers. *J Vis Exp* (100):e52695.
121. Schurmann S*, et al.* (2016) The IsoStretcher: An isotropic cell stretch device to study mechanical biosensor pathways in living cells. *Biosens Bioelectron* 81:363-372.
122. Nakadate H*, et al.* (2017) Strain-Rate Dependency of Axonal Tolerance for Uniaxial Stretching. *Stapp Car Crash J* 61:53-65.
123. Friedrich O*, et al.* (2019) Stretch in Focus: 2D Inplane Cell Stretch Systems for Studies of Cardiac Mechano-Signaling. *Front Bioeng Biotechnol* 7:55.
124. Darnell M & Mooney DJ (2017) Leveraging advances in biology to design biomaterials. *Nat Mater* 16(12):1178-1185.
125. Brusatin G, Panciera T, Gandin A, Citron A, & Piccolo S (2018) Biomaterials and engineered microenvironments to control YAP/TAZ-dependent cell behaviour. *Nat Mater* 17(12):1063-1075.
126. Mitragotri S & Lahann J (2009) Physical approaches to biomaterial design. *Nat Mater* 8(1):15-23.
127. Yang W*, et al.* (2016) Surface topography of hydroxyapatite promotes osteogenic differentiation of human bone marrow mesenchymal stem cells. *Mater Sci Eng C Mater Biol Appl* 60:45-53.
128. Shiu JY, Aires L, Lin Z, & Vogel V (2018) Nanopillar force measurements reveal actin-cap-mediated YAP mechanotransduction. *Nat Cell Biol* 20(3):262-271.
129. Zou J*, et al.* (2019) Microscale roughness regulates laminin-5 secretion of bone marrow mesenchymal stem cells. *Clin Hemorheol Microcirc* 73(1):237-247.
130. Cosgrove BD*, et al.* (2016) N-cadherin adhesive interactions modulate matrix mechanosensing and fate commitment of mesenchymal stem cells. *Nat Mater* 15(12):1297-1306.
131. Kharkar PM, Kloxin AM, & Kiick KL (2014) Dually degradable click hydrogels for controlled degradation and protein release. *J Mater Chem B* 2(34):5511-5521.
132. Foster AA*, et al.* (2018) Protein-engineered hydrogels enhance the survival of induced pluripotent stem cell-derived endothelial cells for treatment of peripheral arterial disease. *Biomater Sci* 6(3):614-622.
133. Hall MS*, et al.* (2016) Fibrous nonlinear elasticity enables positive mechanical feedback between cells and ECMs. *Proc Natl Acad Sci U S A* 113(49):14043-14048.
134. Chaudhuri O*, et al.* (2016) Hydrogels with tunable stress relaxation regulate stem cell fate and activity. *Nat Mater* 15(3):326-334.
135. Sun X*, et al.* (2020) Elasticity of fiber meshes from multiblock copolymers influences endothelial cell behavior. *Clin Hemorheol Microcirc* 74(4):405-415.

136. Sun X*, et al.* (2019) The effect of stiffness variation of electrospun fiber meshes of multiblock copolymers on the osteogenic differentiation of human mesenchymal stem cells. *Clin Hemorheol Microcirc* 73(1):219-228.
137. Discher DE, Janmey P, & Wang YL (2005) Tissue cells feel and respond to the stiffness of their substrate. *Science* 310(5751):1139-1143.
138. Deng Z*, et al.* (2020) Polymeric sheet actuators with programmable bioinstructivity. *Proc Natl Acad Sci U S A* 117(4):1895-1901.
139. Caliari SR*, et al.* (2016) Stiffening hydrogels for investigating the dynamics of hepatic stellate cell mechanotransduction during myofibroblast activation. *Sci Rep* 6:21387.
140. Totaro A*, et al.* (2017) YAP/TAZ link cell mechanics to Notch signalling to control epidermal stem cell fate. *Nat Commun* 8:15206.
141. Zhong W, Zhang W, Wang S, & Qin J (2013) Regulation of fibrochondrogenesis of mesenchymal stem cells in an integrated microfluidic platform embedded with biomimetic nanofibrous scaffolds. *PLoS One* 8(4):e61283.
142. Li L*, et al.* (2019) Nanotopography on titanium promotes osteogenesis via autophagy-mediated signaling between YAP and beta-catenin. *Acta Biomater* 96:674-685.
143. Tang J*, et al.* (2019) Outer-inner dual reinforced micro/nano hierarchical scaffolds for promoting osteogenesis. *Nanoscale* 11(34):15794-15803.
144. Elosegui-Artola A*, et al.* (2017) Force Triggers YAP Nuclear Entry by Regulating Transport across Nuclear Pores. *Cell* 171(6):1397-1410 e1314.
145. Cui Y*, et al.* (2015) Cyclic stretching of soft substrates induces spreading and growth. *Nat Commun* 6:6333.
146. Benham-Pyle BW, Pruitt BL, & Nelson WJ (2015) Cell adhesion. Mechanical strain induces E-cadherin-dependent Yap1 and beta-catenin activation to drive cell cycle entry. *Science* 348(6238):1024-1027.
147. Totaro A, Panciera T, & Piccolo S (2018) YAP/TAZ upstream signals and downstream responses. *Nat Cell Biol* 20(8):888-899.
148. Zhang B*, et al.* (2015) Cyclic mechanical stretching promotes migration but inhibits invasion of rat bone marrow stromal cells. *Stem Cell Res* 14(2):155-164.
149. Liang X, Huang X, Zhou Y, Jin R, & Li Q (2016) Mechanical Stretching Promotes Skin Tissue Regeneration via Enhancing Mesenchymal Stem Cell Homing and Transdifferentiation. *Stem Cells Transl Med* 5(7):960-969.
150. Yuan L, Sakamoto N, Song G, & Sato M (2012) Migration of human mesenchymal stem cells under low shear stress mediated by mitogen-activated protein kinase signaling. *Stem Cells Dev* 21(13):2520-2530.
151. Raab M & Discher DE (2017) Matrix rigidity regulates microtubule network polarization in migration. *Cytoskeleton (Hoboken)* 74(3):114-124.
152. Vincent LG, Choi YS, Alonso-Latorre B, del Alamo JC, & Engler AJ (2013) Mesenchymal stem cell durotaxis depends on substrate stiffness gradient strength. *Biotechnol J* 8(4):472-484.
153. Raab M*, et al.* (2012) Crawling from soft to stiff matrix polarizes the cytoskeleton and phosphoregulates myosin-II heavy chain. *J Cell Biol* 199(4):669-683.
154. Skardal A, Mack D, Atala A, & Soker S (2013) Substrate elasticity controls cell proliferation, surface marker expression and motile phenotype in amniotic fluid-derived stem cells. *J Mech Behav Biomed Mater* 17:307-316.
155. Cote JA, Ostinelli G, Gauthier MF, Lacasse A, & Tchernof A (2019) Focus on dedifferentiated adipocytes: characteristics, mechanisms, and possible applications. *Cell Tissue Res* 378(3):385-398.

156. Lessard J*, et al.* (2015) Generation of human adipose stem cells through dedifferentiation of mature adipocytes in ceiling cultures. *J Vis Exp* (97):52485.
157. Wei S*, et al.* (2013) Bovine dedifferentiated adipose tissue (DFAT) cells: DFAT cell isolation. *Adipocyte* 2(3):148-159.
158. Huber B & Kluger PJ (2015) Decelerating Mature Adipocyte Dedifferentiation by Media Composition. *Tissue Eng Part C Methods* 21(12):1237-1245.
159. Zoico E*, et al.* (2016) Adipocytes WNT5a mediated dedifferentiation: a possible target in pancreatic cancer microenvironment. *Oncotarget* 7(15):20223-20235.
160. Gustafson B & Smith U (2010) Activation of canonical wingless-type MMTV integration site family (Wnt) signaling in mature adipocytes increases beta-catenin levels and leads to cell dedifferentiation and insulin resistance. *J Biol Chem* 285(18):14031-14041.
161. Bi P*, et al.* (2016) Notch activation drives adipocyte dedifferentiation and tumorigenic transformation in mice. *J Exp Med* 213(10):2019-2037.

9. Curriculum Vitae

For reasons of data protection, the curriculum vitae is not published in the electronic version.

Publications:

1. **Deng, Z.**, Wang, W., Xu, X., Ma, N., & Lendlein, A. Polydopamine Based Biofunctional Substrate Coating Promotes Mesenchymal Stem Cell Migration. *MRS Advances* 2021.

2. **Deng, Z**.; Wang, W.; Xu, X.; Nie, Y.; Liu, Y.; Gould, O. E. C.; Ma, N.; Lendlein, A., Biofunction of Polydopamine Coating in Stem Cell Culture. *ACS Appl Mater Interfaces* 2021, 13 (9), 10748-10759.

3. **Deng, Z.**; Wang, W.; Xu, X.; Gould, O. E. C.; Kratz, K.; Ma, N.; Lendlein, A., Polymeric sheet actuators with programmable bioinstructivity. *Proc Natl Acad Sci U S A* 2020, 117 (4), 1895-1901.

4. **Deng, Z.**, Wang, W., Xu, X., Ma, N., & Lendlein, A. Modulation of Mesenchymal Stem Cell Migration using Programmable Polymer Sheet Actuators. *MRS Advances* 2020; 5(46-47), 2381-2390.

5. **Deng, Z.**; Zou, J.; Wang, W.; Nie, Y.; Tung, W. T.; Ma, N.; Lendlein, A., Dedifferentiation of mature adipocytes with periodic exposure to cold. *Clin Hemorheol Microcirc* 2019, 71 (4), 415-424.

6. Nie, Y.; **Deng, Z**.; Wang, W.; Bhuvanesh, T.; Ma, N.; Lendlein, A. Polydopamine-Mediated Surface Modification Promotes the Adhesion and Proliferation of Human Induced Pluripotent Stem Cells. *MRS Advances* 2020, 5 (12-13), 591–599.

7. Zou, J.; Wang, W.; Neffe, A. T.; Xu, X.; Li, Z.; **Deng, Z.**; Sun, X.; Ma, N.; Lendlein, A., Adipogenic differentiation of human adipose derived mesenchymal stem cells in 3D architectured gelatin based hydrogels (ArcGel). *Clin Hemorheol Microcirc* 2017, 67 (3-4), 297-307.

8. Wang, W.; Naolou, T.; Ma, N.; **Deng, Z.**; Xu, X.; Mansfeld, U.; Wischke, C.; Gossen, M.; Neffe, A. T.; Lendlein, A., Polydepsipeptide Block-Stabilized Polyplexes for Efficient Transfection of Primary Human Cells. *Biomacromolecules* 2017, 18 (11), 3819-3833.

9. Wang, W.; **Deng, Z.**; Xu, X.; Li, Z.; Jung, F.; Ma, N.; Lendlein, A., Functional Nanoparticles and their Interactions with Mesenchymal Stem Cells. *Curr Pharm Des* 2017, 23 (26), 3814-3832.

10. Li, Z.; Xu, X.; Wang, W.; Kratz, K.; Sun, X.; Zou, J.; **Deng, Z.**; Jung, F.; Gossen, M.; Ma, N.; Lendlein, A., Modulation of the mesenchymal stem cell migration capacity via preconditioning with topographic microstructure. *Clin Hemorheol Microcirc* 2017, 67 (3-4), 267-278.

11. Wang, W.; Balk, M.; **Deng, Z.**; Wischke, C.; Gossen, M.; Behl, M.; Ma, N.; Lendlein, A., Engineering biodegradable micelles of polyethylenimine-based amphiphilic block copolymers for efficient DNA and siRNA delivery. *J Control Release* 2016, 242, 71-79.

12. Li, Z.; Wang, W.; Kratz, K.; Kuchler, J.; Xu, X.; Zou, J.; **Deng, Z.**; Sun, X.; Gossen, M.; Ma, N.; Lendlein, A., Influence of surface roughness on neural differentiation of

human induced pluripotent stem cells. *Clin Hemorheol Microcirc* 2016, 64 (3), 355-366.

Contribution of conferences:

1. Conference Poster: Modulation of Mesenchymal Stem Cell Migration using Programmable Polymer Sheet Actuators. 2020. Virtual MRS Spring/Fall Meeting. Virtual. 27.11.2020 - 04.12.2020.
2. Conference Poster: Inhibition of cellular senescence by polydopamine coating to maintain mesenchymal stem cells. 2019. Advanced Functional Polymers for Medicine (AFPM). Espoo, Finland. 05.06.2019 - 07.06.2019.
3. Conference Presentation: Dedifferentiation of mature adipocytes with periodic exposure to cold. 2018. 37th Conference of the German Society for Clinical Microcirculation and Hemorheology, DGKMH 2018. Neubrandenburg, Germany. 08.06.2018-09.06.2018.

Appendix I

Polymeric Sheet Actuators with Programmable Bioinstructivity

Zijun Deng[1,2#], Weiwei Wang[1#], Xun Xu[1#], Oliver Gould[1], Karl Kratz[1], Nan Ma[1,2*], Andreas Lendlein[1,2,3*]

1 Institute of Biomaterial Science and Berlin-Brandenburg Centre for Regenerative Therapies, Helmholtz-Zentrum Geesthacht, Teltow, Germany

2 Institute of Chemistry and Biochemistry, Free University of Berlin, Berlin, Germany

3 Helmholtz Virtual Institute − Multifunctional Materials in Medicine, Berlin and Teltow, Germany

# These authors contributed equally to this work.

Email: nan.ma@hzg.de , andreas.lendlein@hzg.de

Reprinted from Proc Natl Acad Sci U S A, 117. Zijun Deng, Weiwei Wang, Xun Xu, Oliver E C Gould, Karl Kratz, Nan Ma, Andreas Lendlein. Polymeric sheet actuators with programmable bioinstructivity, 415-424. Copyright (2019), with permission from the National Academy of Sciences.

The publication is available through https://doi.org/10.1073/pnas.1910668117

Key words

shape-memory polymer actuator, mesenchymal stem cells, calcium influx, HDAC1, RUNX2

Classification

Physical Sciences - Engineering; Biological Sciences Biophysics and Computational Biology

Author Contributions

Z. Deng, W. Wang, and X.Xu designed research, performed research, contributed new reagents/analytic tools, analyzed data and wrote the paper,

O. Gould analyzed data and wrote the paper,

K. Kratz designed research and analyzed data

N. Ma and A. Lendlein designed research, analyzed data and wrote the paper.

Abstract

Stem cells are capable of sensing and processing environmental inputs, converting this information to output a specific cell lineage through signaling cascades. Despite the combinatorial nature of mechanical, thermal and biochemical signals, these stimuli have typically been decoupled and applied independently, requiring continuous regulation by controlling units. We employ a programmable polymer actuator sheet to autonomously synchronize thermal and mechanical signals applied to mesenchymal stem cells (MSCs). Using a grid on its underside, the shape change of polymer sheet, as well as cell morphology, calcium (Ca^{2+}) influx and focal adhesion assembly, could be visualized and quantified. This paper gives compelling evidence that the temperature sensing and mechanosensing of MSCs are interconnected via intracellular Ca^{2+}. Upregulated Ca^{2+} levels lead to a remarkable alteration of histone H3K9 acetylation and activation of osteogenic related genes. The interplay of physical, thermal and biochemical signaling was utilized to accelerate the cell differentiation towards osteogenic lineage. The approach of programmable bioinstructivity provides a fundamental principle for functional biomaterials exhibiting multifaceted stimuli on differentiation programs. Technological impact is expected in the tissue engineering of periosteum for treating bone defects.

Significance Statement

Stem cells can be conceptualized as computational processors capable of sensing, processing and converting environmental information (input) to yield a specific differentiation pathway (output). In this study, we employ a temperature-controlled polymer sheet actuator to interpret and transfer information, controlled by the material's programming, to mesenchymal stem cells. The cell's interpretation of mechanical, thermal and biochemical signaling is shown to be dependent on the actuator's activity, utilized to accelerate differentiation towards bone cells, further elucidating the role of microenvironmental parameters on mammalian cells. Our method provides a unique approach to processing two discrete stimuli into one biochemical signal, calcium ions, providing a basis for the logical control of the flow of biological signals and the design of new cellular functions.

Introduction

In bioinformatics, the mass collection and mass distribution of biological information has enabled the unparalleled collaborative examination of complex cellular systems, detecting previously hidden patterns in the behavior of a variety of organisms. Current cell signaling methods, however, rely on bulky controlling devices that regulate the transmission of decoupled thermomechanical information, limiting our control of the cellular microenvironment, but because of their expense, also the standardization of protocols that comes with widespread adoption by the scientific community (1, 2). Programmable materials are needed that enable the encoding of information into cell culture substrates, allowing multiple physical signals or inputs to be communicated to cells controllably and autonomously. To effectively replicate the complex microenvironment occupied by in vivo mammalian cells, multiple dynamic inputs are necessary that can be separately controlled and simultaneously applied (3). This allows the differentiation pathway of the cell, or the output, to be modified. Additionally, how the cell senses, processes and interconnects complex physical signals from its microenvironment is not well understood. Transmitted physical signals are converted by the cell into biochemically relevant information, allowing the regulation of cell behavior. Despite the synergistic nature of this relationship, the roles of mechanical, thermal, and biochemical signaling have traditionally been decoupled and studied separately. Furthermore, methods that allow the in-situ analysis of the cells' shape change during stimulation are needed.

Mesenchymal stem cells (MSCs), a type of multipotent stem cell, are highly sensitive to physical characteristics of their microenvironment such as temperature, differentiated stiffness stress, topography and extra-cellular matrix (ECM) mechanics (4). A range of physical stimuli is able to influence cell behavior, allowing control over lineage commitment (5). The activity of MSCs can be steered via various mechano-signals, as physical cues are sensed via surface receptors such as integrin, and intracellular components can be activated via a mechanotransduction pathway such as Yes-associated protein (YAP) and transcriptional coactivator with PDZ binding domain (TAZ) signaling (6-9). As one of the most important environmental interventions, temperature change has a profound effect on an animal's physiological response. The reduction of core body temperature extends life span in invertebrates (10), African killifish (11), and even mice (12). Exposure to low temperature can slow

the process of cellular energy metabolism. The lineage commitment of stem cells can be regulated by local temperature. For example, culturing MSCs under hypothermal conditions (32 °C) drives cell differentiation into beige-like adipocytes (13). An increased Schwann-like cell differentiation of MSCs was found when culturing at 35 °C (14). When MSCs were exposed to a cyclic cold stress (18 °C for 12 h/day), they preferentially differentiated into the osteogenic lineage (15). Temperature change can be sensed via thermosensitive ion channels in the cell membrane, such as certain transient receptor potential (TRP) channels, and further influences calcium (Ca^{2+}) influx (16, 17). However, how mechanical and thermal inputs are sensed and processed simultaneously, or the nature of the biochemical signaling responsible for regulating these pathways is poorly understood.

To explore these questions, this study used programmable shape-memory polymer actuator (SMPA) sheets, capable of reversibly and responsively changing between two different pre-defined shapes (actuation) (18-21). SMPAs are unique among shape changing materials in that their actuation can be dictated during an initial thermomechanical programming process. In this initial programming period, information is encoded into the material that governs its reaction to an external stimulus. Within the material, crystallizable actuation domains provide the driving force for shape change, while geometry-determining domains provide the network anisotropy necessary to coordinate the change in macromolecular orientation during crystallization and melting (19, 21). We hypothesize that by programming the SMPA sheet it is possible to logically couple thermal and mechanical stimuli synchronously, and use this active substrate to regulate the behavior of human adipose derived stem cells (hADSCs) (Fig. 1A). A cyclic temperature change (ΔT) results in a bidirectional 2D actuation (Δε) of the programmed SMPA (p-SMPA), transmitting both thermal and mechanical stimuli (ΔT+, Δε+) to the cells (Fig. 1B). For a non-programmed SMPA (np-SMPA), a cyclic temperature change generates only a thermal signal (ΔT+, Δε-). A np-SMPA sheet, periodically deformed by a stretch chamber, is used to produce a mechanical stimulus without a cyclic temperature change (ΔT-, Δε+). Finally, a p-SMPA held at a constant temperature generates neither thermal nor mechanical stimuli (ΔT-, Δε-).

Here, a temperature decrease from 37 °C to 10 °C leads to a simultaneous elongation of the sheet in the direction of deformation during programming, and compression in the perpendicular direction. The unstretched shape can then be recovered by

increasing the temperature to 37 °C again (Fig. 1B). This cyclic actuation of the p-SMPA drives the shape change of the cells cultured on it, immediately leading to cell response. By molding 50 x 50 µm grids on the underside of the sheet, the accurate real-time visualization of the microscale movement of materials and cells is possible, without influencing the cells cultured on the surface of the sheet. We hypothesize that cyclic temperature-induced shape change of the p-SMPA sheet results in the synchronized shape change of cells. These dual stimuli activate Ca^{2+} signaling, leading to the enhancement of Ca^{2+} influx. YAP signaling is activated by mechanical stimulation but suppressed by Ca^{2+} influx. Acetylation at histone H3 lysine 9 (H3K9ac) on osteogenesis-related gene promoters is promoted by dual stimuli, enhancing osteogenesis and suppressing adipogenesis of hADSCs.

Results and Discussion

Synchronization of the Cyclic Shape Change of p-SMPA Sheets and hADSCs.

In this work, semi-crystalline linear poly(ε-caprolactone) (PCL) polymers were used as starting materials for the preparation of the polymer networks forming the actuating sheets. The low and broad melting transition (25 - 50 °C), relatively slow degradation rate, and commercial viability make these materials attractive candidates for many biomedical applications. Its elastic deformation in the temperature range 10 - 37 °C fulfills the requirements of this study (20).The shape switching temperatures were set within the viability range of the cells between 37 °C and 10 °C, with a cycle time of 60 minutes. Although hADSCs showed a detectable cell death when subjected to 10 °C for more than 6 hours (SI Appendix, Fig. S4A), a high cell viability over 7 days (>80%) was sustained under cyclically changed temperature (SI Appendix, Fig. S4 B, C), suggesting the 37 °C temperature (22 min per cycle) allowed for cell recovery. For each cycle, elongation of p-SMPA sheets occurred in the direction of deformation during programming during cooling, with compression occurring in the perpendicular direction, and an overall increase of the material surface area (Fig. 1C, SI Appendix: Fig. S1A and Video S1). The average elongation of the p-SMPA at 10 °C in cell culture medium was measured as 13.6 ± 0.8% after 24 temperature cycles (day 1), while the non-programmed SMPA sheets (np-SMPA) displayed an elongation of less than 1% with no distinguishable difference in both macroscopic shape and grid dimensions (SI Appendix, Fig. S1B and Video S2).

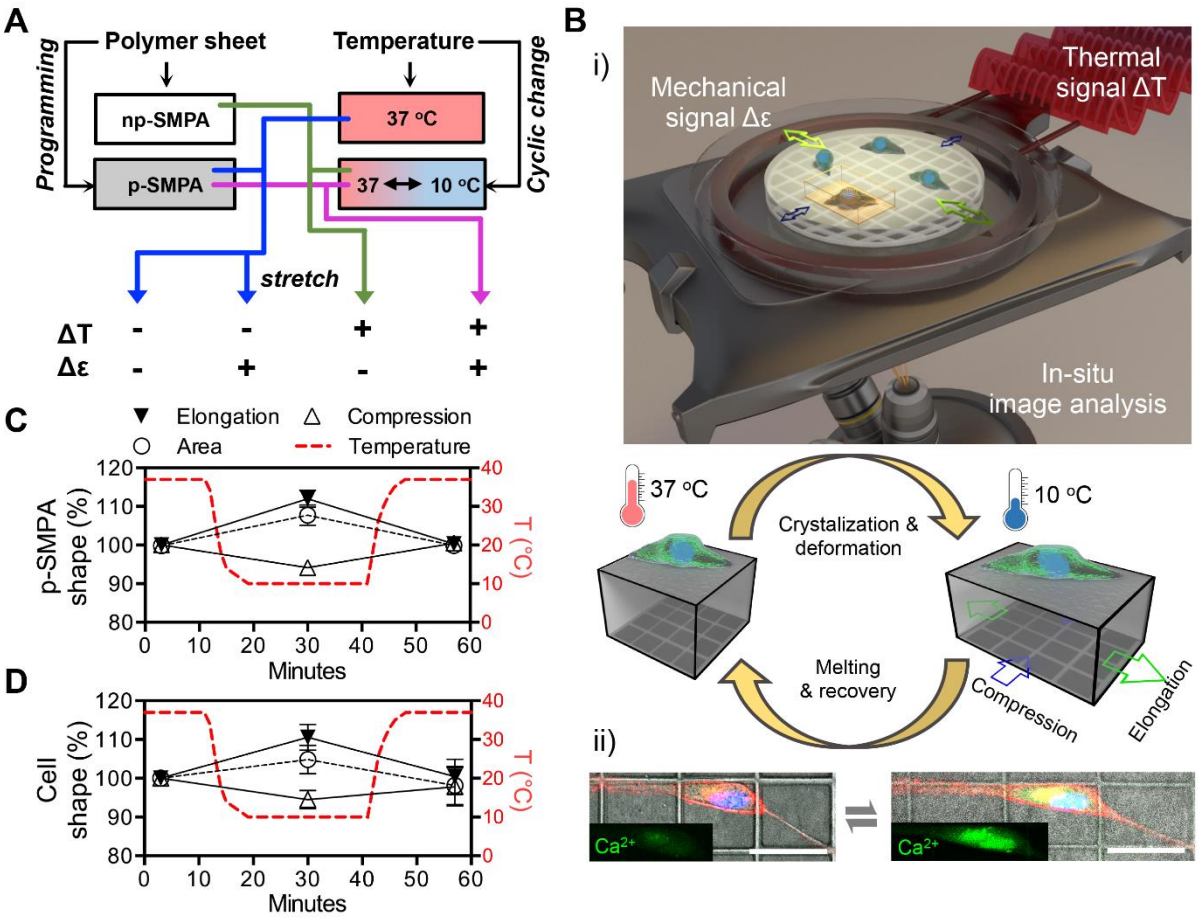

Fig. 1. Temperature-controlled p-SMPA sheet exerts synchronized thermal and mechanical stimuli on hADSCs. (A) To ascertain the role of each input in logical regulation of hADSCs, cells cultured on SMPA sheets were compared to those exposed to either a constant 37 °C and mechanical stimulation, or a constant temperature and no mechanical stimulation. (B) (i) Schematic illustration showing the generation of mechanical and thermal signals. The 50 × 50 μm grids on the underside of the sheet enabled the real-time monitoring of the movement of material and cells. (ii) Representative images of p-SMPA actuationinduced cell shape change and Ca^{2+} influx showing cytoplasmic membrane (red) and nucleus (blue) and intracellular Ca^{2+} (green). (Scale bars, 50 μm.) (C andD) Measurements of the temperature-controlled cyclic shape change of the p-SMPA sheet (C), and hADSCs cultured on top (D), in the direction of elongation and compression, and the change in surface area. The cells were cultured in growth medium on a p-SMPA sheet exposed to cyclic temperature change for 1 d, quantification based on six cells from three randomly selected p-SMPA sheets.

To verify the long-term behavior of the p-SMPA sheets, necessary to facilitate stem cell differentiation, their shape change in cell culture medium was recorded for up to 3 weeks, with more than 500 temperature-change cycles. An elongation >10% was still observed after 3 weeks (SI Appendix, Fig. S1B). The uniformity of the elongation of the grid squares at different locations of the p-SMPA sheet suggested homogeneous actuation during temperature change (SI Appendix, Fig. S1C).To ensure that the shape change of the sheet was sufficiently fast relative to the migratory movement of the cells, a temperature program was used to cool from 37 °C to 10 °C in 8 minutes and heat from 10 °C to 37 °C in 8 minutes. This greatly increased the speed of the shape change of the sheet (SI Appendix, Fig. S1D). By measuring the change in the distance of two points initially separated by 100 μm, the speed of elongation and compression was measured as 3.6 ± 2.6 μm/min (temperature decrease) and (5.6 ± 1.5) μm/min (temperature increase). The movement speed in the compression direction was measured 2.4 ± 2.2 μm/min (temperature decrease) and 2.7 ± 1.5 μm/min (temperature increase) (SI Appendix, Fig. S1E). The migration velocity of hADSCs on SMPA sheets was approximately 0.6 ± 0.3 μm/min, as quantified via time-lapse microscopy using a previously reported method (22). Therefore, the p-SMPA shape change was sufficiently fast to counteract the migration of hADSCs, which have an average dimension around 100 μm in length, allowing them to feel the mechanical stimulus.

We found no evidence that the presence of cells affected the shape change of the pSMPA sheets (SI Appendix, Fig. S1F). This is supported by work elsewhere (23, 24), where the force exerted by cells on a surface has been shown to be more than an order of magnitude less than that of comparable SMPA sheets.

The effect of the actuation on morphology of cells was determined by measuring their change of dimensions during shape change. The cells were stretched and compressed by the shape change of p-SMPA, regardless of their orientation on the surface (SI Appendix, Fig. S1 G, H, Video S3 and S4). The changes in several key spatial cell parameters, such as the area covered and the length in the direction of elongation and compression, were similar to that of the p-SMPA sheet (Fig. 1C, D), suggesting the shape change of the cells was synchronized with the material shape change.

Given that the magnitude of the material shape change is dependent on direction, with a greater shape change in the direction of elongation, cyclic actuation of the sheets

should influence the cell orientation. To verify this, cells were seeded at a lower density to ensure the sufficient freedom of movement. After 3 days (72 cycles of actuation), the cells on the p-SMPA sheet aligned preferentially along the direction of elongation, when compared to those on a np-SMPA sheet (SI Appendix, Fig. S2). Furthermore, the influence of both stimuli on cell proliferation was assessed. The cell proliferation was inhibited by cyclic temperature change but promoted by mechanical stimulus, as evidenced by the staining of cell proliferation marker Ki67 as well as the quantification of cell number (SI Appendix, Fig. S3).

Regulation of the Ca^{2+} Dynamics of hADSCs by Thermal and Mechanical Dual Stimuli.

As a signaling messenger, Ca^{2+} plays a key role in the cellular signaling cascades that regulate the migration, proliferation and differentiation of MSCs (25, 26). Here, the intracellular Ca^{2+} concentration is likely mediated by different Ca^{2+} influx/efflux pathways including entry into the cell membrane, release from intracellular stores such as the endoplasmic reticulum, and being pumped back from cytosol to the extracellular environment or into intracellular stores (27). Given that thermal and mechanical dual stimuli generated shape and orientation change in hADSCs, we investigated their effect on thermo- and mechanosensitive ion channels, and subsequent intracellular Ca^{2+} concentration. A significantly higher percentage of cells (87 ± 4.5% on np-SMPA and 90.9 ± 4.6% on p-SMPA) exposed to cyclic temperature change displayed visible Ca^{2+} influx (Fig. 2A, SI Appendix Video S5 and S6). In contrast, only a small fraction of cells showed visible Ca^{2+} influx when cultured at 37 °C (7.3 ± 2.6% on np-SMPA and 8.1 ± 4.8% on p-SMPA) and at 10 °C (5.9 ± 4% on np-SMPA and 4.9 ± 4.7% on p-SMPA) (Fig. 2A), while the majority of cells displayed no visible Ca^{2+} influx (Fig. 2B, C and SI Appendix, Fig. S6 A, B).

The analysis of the dynamic intracellular Ca^{2+} levels suggested a rapid variation Ca^{2+} concentration with temperature change (Fig. 2D, E, F). Given that the properties of the SMPA, such as polymer crystallization and elasticity, are temperature dependent, these experiments were repeated on glass, with similar results observed (SI Appendix,

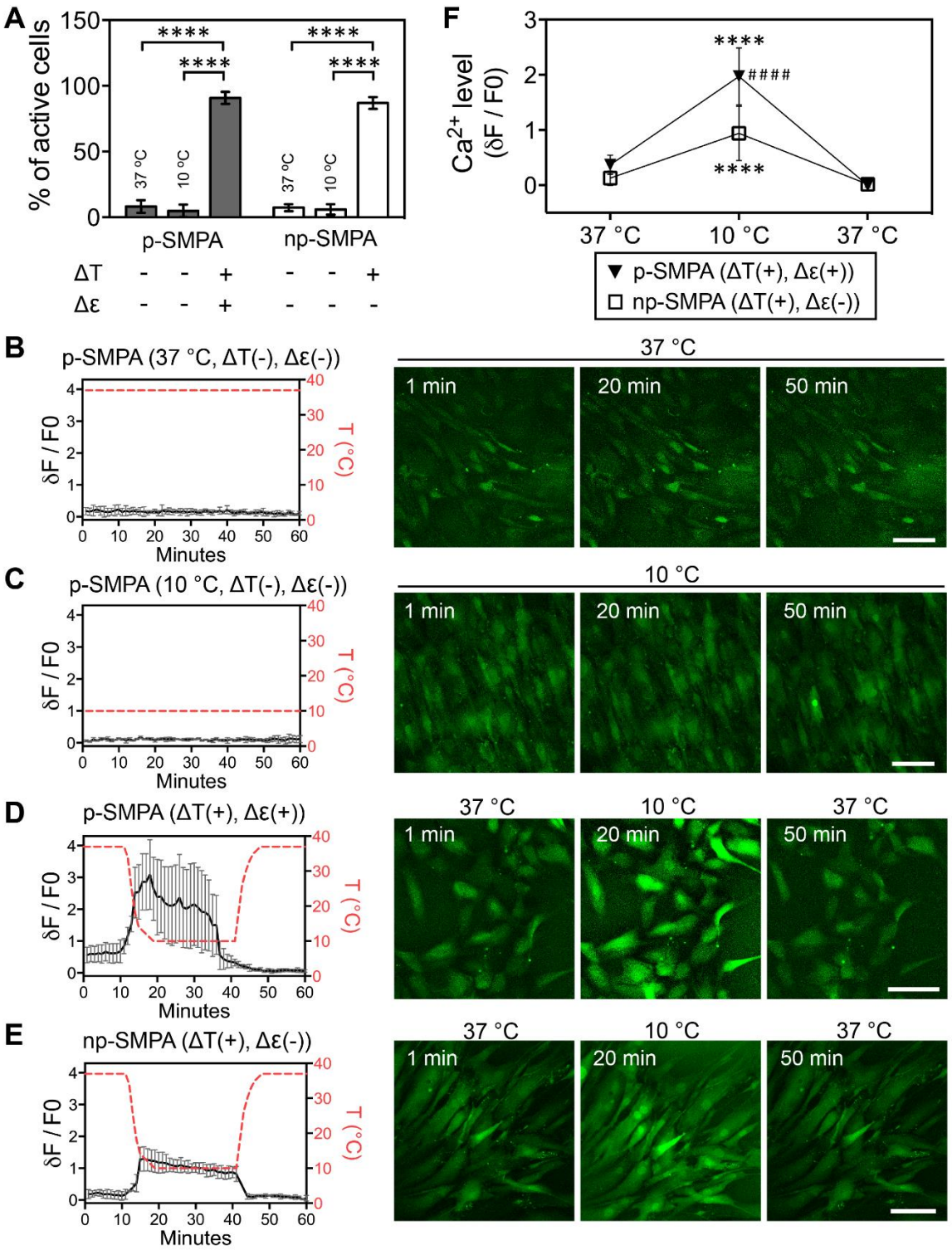

Fig. 2. Ca^{2+} dynamics of hADSCs exposed to thermal and mechanical dual stimuli. (A) Percentage of cells with visible active Ca^{2+} influx in one temperature change cycle on p-SMPA and np-SMPA sheets. The cells were cultured in competitive differentiation medium and the intracellular Ca^{2+} was labeled with Fluo-4 calcium indicator. Quantification was based on ⩾3 randomly selected SMPA sheets with more than 46 cells per group (****P < 0.0001, one-way ANOVA with Tukey's multiple comparisons

test). (B and C) Intracellular Ca^{2+} fluorescence in hADSCs without active Ca^{2+} influx on p-SMPA sheets exposed to a constant temperature of either 37 or 10 ° C ($n \geqslant 3$). (D and E) Intracellular Ca^{2+} fluorescence in hADSCs with active Ca^{2+} influx growing on p-SMPA (n = 7) and np-SMPA (n = 4) exposed to cyclic temperature change. The representative confocal images in B–E showed the fluorescence of intracellular Ca^{2+}. (Scale bar, 100 μm.) (F) Intracellular Ca^{2+} of hADSCs in one temperature-changing cycle on p-SMPA (n = 50) and np-SMPA (n = 26) (****P < 0.0001, compared to corresponding values at 37 °C; ####P < 0.0001, p-SMPA vs. np-SMPA at 10 °C; one-way ANOVA with Tukey's multiple comparisons test).

Fig. S5A and Video S7). The cyclic temperature change between 37 °C and 10 °C induced a greater Ca^{2+} influx and activation than with the temperature range 37 °C and 30 °C (SI Appendix, Fig. S5 B, C, D). This observation verified that certain thermosensitive channels were responsible for the temperature induced Ca^{2+} influx. For example, the thermosensitive TRPM8 channel is activated below 20 °C, facilitating the intracellular entry of Ca^{2+} (16). The inhibition of Ca^{2+} entry and release using 2APB would effectively decrease the temperature-induced elevation of intracellular Ca^{2+} (SI Appendix, Fig. S5 E, F). Despite the actuation's negligible influence on the percentage of cells which experienced Ca^{2+} influx, it contributed to the Ca^{2+} signaling by increasing the intracellular Ca^{2+} level. The cells exposed to dual stimuli presented a higher concentration of intracellular Ca^{2+} than those exposed to thermal stimulus (Fig. 2D, E, F and SI Appendix, Fig. S6C). Compared to the control, a significantly higher intracellular Ca^{2+} level was observed in the group with only mechanical stimulus (SI Appendix, Fig. S6C). This confirmed that the actuation of the sheet might activate some mechanosensitive channels, such as TRPM7 (28) and PIEZO1 (29). Previous work has shown that the proliferation and differentiation of stem cells can be regulated by spontaneous Ca^{2+} oscillations (30, 31). Dynamic intracellular Ca^{2+} imaging showed that the spontaneous Ca^{2+} oscillations could be still observed (SI Appendix, Fig. S5G), indicating the preservation of spontaneous Ca^{2+} oscillations under the dual stimuli.

The Role of Mechanical Stimuli and Intracellular Ca^{2+} on YAP Signaling Activation and Suppression.

When incident on cells, an external mechanical signal can regulate integrin activation, focal adhesion composition and cytoskeleton organization to transduce the mechanical signal intracellularly and activate a series of down-stream pathways. Talin, a vital component of integrin adhesion complex which mediates integrin activation and connects integrin to cytoskeleton (32), was enriched at the lamellipodia of hADSCs upon SMPA actuation (SI Appendix, Fig. S7A). Compared to the cells without stimuli and only thermal stimulus, the cells in the group of dual stimuli expressed increased integrin β1 as well as enhanced fibronectin fibrillogenesis (SI Appendix, Fig. S7 B, C), suggesting an effect of mechanical stimuli on matrix protein assembly and activation of integrin adhesion complexes.

It has been suggested that YAP and TAZ are sensors for mechanical signals and act as an intracellular rheostat, storing past mechanical information and regulating differentiation of stem cells. Particularly, YAP/TAZ play a key role in mediating the translation of incoming mechanical information into the expression of osteogenesis related transcriptional factors (9). The shape change of the p-SMPA sheet significantly enhanced YAP and RUNX2 activity (nuclear localization) (Fig. 3A, B, D and SI Appendix, Fig. S8). Inhibiting of actin polymerization with cytochalasin D (CytoD) to block the mechanotransduction pathway resulted in significantly decreased YAP and RUNX2 activity (SI Appendix, Fig. S9 B, D). However, the nuclear localization of YAP was suppressed by the cyclic temperature change (Fig. 3B). The elevation of cytosolic Ca^{2+} could inhibit YAP/TAZ activity through the Hippo pathway, phosphorylating YAP/TAZ and preventing their nuclear accumulation (33). Therefore, the decreased YAP activity could be attributed to the enhanced intracellular Ca^{2+} concentration during temperature change. Inhibition of Ca^{2+} influx with 2APB suppressed YAP phosphorylation and the expression of total YAP (Fig. 3C), but increased the percentage of nuclear YAP active cells (SI Appendix, Fig. S9 A, C), which confirmed the role of Ca^{2+} in regulating YAP activity. The SMPA sheet's geometric and temperature changes could regulate RUNX2 activity through a signaling network consisting of multiple pathways, as summarized in Fig. 6. Either mechanical stress could activate RUNX2 through the activation of YAP, or an increase of intracellular Ca^{2+} concentration, induced by stretch and temperature change, might exert both a negative and positive regulatory effect on RUNX2 activity. For example, Ca^{2+} could inhibit RUNX2 through deactivation of YAP but activate RUNX2 via Ras/ERK1/2,

MAPK and CaMKII signaling (34-36). Here, the nuclear localization of RUNX2 was influenced by the SPMA sheet deformation but not by temperature change (Fig. 3D).

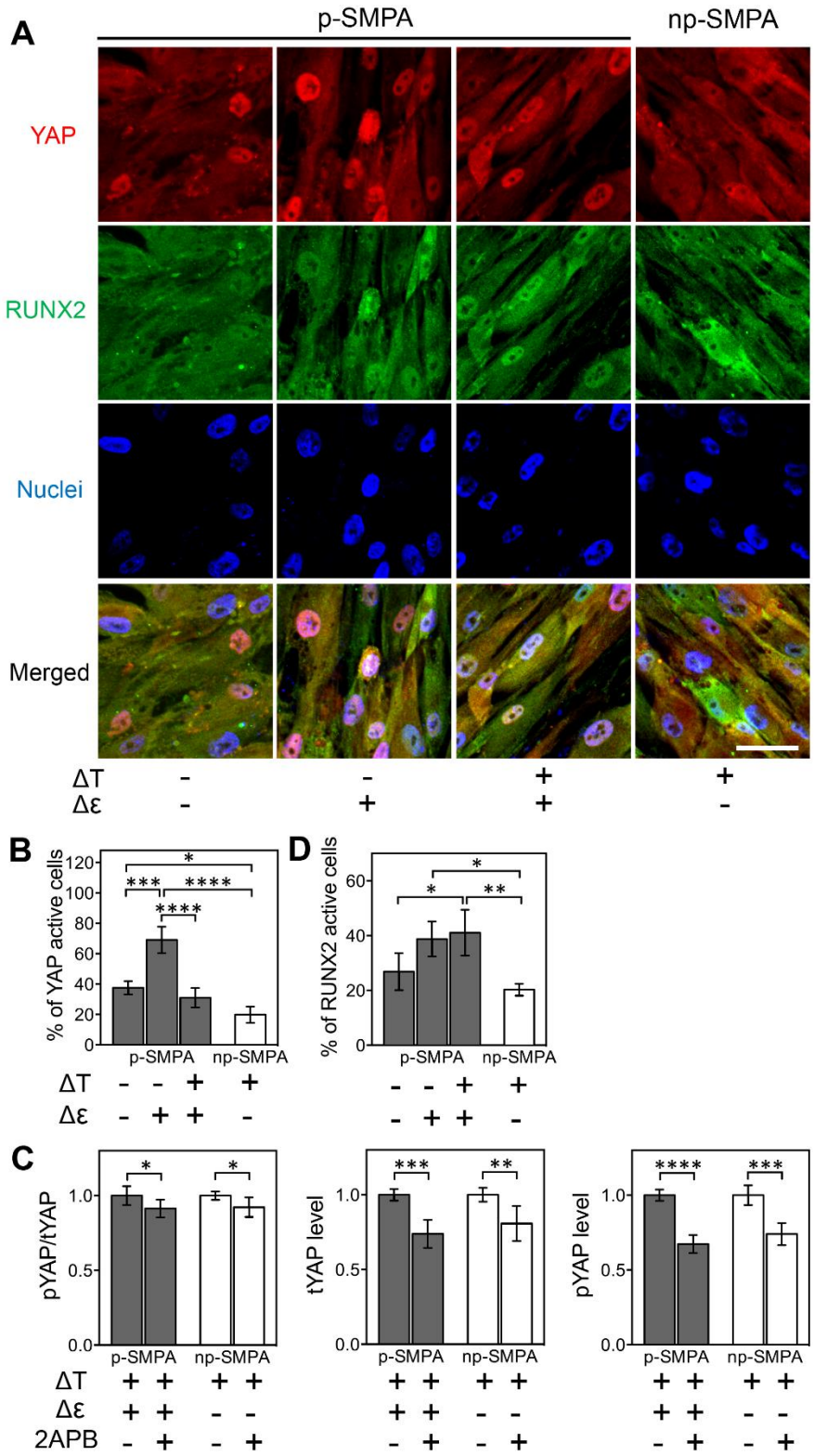

Fig. 3. Regulation of YAP and RUNX2 nuclear translocation by thermal and mechanical stimuli. (A) Representative images of YAP and RUNX2 immunostaining.

(Scale bar, 50 μm.) (B) Percentage of nuclear YAP positive cells (two-way ANOVA, $P < 0.0001$ for effect of ΔT, $P < 0.001$ for effect of Δε, $P < 0.05$ for ΔT × Δε interaction; *$P < 0.05$, ***$P < 0.001$, ****$P < 0.0001$, Tukey's multiple comparisons test). (C) Ratio of phosphorylated YAP (pYAP) to total YAP (tYAP), levels of pYAP and tYAP of hADSCs cultured on SMPA sheets with and without Ca^{2+} inhibition. The enzyme-linked immunosorbent assay was based on lysate of cells on ⩾5 independent SMPA sheets in each group, and the obtained value were normalized to the amount of total protein in the cell lysate (*$P < 0.05$, **$P < 0.01$, ***$P < 0.001$, ****$P < 0.0001$, Student's t test). The value of the group without inhibition was set to 1 as a reference point. (D) Percentage of nuclear RUNX2 positive cells (two-way ANOVA, $P < 0.001$ for effect of Δε, nonsignificant for effect of ΔT and ΔT x Δε interaction; *$P < 0.05$, **$P < 0.01$, Tukey's multiple comparisons test). For B and D, ⩾3 randomly selected images containing more than 200 cells in each group were analyzed. The cells were cultured in competitive differentiation medium for 10 d.

Histone Modification Induced by Thermal and Mechanical Stimuli.

To gain insight into the effect of the dual stimuli at the epigenetic level, histone modification was evaluated after 10 days. The H3K9 acetylation (H3K9ac) at promoters of osteogenesis-related genes, including RUNX2, alkaline phosphatase (ALP) and osteocalcin (OCN), was significantly enhanced in the cells treated with dual stimuli (Fig. 4A). Inhibition of intracellular Ca^{2+} with 2APB significantly decreased the level of H3K9ac at ALP and OCN promoters. Treatment with CytoD, which inhibits actin, decreased the H3K9ac at OCN promoter but not at RUNX2 and ALP promoters (Fig. 4B). The effect of thermal or mechanical stimulus on histone modification was also observed in H3K27 trimethylation (H3K27me3). Treatment with 2APB increased the H3K27me3 at the promoters of RUNX2 and ALP, and inhibition of actin led to the elevation of H3K27me3 at ALP promoter. However, neither 2APB nor CytoD treatment showed effect on H3K27me3 at OCN promoter (SI Appendix, Fig. S10). These results suggested that both Ca^{2+} and mechanical signals could modulate histone modification, with different role for different types of histone modification.

The histone deacetylase 1 (HDAC1) is an important regulator of histone acetylation. Phosphorylation of HDAC1 at Ser421 increases its de-acetylation activity. Previous studies have demonstrated the response of HDAC1 expression, nuclear localization

and phosphorylation to external mechanical cues and Ca^{2+} signaling. For example, HDAC1 expression was down-regulated by cyclic stretch (37). Mechanical stimuli of interstitial flow stimulated HDAC1 phosphorylation and increased the localization of phosphorylated HDAC1 (p-HDAC1) to the cytoplasm (38). Intracellular Ca^{2+} inhibited nuclear localization and phosphorylation of HDAC1 (39, 40). Here, the subcellular localization of p-HDAC1 was investigated by analyzing the fluorescence intensity of immunostained p-HDAC1 in cytosol and nuclei (Fig. 4C, D). Both thermal and mechanical changes stimulated the nuclear export of p-HDAC1 and when synchronized generated the highest level of cytosolic localization of p-HDAC1. Inhibition of Ca^{2+} eliminated the increased nuclear export of p-HDAC1, suggesting that Ca^{2+} plays a key role in regulating the subcellular distribution of p-HDAC1. Therefore, the potential mechanism for enhanced H3K9ac at the promotors of osteogenic genes can be attributed to the regulation of dual stimuli on histone deacetylase.

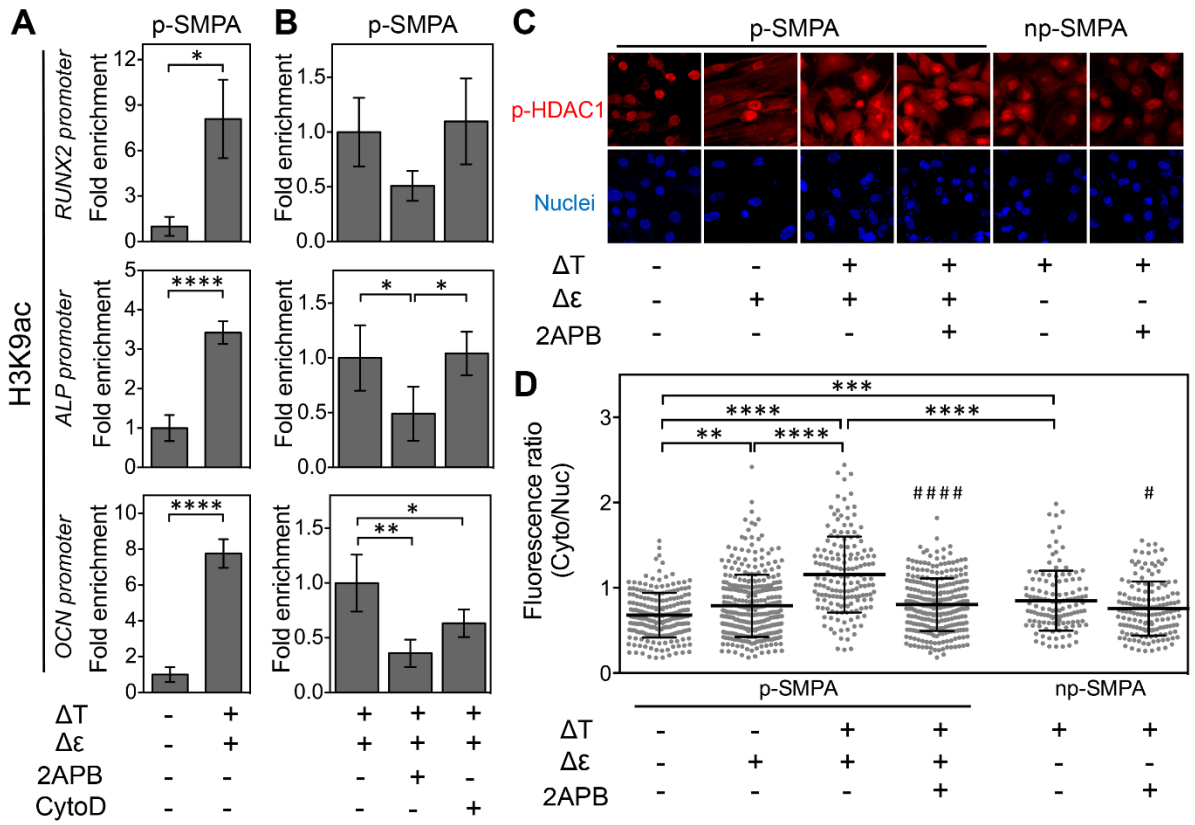

Fig. 4. Epigenetic alternation of hADSCs exposed to thermal and mechanical stimuli. (A) H3K9 acetylation level at the promoters of RUNX2, ALP, and OCN genes on p-SMPA sheet without and with cyclic temperature change. The values of the group without temperature change were set as 1 (n ⩾ 4; *$P < 0.05$, ****$P < 0.0001$, Student's

t test). (B) Regulation of Ca^{2+} signaling and mechanotransduction on H3K9 acetylation in hADSCs perceiving dual stimuli. Cells were treated with Ca^{2+} inhibitor (2APB) and actin inhibitor (CytoD). The values of the group without inhibition were set as 1 (n = 4; *P < 0.05, **P < 0.01, one-way ANOVA with Tukey's multiple comparisons test). (C) Staining of p-HDAC1 (red) and nuclei (blue) of hADSCs cultured in different conditions. (Scale bar, 20 μm.) (D) Ratio of fluorescence intensity of the cytoplasm and nuclear p-HDAC1 on SMPA sheets. This quantification was based on the images of more than 126 cells from 3 randomly selected SMPA sheets in each group [two-way ANOVA, P < 0.0001 for effects of ΔT and Δε, P < 0.001 for ΔT × Δε interaction in the absence of 2APB; **P < 0.01, ***P < 0.001, ****P < 0.0001, Tukey's multiple comparisons test; #P < 0.05, ####P < 0.0001, 2APB(+) vs. 2APB(−) with the same stimuli, Student's t test]. The cells were examined after being cultured in competitive differentiation medium for 10 d.

Promotion of Osteogenesis and Suppression of Adipogenesis of hADSCs by Thermal and Mechanical Stimuli.

To investigate the effect of dual stimuli on hADSCs' fate decision, differentiation markers were quantified at mRNA and protein levels (Fig. 5). Both temperature change and p-SMPA actuation promoted the osteogenesis of hADSCs. Although no dramatic influence on OCN was observed, temperature change significantly increased ALP mRNA and protein activity (Fig. 5A, B, C). The actuation of p-SMPA sheet enhanced the gene expression of ALP and OCN, as well as the protein level of OCN and ALP activity (Fig. 5A-D), and increased the cellular mineralization of differentiated hADSCs (SI Appendix, Fig. S11A). The OCN level under dual stimuli was significantly higher than that under mechanical stretch only (SI Appendix, Fig. S11 B, C), suggesting a cumulative effect of temperature change and p-SMPA actuation on osteogenesis. The adipogenesis of hADSCs was shown to be inhibited by temperature change and p-SMPA actuation. The adipogenesis marker FABP4 was down-regulated in samples exposed to cyclic temperature change and was further decreased in the presence of both stimuli (Fig. 5A, E). The amount and size of lipid droplets identified via ORO staining significantly decreased in cells exposed to cyclic temperature change compared to those held at 37 °C (SI Appendix, Fig. S11 D, E).

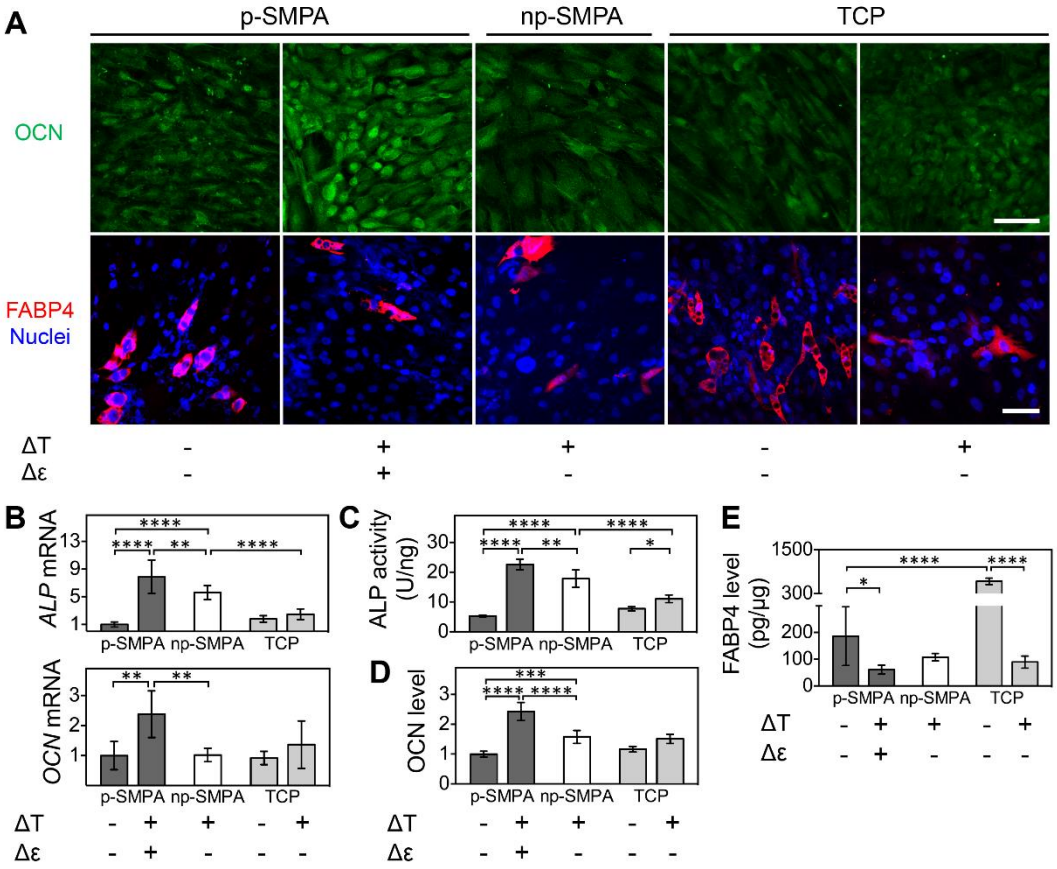

Fig. 5. The effect of thermal and mechanical dual stimuli on hADSC differentiation. (A) OCN (green) and FABP4 (red) immunostaining on SMPA sheets and TCP under different conditions. (Scale bar, 100 μm.) (B) Expression levels of ALP and OCN mRNA (n ⩾ 5). The values of the group on SMPA without thermal and mechanical stimuli were set as 1. (C) ALP activity of hADSCs cultured under different conditions (n ⩾ 3). (D) OCN fluorescence intensity normalized to cell number. The analysis was based on five randomly selected images in each group. (E) The enzyme-linked immunosorbent assay of FABP4 of hADSCs (n ⩾ 4). To induce cell differentiation, the competitive differentiation medium was applied for 3 wk. (*P < 0.05, **P < 0.01, ***P < 0.001, ****P < 0.0001, one-way ANOVA with Tukey's multiple comparisons test.)

In summary, a thermally controlled SMPA sheet was employed to control the differentiation process of MSCs. In this work, we demonstrate that multiple physical stimuli (physical force, temperature etc.) provided by a programmed polymeric actuator sheet could be used as basic inputs to guide the construction of the internal signal processing architecture of living cells (Fig. 6). The results of our study suggest that the thermo- and mechanosensing networks of stem cells are interconnected via

a universal intracellular component. The actuation of a sheet during cyclic temperature change imparts a mechanical and cold stress on hADSCs, which are logically connected to their discrete networks by Ca^{2+}. Ca^{2+} dynamics regulate the intercellular connection of mechano- and thermosensing components, serving as a cellular basis for the osteogenic differentiation of MSCs. Polymer actuation activates the mechanosensor YAP, and subsequently promotes RUNX2 nuclear localization. Meanwhile, the cyclic temperature change and interlinked polymer sheet actuation decreased nuclear localization of phosphorylated HDAC1 via Ca^{2+} signaling, and maintained a high level of histone H3K9 acetylation on osteogenesis-related gene promoters. Thermal and mechanical dual effects work cooperatively to promote osteogenic differentiation of hADSCs. This dual stimuli system could serve as a culture device to modulate stem cell function, demonstrating the cooperative use of multiple external signals to achieve biological outputs. The p-SMPA sheet shows great potential to meet the clinical requirements for the tissue engineering of periosteum to treat bone defects. MSCs could be cultured in vitro where both thermal and mechanical stimuli are used to induce a high level of osteogenesis. After transplantation, the shape-memory effect of a p-SMPA sheet could allow self-tightening when exposed to the relatively higher temperature of the body, facilitating the attachment of the cell-laden sheet onto bone and accelerating its restoration process. In the future, detailed knowledge of signaling mechanisms with both spatial and temporal resolution is required. It is important to use a systemic approach, logically dissect the thermal and mechanical stimuli, and establish a precise and faithful model system, which enables a more effective combination of different stimuli.

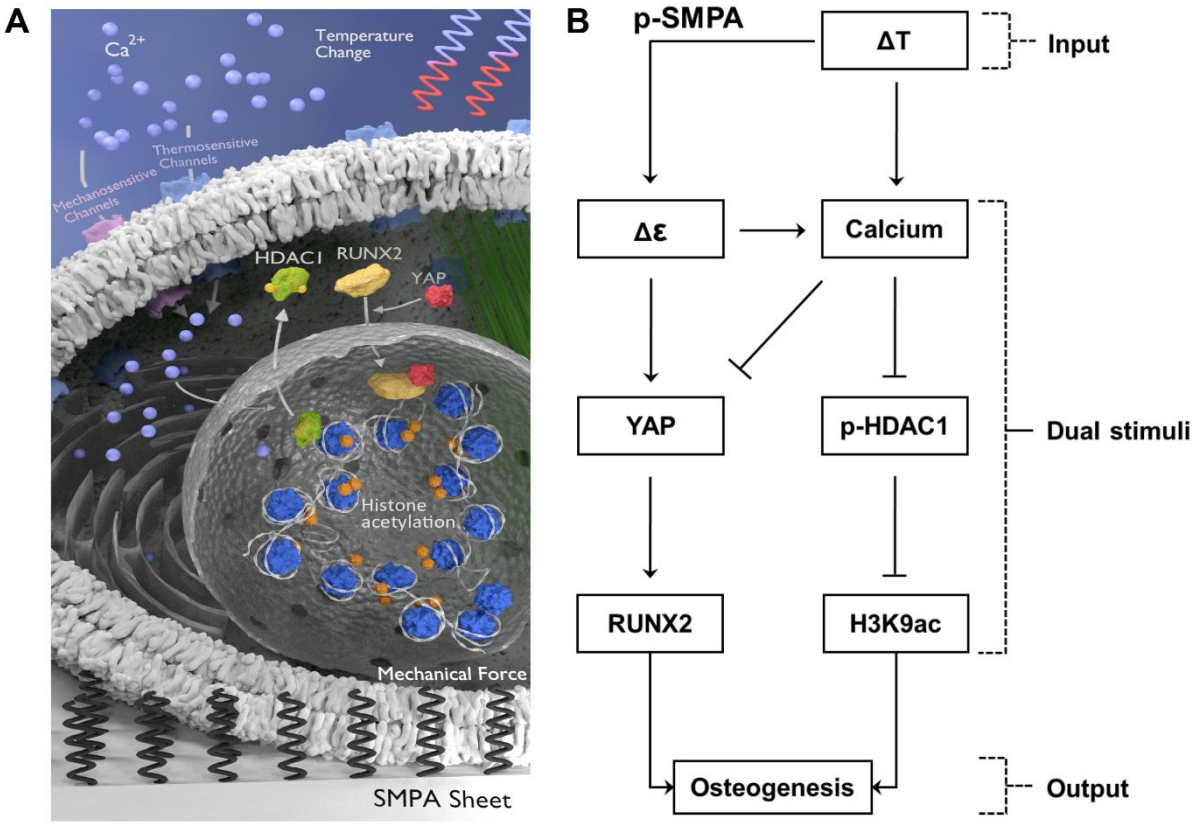

Fig. 6. The influence of thermal and mechanical dual stimuli on hADSCs. (A) A schematic illustration showing the effect of temperature change and the actuation of the p-SMPA on Ca^{2+} signaling via thermo- and mechanosensitive channels as well as on YAP activity via mechanotransduction. Ca^{2+} signaling enhanced H3K9 acetylation while YAP activated RUNX2, both of which promoted osteogenesis of hADSCs. (B) Flowchart illustrating the function of p-SMPA as a signal processer to convert an input (temperature change) into dual stimuli, subsequently regulating the differentiation of hADSCs as an output.

Materials and Methods

Detailed descriptions appear in the SI appendix.

Generation of Thermal and Mechanical Stimuli and Cyclic Temperature Change. The cyclic temperature change between 37 °C and 10 °C was realized by computer-controlled thermochambers (Instec, Colordao, USA). Thermal and mechanical dual stimuli were generated by subjecting p-SMPA to temperature cycles. In the case of non-programmed SMPA sheet only a thermal stimulus is provided, and a mechanical stretching device was used to generate mechanical stimulation.

In-Situ Measurement of Temperature, SMPA Sheet Shape and Cell Morphology. Temperature and cell morphology were measured using a digital thermometer and laser scanning microscopy respectively, where the 50 X 50 µm grid printed on the SMPA sheet was used to provide information about the actuation of the cell substrate during characterization.

Acknowledgements

Nicole Schneider for the synthesis of PCL-DIEMA, Daniela Radzik and Patrick Budach for preparation of SMPA sheets, Dr. Tian Liu for providing advice on statistical analysis. This work was financially supported by the Helmholtz Association of German Research Centers (through program-oriented funding, Helmholtz Cross Program Initiative "Technology and Medicine Adaptive Systems", Helmholtz Virtual Institute, Multifunctional Biomaterials for Medicine (grant no. VH-VI-423), and the Federal Ministry of Education and Research, Germany, through the Program Health Research (grant no. 13GW0098, and project number 0315696A "Poly4BioBB").

Conflict of interest

A.L and K.K are co-inventors on patents / patent applications in the area of shape-memory polymer actuators.

Data availability

The raw data for figures 1-5 are available at DOI: 10.6084/m9.figshare.c.4682696.

References

1. Pedrigi RM, et al. (2017) Disturbed Cyclical Stretch of Endothelial Cells Promotes Nuclear Expression of the Pro-Atherogenic Transcription Factor NF-kappaB. Ann Biomed Eng 45(4):898-909.
2. Rapalo G, et al. (2015) Live Cell Imaging during Mechanical Stretch. J Vis Exp (102):e52737.
3. Purvis JE & Lahav G (2013) Encoding and decoding cellular information through signaling dynamics. Cell 152(5):945-956.
4. Higuera GA, van Boxtel A, van Blitterswijk CA, & Moroni L (2012) The physics of tissue formation with mesenchymal stem cells. Trends Biotechnol 30(11):583-590.

5. Huang C, Dai J, & Zhang XA (2015) Environmental physical cues determine the lineage specification of mesenchymal stem cells. Biochim Biophys Acta 1850(6):1261-1266.
6. Lee DA, Knight MM, Campbell JJ, & Bader DL (2011) Stem cell mechanobiology. J Cell Biochem 112(1):1-9.
7. Wozniak MA & Chen CS (2009) Mechanotransduction in development: a growing role for contractility. Nat Rev Mol Cell Biol 10(1):34-43.
8. Heo S-J, et al. (2016) Differentiation alters stem cell nuclear architecture, mechanics, and mechano-sensitivity. eLife 5:e18207.
9. Yang C, Tibbitt MW, Basta L, & Anseth KS (2014) Mechanical memory and dosing influence stem cell fate. Nat Mater 13(6):645-652.
10. Tao C, et al. (2015) Changes in white and brown adipose tissue microRNA expression in cold-induced mice. Biochem Biophys Res Commun 463(3):193-199.
11. Kim Y, Nam HG, & Valenzano DR (2016) The short-lived African turquoise killifish: an emerging experimental model for ageing. Dis Model Mech 9(2):115-129.
12. Conti B, et al. (2006) Transgenic mice with a reduced core body temperature have an increased life span. Science 314(5800):825-828.
13. Velickovic K, et al. (2018) Low temperature exposure induces browning of bone marrow stem cell derived adipocytes in vitro. Sci Rep 8(1):4974.
14. Yoon HH, Han MJ, Park JK, Lee JH, & Seo YK (2015) Effect of Low Temperature on Schwann-Like Cell Differentiation of Bone Marrow Mesenchymal Stem Cells. Tissue Eng Regen Med 12(4):259-267.
15. Nie Y, Yan Z, Yan W, Xia Q, & Zhang Y (2015) Cold exposure stimulates lipid metabolism, induces inflammatory response in the adipose tissue of mice and promotes the osteogenic differentiation of BMMSCs via the p38 MAPK pathway in vitro. Int J Clin Exp Pathol 8(9):10875-10886.
16. Zheng J (2013) Molecular mechanism of TRP channels. Compr Physiol 3(1):221-242.
17. Tansey EA & Johnson CD (2015) Recent advances in thermoregulation. Adv Physiol Educ 39(3):139-148.
18. Behl M, Kratz K, Noechel U, Sauter T, & Lendlein A (2013) Temperature-memory polymer actuators. Proc Natl Acad Sci U S A 110(31):12555-12559.
19. Behl M, Kratz K, Zotzmann J, Nochel U, & Lendlein A (2013) Reversible bidirectional shape-memory polymers. Adv Mater 25(32):4466-4469.

20. Saatchi M, Behl M, Nöchel U, & Lendlein A (2015) Copolymer Networks From Oligo(ε-caprolactone) and n-Butyl Acrylate Enable a Reversible Bidirectional Shape-Memory Effect at Human Body Temperature. Macromol. Rapid Commun. 36(10):880-884.
21. Lendlein A & Gould OEC (2019) Reprogrammable recovery and actuation behaviour of shape-memory polymers. Nat Rev Mater 4(2):116-133.
22. Xu X, et al. (2014) Controlling Major Cellular Processes of Human Mesenchymal Stem Cells using Microwell Structures. Adv Healthc Mater 3(12):1991-2003.
23. Maskarinec SA, Franck C, Tirrell DA, & Ravichandran G (2009) Quantifying cellular traction forces in three dimensions. Proc Natl Acad Sci U S A 106(52):22108-22113.
24. Polacheck WJ & Chen CS (2016) Measuring cell-generated forces: a guide to the available tools. Nat Methods 13(5):415-423.
25. Lee MN, et al. (2018) Elevated extracellular calcium ions promote proliferation and migration of mesenchymal stem cells via increasing osteopontin expression. Exp Mol Med 50:e142.
26. Barradas AMC, et al. (2012) A calcium-induced signaling cascade leading to osteogenic differentiation of human bone marrow-derived mesenchymal stromal cells. Biomaterials 33(11):3205-3215.
27. Titushkin I, Sun S, Shin J, & Cho M (2010) Physicochemical Control of Adult Stem Cell Differentiation: Shedding Light on Potential Molecular Mechanisms. J Biomed Biotechnol 2010:Artn 743476.
28. Xiao E, et al. (2015) Brief Reports: TRPM7 Senses Mechanical Stimulation Inducing Osteogenesis in Human Bone Marrow Mesenchymal Stem Cells. Stem Cells 33(2):615-621.
29. Sugimoto A, et al. (2017) Piezo type mechanosensitive ion channel component 1 functions as a regulator of the cell fate determination of mesenchymal stem cells. Sci Rep 7(1):17696.
30. Resende RR, et al. (2010) Influence of spontaneous calcium events on cell-cycle progression in embryonal carcinoma and adult stem cells. Bba-Mol Cell Res 1803(2):246-260.
31. Sun S, Liu YM, Lipsky S, & Cho M (2007) Physical manipulation of calcium oscillations facilitates osteodifferentiation of human mesenchymal stem cells. Faseb J 21(7):1472-1480.

32. Das M, Ithychanda SS, Qin J, & Plow EF (2014) Mechanisms of talin-dependent integrin signaling and crosstalk. Bba-Biomembranes 1838(2):579-588.
33. Liu ZJ, et al. (2019) Induction of store-operated calcium entry (SOCE) suppresses glioblastoma growth by inhibiting the Hippo pathway transcriptional coactivators YAP/TAZ. Oncogene 38(1):120-139.
34. Zayzafoon M (2006) Calcium/calmodulin signaling controls osteoblast growth and differentiation. J Cell Biochem 97(1):56-70.
35. Li J, et al. (2019) TMCO1-mediated Ca(2+) leak underlies osteoblast functions via CaMKII signaling. Nat Commun 10(1):1589.
36. Kanno T, Takahashi T, Tsujisawa T, Ariyoshi W, & Nishihara T (2007) Mechanical stress-mediated Runx2 activation is dependent on Ras/ERK1/2 MAPK signaling in Osteoblasts. J Cell Biochem 101(5):1266-1277.
37. Wang J, et al. (2016) Mechanical stimulation orchestrates the osteogenic differentiation of human bone marrow stromal cells by regulating HDAC1. Cell Death Dis 7:e2221.
38. Bazou D, et al. (2016) Flow-induced HDAC1 phosphorylation and nuclear export in angiogenic sprouting. Sci Rep 6:34046.
39. Kim JY, et al. (2010) HDAC1 nuclear export induced by pathological conditions is essential for the onset of axonal damage. Nat Neurosci 13(2):180-U163.
40. Zhu YJ, et al. (2017) Subcellular Distribution of HDAC1 in Neurotoxic Conditions Is Dependent on Serine Phosphorylation. J Neurosci 37(31):7547-7559.

Supplementary Information for

Polymeric Sheet Actuators with Programmable Bioinstructivity

Zijun Deng[#], Weiwei Wang[#], Xun Xu[#], Oliver Gould, Karl Kratz, Nan Ma and Andreas Lendlein
# These authors contributed equally to this work.

Nan Ma, Andreas Lendlein
Email: nan.ma@hzg.de, andreas.lendlein@hzg.de

Supplementary text
Figures S1 to S12
Legends for Movies S1 to S7
SI References

Other supplementary materials for this manuscript include the following:
Movies S1 to S7

Supplementary Materials and Methods.

SMPA Preparation. Linear poly(ε-caprolactone) - diisocyanatoethyl dimethacrylate (PCL-DIEMA) was synthesized according to a previously reported free radical polymerization method (1). 2,2'-Azobisisobutyronitrile (AIBN), chloroform, and inhibitor remover were purchased from Sigma Aldrich. AIBN was used after crystallization from ethanol. N-butyl acrylate (Merck) was passed over inhibitor remover before use. Hexane was purchased from Acros and used as received. Diisocyanatoethyl dimethacrylate was synthesized according to a previously reported method (2).
Polymers of Mn of 3,000 g.mol-1 and 8,000 g.mol-1 were mixed in a weight ratio of 1:5 and ground into a homogenous mixture according to (2). 40% wt of this mixture to 60% wt of n-butyl acrylate was heated to 50 °C for 15 minutes before the initiator AIBN (1 wt%) was added whilst stirring carefully to prevent air bubbles forming. After 3 min, stirring was stopped. The obtained mixture was poured into a mold consisting of a glass plate patterned with 50 x 50 µm grids, a flat glass plate and a spacer of 0.5 mm

in thickness, then kept in an oven at 80 °C overnight. The sheet was cut into strips, washed with chloroform twice, then once with a 50:50 mixture of chloroform: hexane, and then dried under vacuum at 70 °C for 7 days. Programming of the polymer sheet was performed by stretching to ε_{prog} of 60% at T_{prog} = 50 °C before cooling to - 20°C under constant strain. Finally, the polymer was punched into circular sheets with a diameter of 10 mm, heated to 40 °C and left for 10 minutes.

Generation of Thermal and Mechanical Stimuli and Cyclic Temperature Change. The cyclic temperature change between 37 °C and 10 °C was realized by computer controlled thermochambers (Instec, Colordao, USA) suitable for a standard 35 mm cell culture dish (smaller chamber) on an inverted microscope or two standard 24-well tissue culture plates (larger chamber). The 35 mm dish and each well of the 24-well plates were filled with 1.5 mL and 0.6 mL liquid (PBS or cell culture medium), which covered the polymer sheet, and supplied with 5 vol% CO_2 for cell maintenance. For each cycle of temperature change, the time was set to 60 minutes, consisting of 8 minutes to cool from 37 °C to 10 °C, 22 minutes at 37 °C, 8 minutes to heat from 10 °C to 37 °C, and 22 minutes at 10 °C.

Thermal and mechanical dual stimuli were generated by subjecting p-SMPA to temperature cycles. In the case of non-programmed SMPA sheet only a thermal stimulus was provided. A stretching device that enables the cyclic stretch deformation of the SMPA sheet at 37 °C was used to produce to expose the cells to the mechanical stimulus. SMPA at constant temperature (37 °C) exhibited neither thermal nor mechanical stimulus.

Mechanical Stimulation at Constant Temperature A stretching device (MCB1, CellScale, Ontario, Canada) was used to generate the cyclic stretch of the SMPA sheet at a constant temperature of 37 °C. The device was put into a cell culture incubator (37 °C, 5 vol% CO2). The programmed SMPA sheets were fixed and stretched along the direction of programming (Fig. S12). In order to have the same shape change behavior as inside the thermal chamber, the time was set to 60 minutes for each stretching cycle, consisting of 8 minutes of stretching, 22 minutes to hold, 8 minutes to release, 22 minutes to hold. The SMPA sheet was stretched to 10% elongation in each cycle to match the cyclic temperature change experiments.

hADSC Culture and Differentiation The hADSCs were isolated from human adipose tissue after informed consent (No.: EA2/127/07; Ethics Committee of the Charité – Universitätsmedizin Berlin, approval from 17.10.2008), as described in a previous study (3). The cells were held at a constant temperature of 37 °C in an incubator supplied with 5 vol% CO_2, in cell growth medium - DMEM medium (Thermo Fisher Scientific, Schwerte, Germany) suppled with 10 vol% fetal bovine serum (Sigma Aldrich, Hamburg, Germany) and 1 vol% non-essential amino acids (Thermo Fisher Scientific, Schwerte, Germany). The medium was changed every 2 days and the cells were passaged at a ratio of 1:3 when the confluence reached ~90%.

In order to examine the cell differentiation on SMPA sheets, the competitive differentiation medium consisting of 1:1 (v:v) adipogenesis medium (StemPro® adipogenesis differentiation kit, Thermo Fisher Scientific, Schwerte, Germany) and osteogenesis medium (StemPro® osteogenesis differentiation kit, Thermo Fisher Scientific, Schwerte, Germany) were used. The medium was changed every 3 days.

In-Situ Measurement of SMPA Sheet Shape and Cell Morphology

The temperature of the liquid surrounding the SMPA sheet was measured using a digital thermometer. The SMPA sheets and the cells were monitored using laser scanning confocal microscopy (LSM 780, Carl Zeiss, Jena, Germany) or a fluorescence microscope (Axiovert 200M, Carl Zeiss, Jena, Germany).

The 50 x 50 µm grid squares created on the bottom of SMPA sheet were measured in the direction of elongation and compression to analyze the shape change of SMPA sheets (ImageJ software, National Institutes of Health). The movement speed of the p-SMPA sheet during actuation was calculated according to the measurements of dynamic shape change using a benchmark point 100 µm away.

The shape change of the cells growing upon p-SMPA sheet actuation was quantified by measuring the cell dimension in the direction of p-SMPA sheet elongation and compression as well as the cell surface area. The cell membrane, cytoplasm and nuclei were stained using a CellMask™ Deep Red plasma membrane staining kit, CFSE and Hoechst 33342 respectively (Thermo Fisher Scientific, Schwerte, Germany). The orientation of cells on SMPA sheets was analyzed by measuring the angle between the direction of p-SMPA sheet elongation and the long axis of cells. In order to study the focal adhesion dynamics of cells upon p-SMPA actuation, the cells were transfected using CellLight® Talin-GFP, BacMam 2.0 (Thermo Fisher Scientific,

Schwerte, Germany) to label talin with (GFP). The GFP signal of cells cultured on p-SMPA sheets during cyclic temperature change was detected using laser scanning confocal microscopy.

Cell viability assay Live/dead staining of hADSCs was performed using CFSE and propidium iodide (PI) (Thermo Fisher Scientific, Schwerte, Germany). In brief, 25 µM CFSE was loaded to cells before cell seeding. At indicated time points, PI (2 µg/mL) was directly added to cell culture medium for visualizing dead cells. Images were taken by confocal laser scanning microscope (LSM780, Carl Zeiss, Jena, Germany) and analyzed using ImageJ software. CellTiter-Glo Luminescent cell viability assay kit and MultiTox-Fluor Multiplex cytotoxicity assay kit (Promega GmbH, Mannheim, Germany) were used to quantify the viable and dead cells simultaneously. At indicated time points, the conditioned medium was collected and the cell lysate was harvested immediately to determine the relative number of dead and viable cells, respectively. The cell viability was presented as the percentage of viable cell in total cell number (viable+dead cells).

Cell proliferation assay The hADSCs were seeded at a density of 0.25 x $10^4/cm^2$ and cultured in growth medium. After 3 days, the cell proliferation activity was assessed by staining the cell proliferation marker Ki67. In brief, 1 x $10^4/cm^2$ cells (in growth medium) were seeded for image based cell counting. To test the cell proliferation during differentiation, the hADSCs were seeded at a density of 2.5 x $10^4/cm^2$ and cultured in competitive differentiation medium. The cell number was counted based on the carboxyfluorescein succinimidyl ester (CFSE) and nuclear labeling (Hoechest 33342) (Thermo Fisher Scientific, Schwerte, Germany) or examined using a cell counting kit-8 (CCK-8, Dojindo, Offenbach, Germany).

Calcium Imaging. Intracellular Ca^{2+} was measured using a Fluo-4 kit according to the manufacturer's instructions. Real-time fluorescence images were acquired at 1 min intervals using laser scanning confocal microscopy and analyzed using ImageJ software. The fluorescence ratio δF/F0 (δF = Ft-F0) was calculated according to existing literature [40] for each cell, where Ft represents the measured fluorescence intensity and F0 corresponds to the lowest fluorescence level in each cell.

Intracellular calcium quantification. The intracellular calcium level of hADSCs was detected using a calcium quantification assay kit-Red fluorescence (Abcam, Berlin, Germany) according to the product manual. Cells cultured under different conditions were lysed using RIPA buffer (Thermo Fisher Scientific, Schwerte, Germany). Rhod Red calcium indicator was then added to the cell lysis and incubated for 30 min at room temperature. The fluorescence were measured by Tecan Infinite® 200 PRO microplate reader (Tecan Deutschland GmbH, Germany). The results were normalized with the amount of total protein for each sample.

Chemical Inhibition. The 2-aminoetho-xydiphenylborate (2APB, Sigma Aldrich, Hamburg, Germany) was used to block the Ca^{2+} entry through TRP channels as well as calcium release from endoplasmic reticulum by inhibiting Inositol 1,4,5-trisphosphate receptors (InsP3Rs). For the calcium imaging experiments, 2APB was added to the medium 30 min before the experiment to reach a final concentration of 200 µM. For long-term experiments (10 days) into Ca^{2+} inhibition, 100 µM 2APB was applied and refreshed in every 3 days after medium change. Cytochalasin D (CytoD, Sigma Aldrich, Hamburg, Germany) was used to inhibit actin dynamics. The medium containing 0.5 µM CytoD was used to culture hADSCs for 10 days. For short-term inhibition experiments, the cells were incubated with 100 µM 2APB and 0.5 µM CytoD for 3 hours.

Cell Staining. For immunostaining, cells were fixed with 4 wt% paraformaldehyde (Sigma Aldrich, Hamburg, Germany), permeabilized using 0.25 vol% Triton X-100 (Sigma Aldrich, Hamburg, Germany), and blocked using 5 vol% goat serum (Thermo Fisher Scientific, Schwerte, Germany) in PBS. Samples were incubated with primary antibodies overnight at 4 °C, followed by incubation with the secondary antibodies (Thermo Fisher Scientific, Schwerte, Germany) for 1 hour at room temperature. The following primary antibodies were used: Ki67 (rabbit monoclonal, Cell Signaling Technology, Frankfurt am Main, Germany), YAP (rabbit monoclonal, Cell Signaling Technology, Frankfurt am Main, Germany), RUNX2 (mouse monoclonal, Abcam, Berlin, Germany), FABP4 (rabbit polyclonal, Thermo Fisher Scientific, Schwerte, Germany), Osteocalcin (mouse monoclonal, Cell Signaling Technology, Frankfurt am Main, Germany), phosphor-HDAC1 (rabbit polyclonal, Thermo Fisher Scientific, Schwerte, Germany), fibronectin (rabbit polyclonal, Abcam, Berlin, Germany) and

integrin β1 (mouse monoclonal, R&D Systems, Minneapolis, USA). YAP and RUNX2 nuclear localization was analyzed by comparing fluorescence intensity in the nucleus and cytoplasm of each cell using ImageJ (National Institutes of Health). A cell with nuclear/cytoplasm fluorescence ratio > 1.35 was defined as a YAP or RUNX2 active cell. The cell nuclei were stained with 4',6-diamidino-2-phenylindole (DAPI) for 5 minutes at room temperature. A confocal laser scanning microscope (LSM780, Carl Zeiss, Jena, Germany) was used to observe the stained cells.

Oil Red O staining was performed to visualize the lipids of cells undergoing adipogenesis. After 2 weeks of adipogenic induction, the cells were washed with PBS, fixed in 4 wt% paraformaldehyde (Sigma Aldrich, Hamburg, Germany) and stained using 0.1 wt% Oil Red O (Sigma Aldrich, Hamburg, Germany) in isopropanol for 15 minutes. After washing 3 times with water, the Oil Red O was extracted using isopropanol. The absorbance at 490 nm of the mixture was measured using a microplate reader (Infinite 200 Pro, Tecan Group Ltd. Männedorf, Switzerland) to evaluate the efficiency of adipogenesis.

Alizarin Red S (ARS) was used to detect the calcium deposition of hADSCs during osteogenesis. Samples were washed with PBS and fixed in 4 wt% paraformaldehyde (Sigma Aldrich, Hamburg, Germany) at room temperature for 15 minutes. Then, 0.3 ml of 40 mM ARS (Sigma Aldrich, Hamburg, Germany) in water was added to each well. After 20 min incubation at room temperature, the samples were washed for 6 times with water.

Real time-PCR and ChIP-PCR The mRNA expression level of ALP and OCN was quantified with real time-PCR, using GAPDH as house-keeping gene. The total RNA was isolated using a mirVana Kit (Thermo Fisher Scientific, Schwerte, Germany), and quantified with a microplate reader (Infinite 200 Pro, Tecan Group Ltd. Männedorf, Switzerland) equipped with a NanoQuant Plate. The cDNA was synthesized using a RT^2 First Strand kit (Qiagen, Hilden, Germany). Then, the cDNA was mixed with RT^2 SYBR Green ROX qPCR Mastermix (Qiagen, Hilden, Germany) and corresponding primers (ALP 5'-CCCCCGTGGCAACTCTATCT-3' and , 5'-GATGGCAGTGAAGGGCTTCTT-3'; OCN 5'-AGCAAAGGTGCAGCCTTTGT-3' and 5'-GCGCCTGGGTCTCTTCACT-3'; GAPDH 5'-ATGGGGAAGGTGAAGGTCG-3' and 5'-GGGGTCATTGATGGCAACAATA-3'), and amplified using a StepOnePlus real-time PCR System (Thermo Fisher Scientific, Schwerte, Germany).

The chromatin immunoprecipitation (ChIP) was performed using a High-sensitivity ChIP kit (Abcam, Berlin, Germany) pre-coated with H3K9ac or H3K27me3 antibody (rabbit monoclonal, Cell Signaling Technology, Frankfurt am Main, Germany). The real-time PCR was applied to quantify the precipitated DNA using the primers targeting the promoter region of RUNX2, ALP and OCN (RUNX2 5'-AGGCCTTACCACAAGCCTTT-3' and 5'-AGAAAGTTTGCACCGCACTT-3'; ALP 5'-TCCAGGGATAAAGCAGGTC-3' and 5'-TTAGTAAGGCAGGTGCCAAT-3'; OCN 5'-CAAATAGCCCTGGCAGATTC-3' and 5'-GAGGGCTCTCATGGTGTCTC-3').

ELISA and ALP Activity Assay The cells were lysed using a cell lysis buffer. The FABP-4, phosphorylated YAP (pYAP) and total YAP (tYAP) in the cell lysate was quantified using the FABP4 ELISA kit (R&D Systems, Minneapolis, USA), PathScan® Phospho-YAP (Ser127) ELISA kit and PathScan® Total YAP ELISA kit (both were from Cell Signaling Technology, Frankfurt am Main, Germany) respectively. The ALP activity was measured using an alkaline phosphatase assay kit (Abcam, Berlin, Germany). The results were normalized with the amount of total protein for each sample, which was determined using a BCA protein assay kit (Thermo Fisher Scientific, Schwerte, Germany).

Statistical Analysis The number of repetitions for each experiment was indicated in the figure legends for each assay, with all data expressed as mean value ± standard deviation. Statistical analysis was performed using GraphPad Prism (Version 7.04, GraphPad Software, Inc., San Diego, CA, USA). The significance of the difference between two groups was determined using a two-tailed, unpaired Student's *t*-test. Differences among three or more independent groups were analyzed using one-way or two-way ANOVA followed by Tukey's multiple comparisons test. A p value less than 0.05 was considered to be statistically significant.

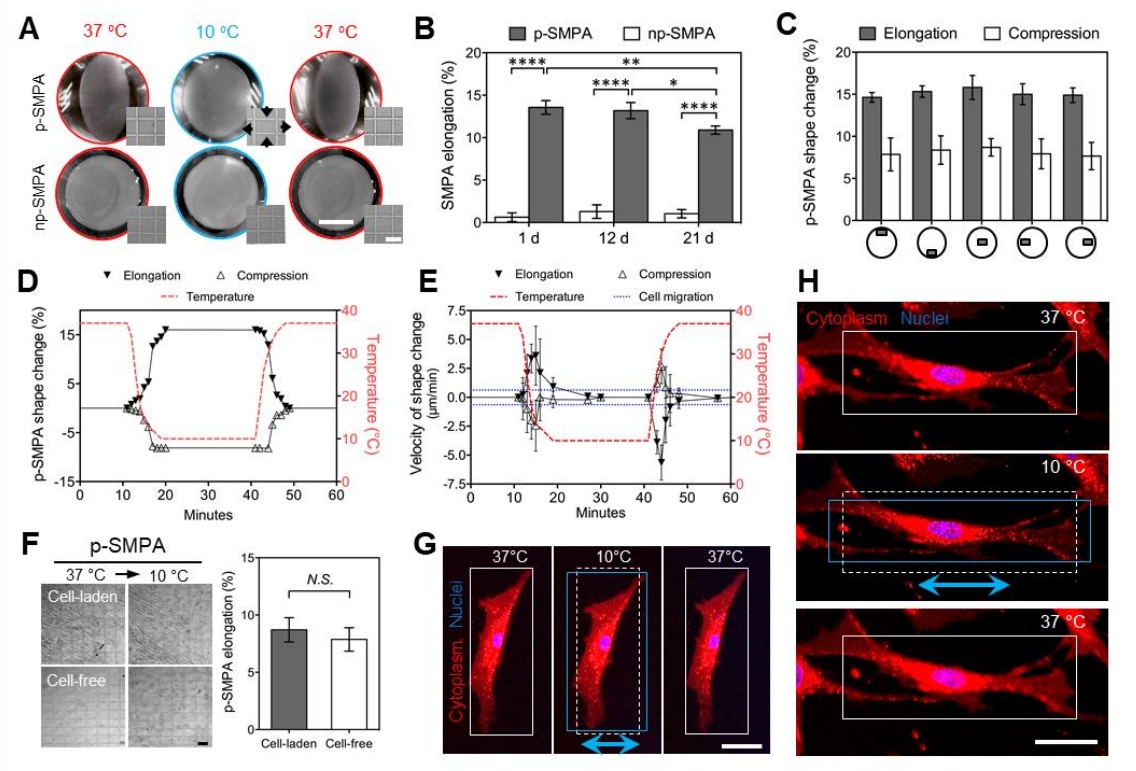

Fig. S1. (A) Representative images showing the macroscale shape change of non-programmed (np) and programmed (p) SMPA sheets in one cycle of temperature change in PBS solution. The elongation and compression of p-SMPA were analyzed according to the shape change of grid squares. Arrows indicate the elongation and compression directions (scale bar = 5 mm for SMPA sheets, scale bar = 50 μm for grid squares). (B) Quantification of p-SMPA shape change in 3 weeks in cell culture medium (n = 3; *p < 0.05, **p < 0.01, ****p < 0.0001, two-way ANOVA with Tukey's multiple comparisons test). (C) Temperature induced shape change of p-SMPA sheet in the center and near the edges of the p-SMPA sheet (n = 6). (D) Elongation and compression of p-SMPA sheet under the cyclic temperature change. (E) Shape change velocity of the p-SMPA sheet during actuation using a point of benchmark 100 μm away (n = 10). (F) Shape change of cell-laden and cell-free p-SMPA sheets under cyclic temperature change. Cells were cultured in growth medium on the p-SMPA sheet for 3 days (scale bar = 50 μm; n >= 12; N.S. non-significant, Student's *t*-test). (G, H) Fluorescent microscopy images of a single cell cultured in growth medium on p-SMPA sheet with temperature induced shape change. The blue arrows represent the direction of elongation. The solid white and blue boxes were used for positioning the cell border at 37 °C and 10 °C respectively (scale bar = 50 μm).

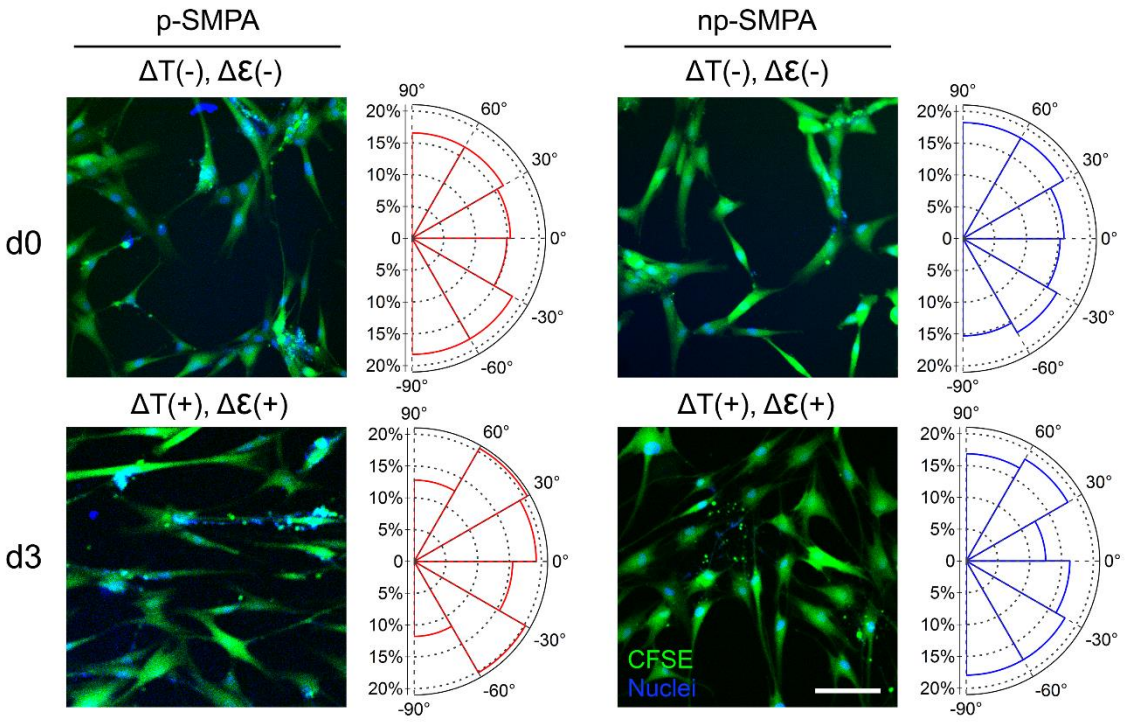

Fig. S2. Cell orientation at day 0 and after 3 days of cyclic temperature change on non-programmed (np) and programmed (p) SMPA sheets. Cells were cultured in competitive differentiation medium, and the living cells were stained with CFSE (green) and Hoechst 33342 (blue) to visualize cytoplasm and nuclei. For each group, more than 170 cells were analyzed to calculate the percentage of cells at different directions (scale bars = 100 μm).

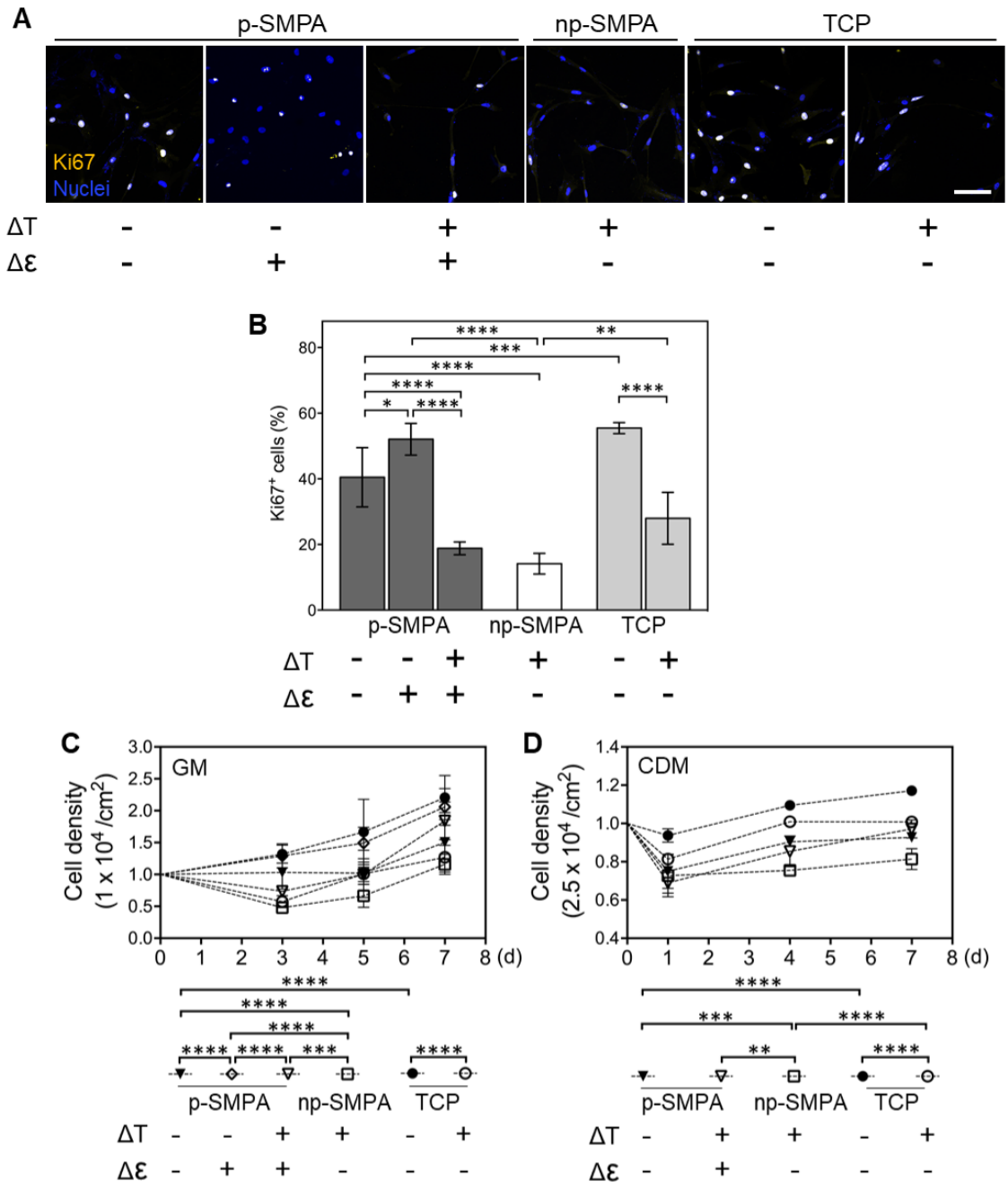

Fig. S3 (A) Ki67 staining (yellow) of cells cultured in growth medium for 3 days at different conditions. Cell nuclei were stained with DAPI (blue) (scale bar = 100 µm). (B) Percentage of Ki67 positive cells in each group. The quantification was based on 6 randomly selected images (*p < 0.05, **p < 0.01, ***p < 0.001, ****p < 0.0001, one-way ANOVA with Tukey's multiple comparisons test). (C) Cell proliferation on TCP and SMPA sheets in growth medium under different stimuli. The cells were stained with CFSE and the images were taken at indicated time points. The cell number were determined by counting the cells on at least 5 randomly selected images using ImageJ

software. (D) Cell proliferation on TCP and SMPA sheets in competitive differentiation medium under different stimuli. The cell number were quantified using a cell counting kit (n = 4). (**p < 0.01, ***p < 0.001, ****p < 0.0001 in C and D, two-way ANOVA with Tukey's multiple comparisons test)

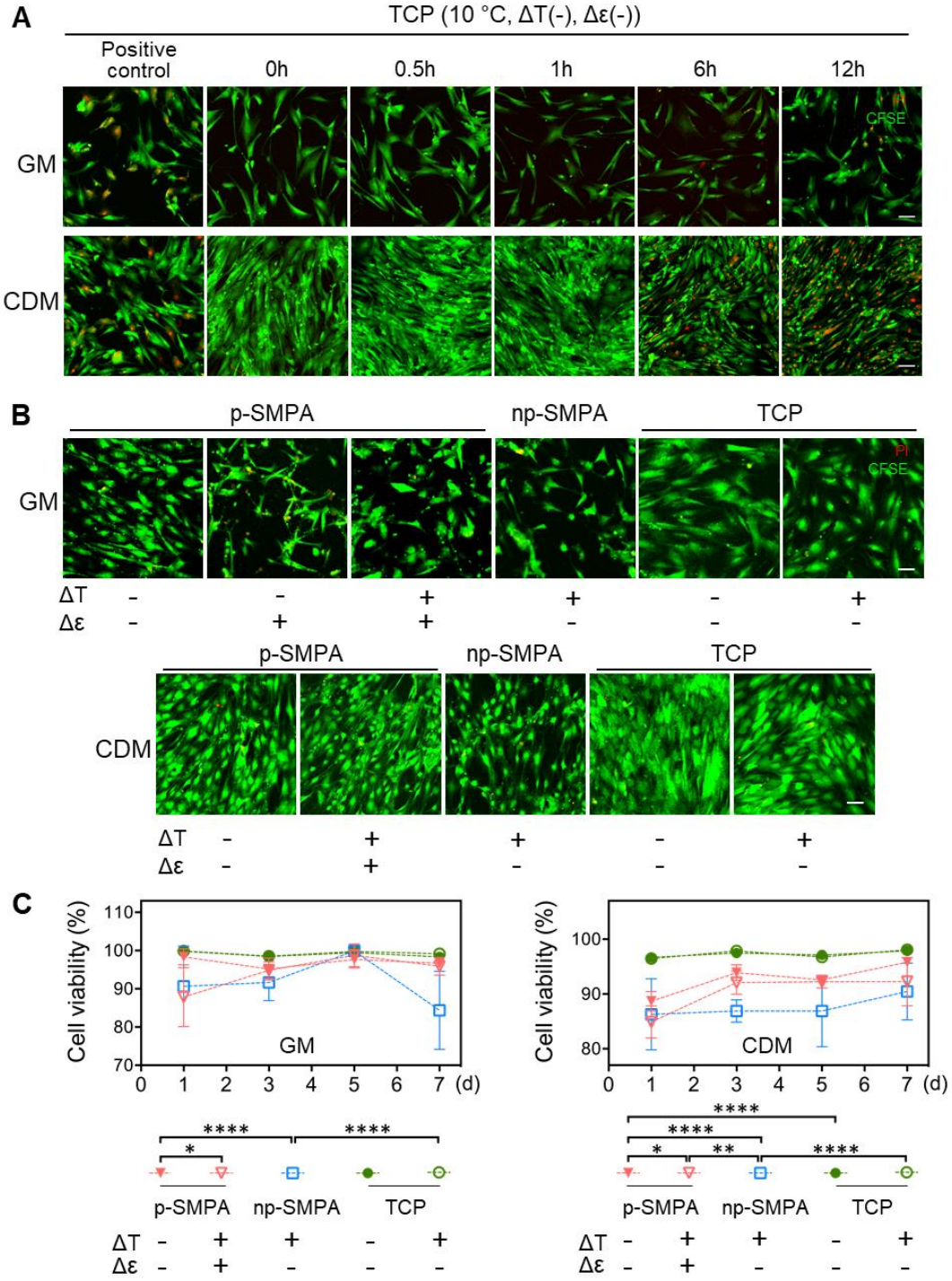

Fig. S4. (A) Live/dead staining of hADSCs cultured at 10 °C on TCP in growth medium (GM) and competitive differentiation medium (CDM). Living and dead cells were

identified using CFSE (green) and propidium Iodide (red) respectively. The cells treated with sonication to disrupt the cell membrane were used as positive control (scale bar = 100 µm). (B) Live/dead staining of hADSCs cultured on SMPA sheets and TCP under different conditions (scale bar = 100 µm). (C) Quantification of cell viability using the cell viability assay kit and cytotoxicity assay kit (n >= 4; *p < 0.05, **p < 0.01, ****p < 0.0001, two-way ANOVA with Tukey's multiple comparisons test).

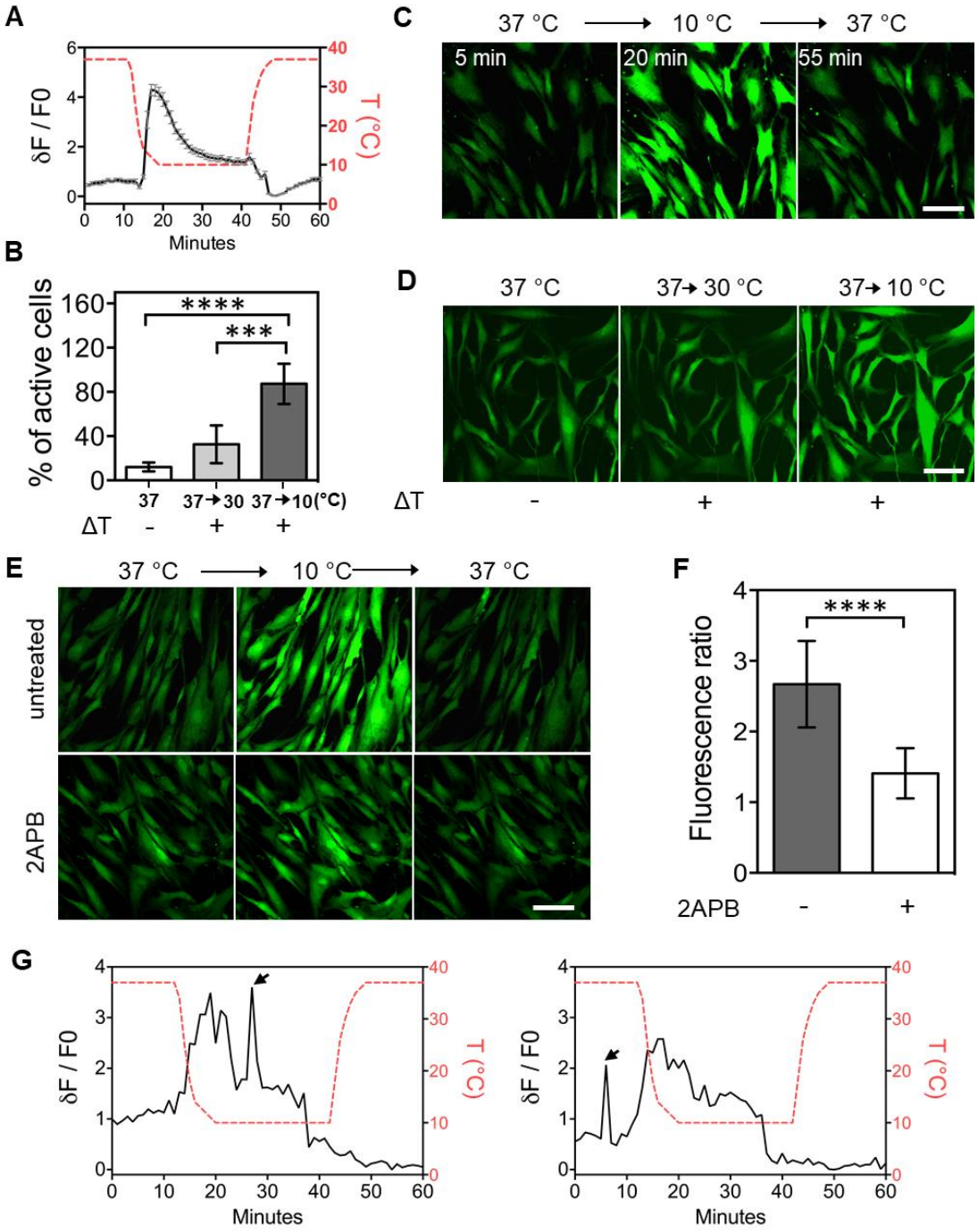

Fig. S5. (A) Dynamics of calcium fluorescence of hADSCs under cyclic temperature change. The cells were cultured on a glass coverslip in competitive differentiation

medium. (B) Percentage of cells with active Ca^{2+} influx. Cells were cultured at 37 °C or in different temperature changing conditions. The analysis was based on at least 4 randomly selected images (***$p < 0.001$, ****$p < 0.0001$, one-way ANOVA with Tukey's multiple comparisons test). (C, D) Time series images of calcium fluorescence of hADSCs cultured on glass with different switching temperatures (scale bar = 100 μm). (E) Comparison of Ca^{2+} fluorescence intensity during temperature change with and without treatment of 2APB (scale bar = 100 μm). (F) Increase of Ca^{2+} fluorescence at low temperature with and without 2APB treatment. The result was expressed as the ratio of Ca^{2+} fluorescence intensity at 10 °C to that at 37 °C. The analysis was based on more than 40 cells on 2 randomly selected images (****$p < 0.0001$, Student's *t*-test). (G) Spontaneous calcium oscillation occurred at 10 °C (left) or 37 °C (right) in hADSCs growing on p-SMPA sheets under changed temperature. The arrows indicated spontaneous calcium oscillations.

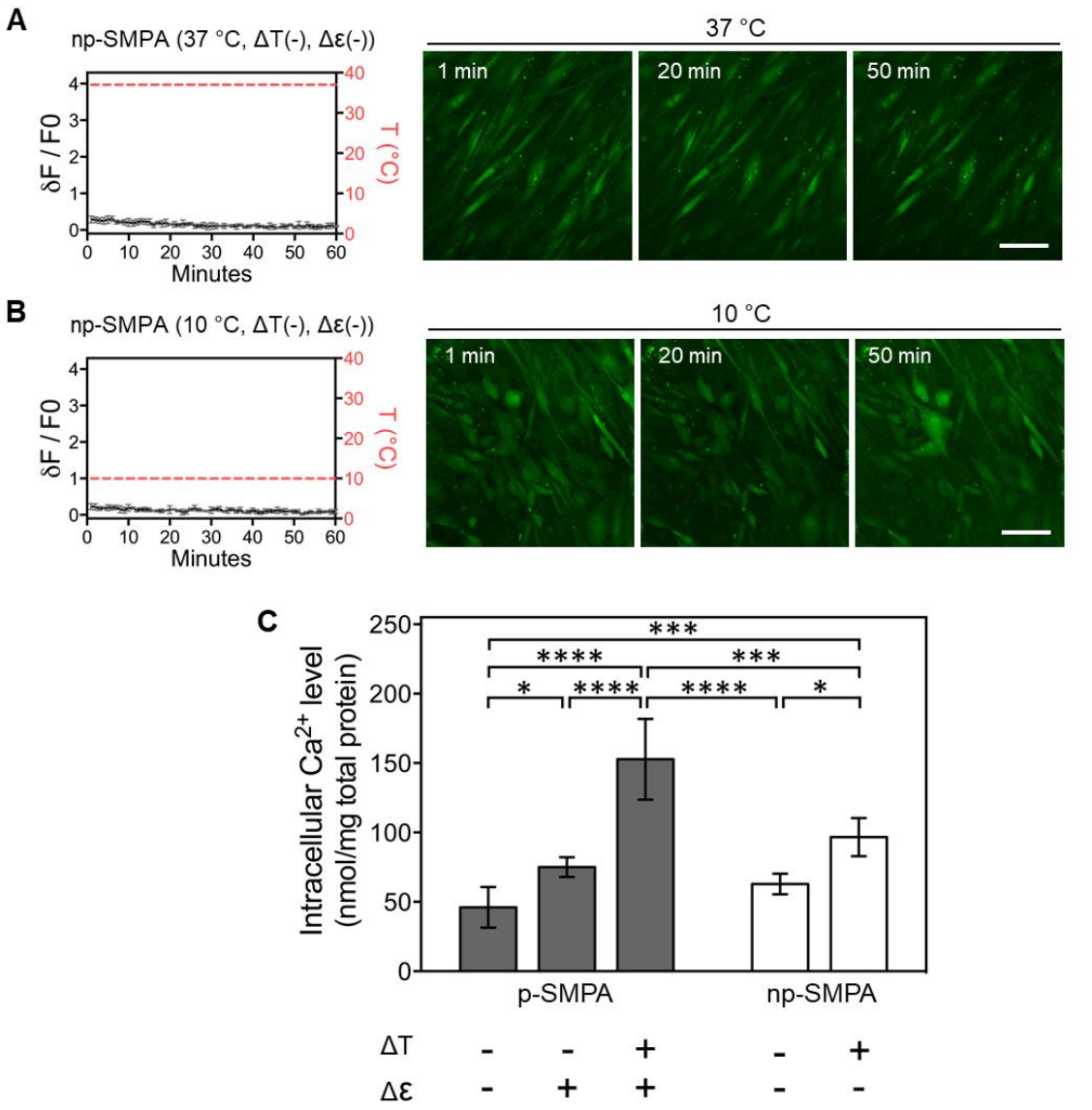

Fig. S6. Intracellular Ca^{2+} fluorescence in hADSCs without active Ca^{2+} influx on np-SMPA sheets exposed to a constant temperature of either 37 °C (A) or 10 °C (B) (n >= 3). (C) Intracellular calcium level in hADSCs cultured in competitive differentiation medium perceiving different stimuli. For ΔT-, Δε+ group, the cells were stretched using a stretching device for one cycle. For ΔT+ groups, the cells were treated with one cycle of temperature change and were lysed when the temperature reached to 10 °C. The Ca^{2+} level was determined using a calcium quantification kit (n >= 4; *p < 0.05, ***p < 0.001, ****p < 0.0001, one-way ANOVA with Tukey's multiple comparisons test).

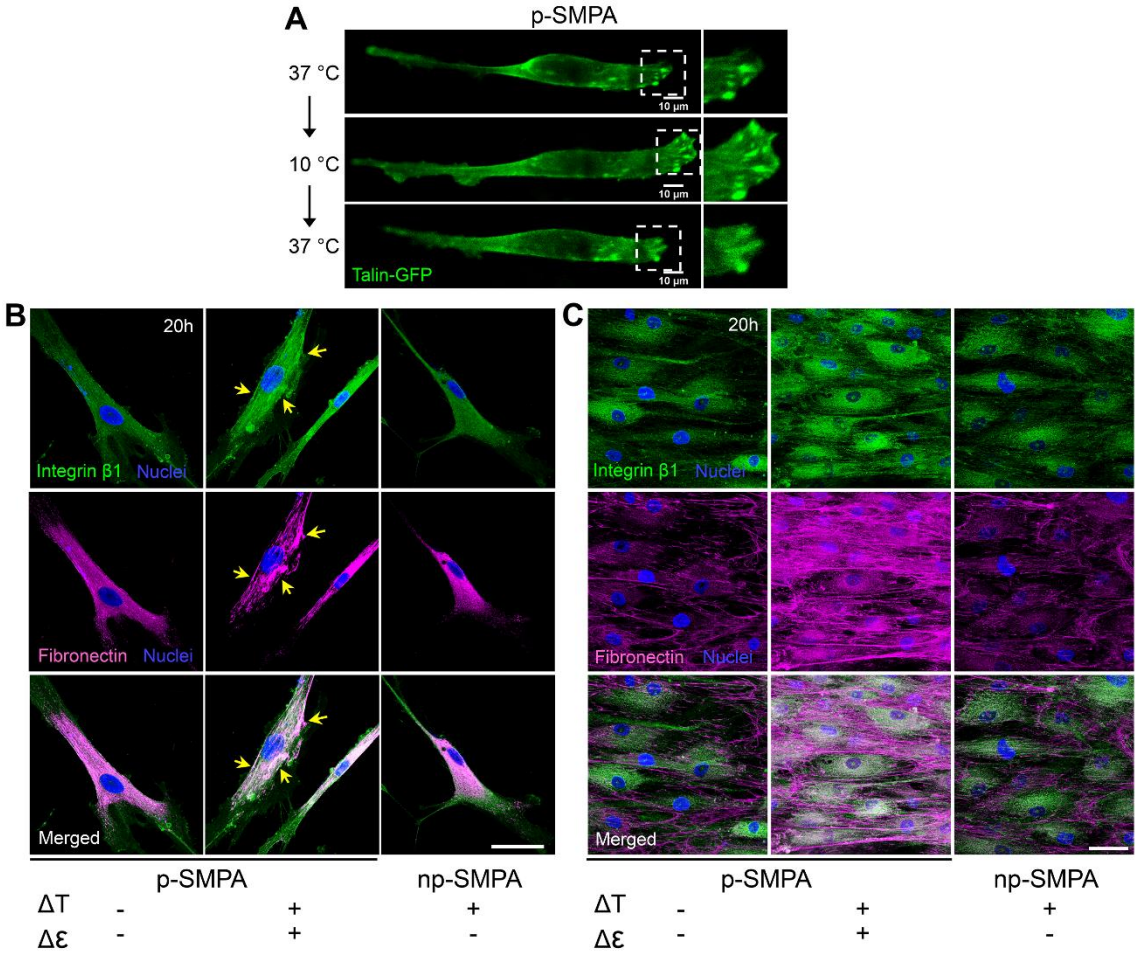

Fig. S7. (A) Representative images of talin (green) dynamics in a hADSC on p-SMPA sheet at indicated temperature. Cells were cultured in growth medium for 1 day (scale bar = 10 μm). (B, C) Fibronectin secretion and integrin β1 expression of hADSCs. The cells were seeded at low and high density to obtain the sparse (B) and confluent (C) cells on SMPA sheets. After 20 hours (20 cycles for ΔT+ groups), the cells were stained to visualize fibronectin (pink), integrin β1 (green) and cell nuclei (blue). The yellow arrows indicated the fibronectin fibrils (scale bar = 50 μm).

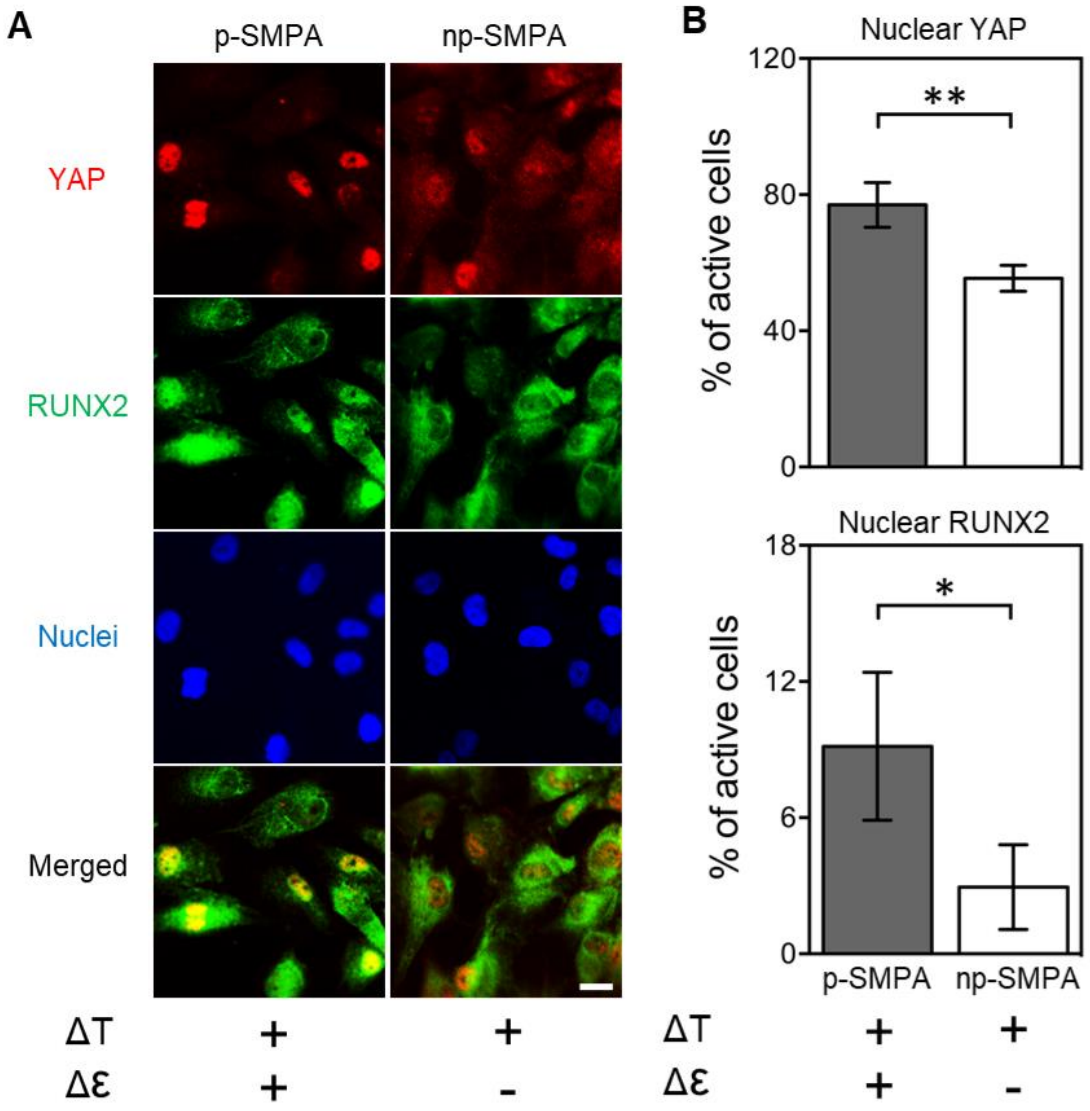

Fig. S8. (A) YAP and RUNX2 immunostaining of hADSCs on non-programmed and programmed SMPA sheets under cyclic temperature change. Cells were cultured in competitive differentiation medium for 3 days (scale bar = 20 μm). (B) Analysis of percentage of YAP and RUNX2 nuclear positive cells according to the immunostaining images. At least 3 images in each group containing more than 151 cells were analyzed (*$p < 0.05$, **$p < 0.01$, Student's *t*-test).

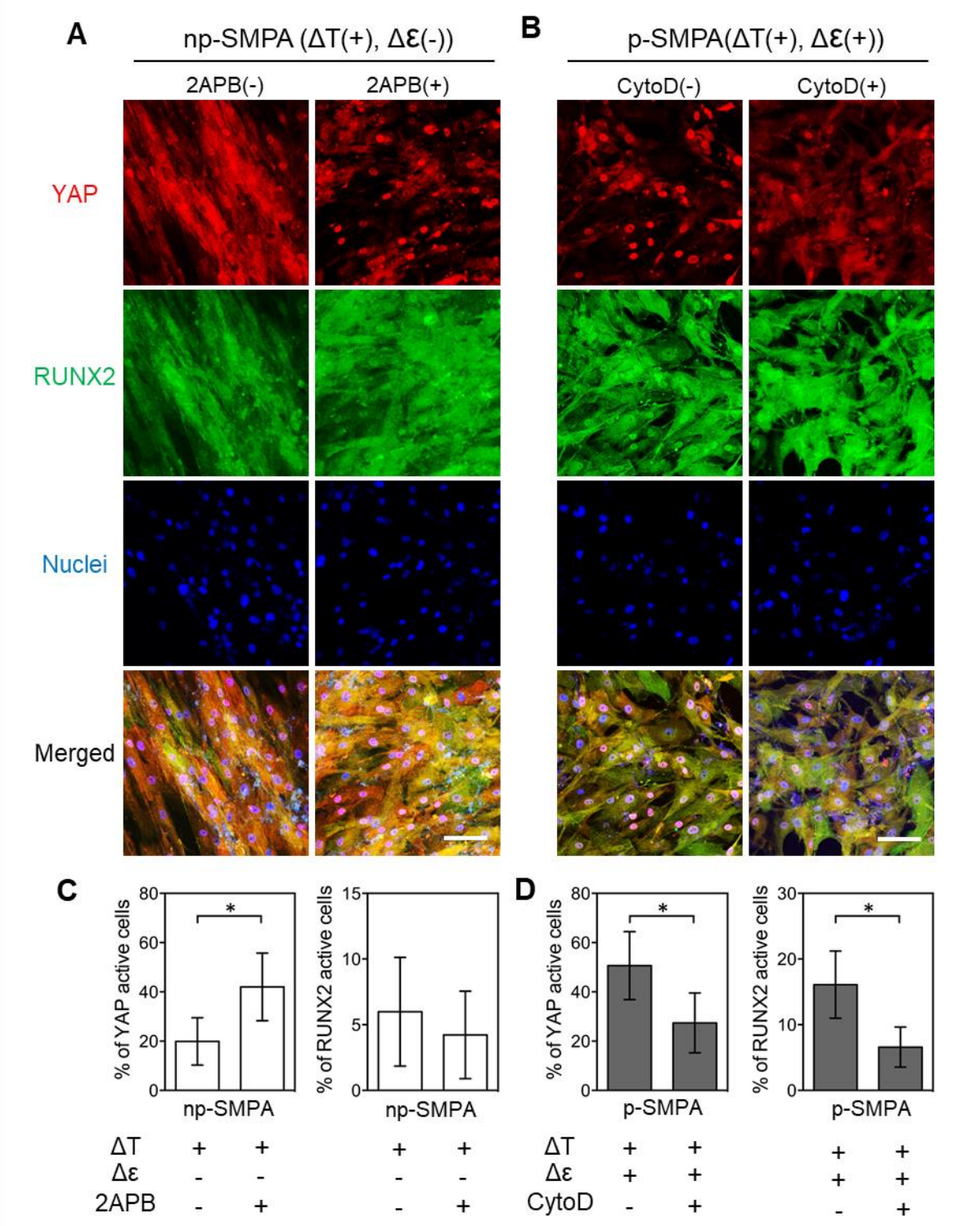

Fig. S9. Effect of calcium signaling (A) and mechanical stimulus (B) on YAP and RUNX2 nuclear translocation. Cells cultured on SMPA sheets under different stimuli were treated with and without 2APB or CytoD for 3 hours. Cells were stained to visualize YAP (red), RUNX2 (green) and nuclei (blue) (scale bar = 100 μm). The analysis of the effect of 2APB (C) or CytoD (D) on YAP and RUNX2 activity was

performed based on the fluorescence images using ImageJ software (*p < 0.05, Student's t-test). For each group, at least 4 randomly selected images were analyzed.

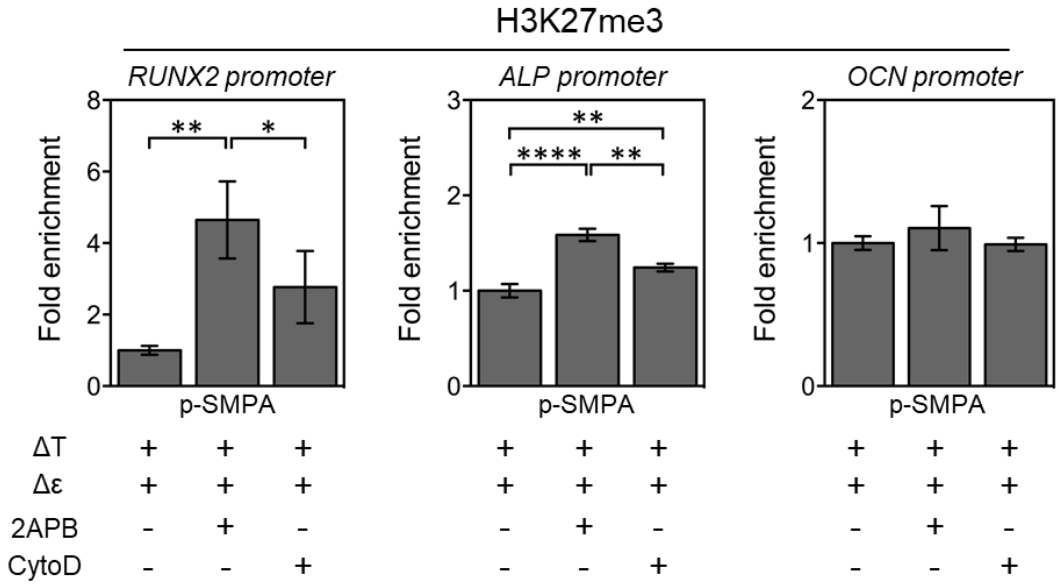

Fig. S10. Regulation of Ca^{2+} signaling and mechanical stimulus on H3K27 trimethylation on the promoters of osteogenesis related genes in hADSCs perceiving dual stimuli. 2APB and CytoD were used to inhibit the intracellular Ca^{2+} and actin polymerization. The values of the group without inhibition were set as 1 (n >= 3; *p < 0.05, **p < 0.01, ****p < 0.0001, one-way ANOVA with Tukey's multiple comparisons test).

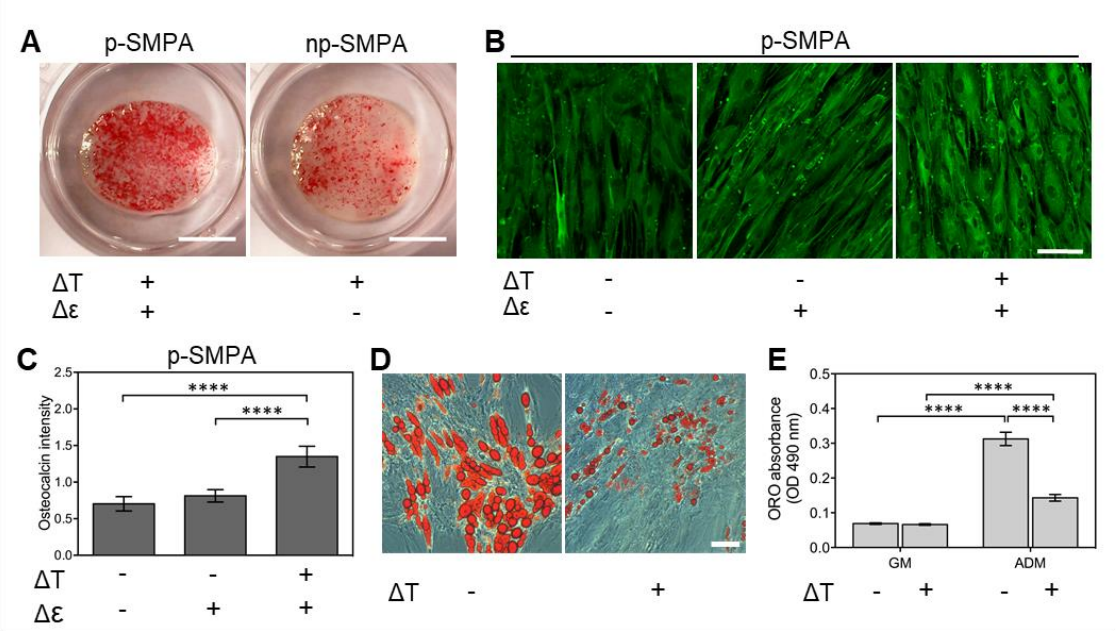

Fig. S11. (A) Alizarin Red S (ARS) staining of hADSCs cultured on programmed (p) and non-programmed (np) SMPA sheets under cyclically changed temperature. The cells were cultured in competitive differentiation medium for 3 weeks (scale bar = 0.5 cm). (B) Osteocalcin immunostaining (green) of hADSCs on p-SMPA sheet with different stimuli. Cells were cultured in competitive differentiation medium for 10 days (scale bar = 100 μm). (C) Quantification of osteocalcin fluorescence intensity according to the immunostaining images. More than 238 cells on 5 randomly selected images in each group were analyzed (****p < 0.0001, one-way ANOVA with Tukey's multiple comparisons test). (D) Oil Red O (ORO) staining of hADSCs induced into adipogenic differentiation. Cells were cultured on TCP in adipogenic induction medium (ADM) for 2 weeks (scale bar = 100 μm). (E) Quantification of ORO by measuring the absorbance value. Cells were cultured on TCP for 2 weeks with and without cyclic temperature change. Cells in growth medium (GM) were used as control (n = 6; ****p < 0.0001, one-way ANOVA with Tukey's multiple comparisons test).

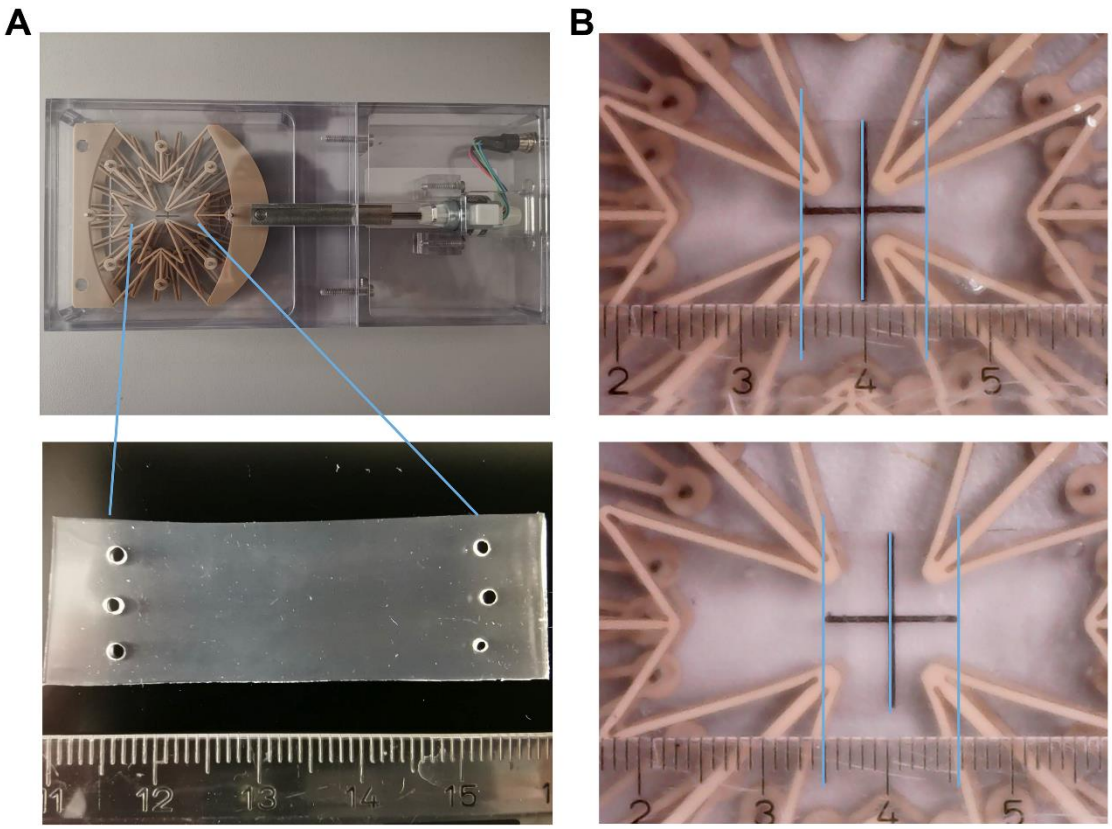

Fig. S12. (A) A stretch device was used to generate mechanical stimulus, without changing temperature. (B) Stretching of the p-SMPA sheet was along the direction of programming, resulting in an elongation about 10%.

Video S1. The p-SMPA sheets exposed to cyclic temperature change in cell growth medium. The videos were generated with the real-time images, which were obtained at 10 s intervals for 30 min using an inverted fluorescence microscopy (Axiovert 200M, Carl Zeiss, Jena, Germany). (Scale bar = 50 μm)

Video S2. The np-SMPA sheets exposed to cyclic temperature change in cell growth medium. The videos were generated with the real-time images, which were obtained at 10 s intervals for 30 min using an inverted fluorescence microscopy (Axiovert 200M, Carl Zeiss, Jena, Germany). (Scale bar = 50 μm)

Video S3. The hADSCs cultured on p-SMPA sheets exposed to cyclic temperature change in cell growth medium. The cells were stained with CFSE. The videos were generated with the real-time images, which were taken at intervals of 10 s for 30 min using an inverted fluorescence microscopy (Axiovert 200M, Carl Zeiss, Jena, Germany). (Scale bar = 50 μm)

Video S4. The hADSCs cultured on np-SMPA sheets exposed to cyclic temperature change in cell growth medium. The cells were stained with CFSE. The videos were generated with the real-time images, which were taken at intervals of 20 s for 30 min using an inverted fluorescence microscopy (Axiovert 200M, Carl Zeiss, Jena, Germany). (Scale bar = 50 μm)

Video S5. The calcium influx of hADSCs on p-SMPA sheet exposed to cyclic temperature change in competitive differentiation medium. The Ca^{2+} was probed using Fluo-4 calcium indicator. The videos were generated with the real-time images, which were taken at 5 s intervals for 18 min using a laser scanning confocal microscopy (LSM 780, Carl Zeiss, Jena, Germany). (Scale bar = 50 μm)

Video S6. The calcium influx of hADSCs on np-SMPA sheet exposed to cyclic temperature change in competitive differentiation medium. The Ca^{2+} was probed using Fluo-4 calcium indicator. The videos were generated with the real-time images, which were taken at 5 s intervals for 18 min using a laser scanning confocal microscopy (LSM 780, Carl Zeiss, Jena, Germany). (Scale bar = 50 μm)

Video S7. The calcium influx of hADSCs on glass exposed to cyclic temperature change in competitive differentiation medium. The Ca^{2+} was probed using Fluo-4 calcium indicator. The videos were generated with the real-time images, which were taken at 5 s intervals for 18 min using a laser scanning confocal microscopy (LSM 780, Carl Zeiss, Jena, Germany). (Scale bar = 50 μm)

References

1. Saatchi M, Behl M, Nöchel U, & Lendlein A (2015) Copolymer Networks From Oligo(ε-caprolactone) and n-Butyl Acrylate Enable a Reversible Bidirectional Shape-Memory Effect at Human Body Temperature. Macromol. Rapid Commun. 36(10):880-884.
2. Kumar UN, Kratz K, Wagermaier W, Behl M, & Lendlein A (2010) Non-contact actuation of triple-shape effect in multiphase polymer network nanocomposites in alternating magnetic field. J. Mater. Chem. 20(17):3404-3415.
3. Xu X, et al. (2014) Controlling Major Cellular Processes of Human Mesenchymal Stem Cells using Microwell Structures. Adv Healthc Mater 3(12):1991-2003.

Appendix II

Modulation of Mesenchymal Stem Cell Migration using Programmable Polymer Sheet Actuators

Zijun Deng[1,2], Weiwei Wang[1], Xun Xu[1], Nan Ma[1,2*], Andreas Lendlein[1,2,3*]

1 Institute of Biomaterial Science and Berlin-Brandenburg Centre for Regenerative Therapies, Helmholtz-Zentrum Geesthacht, 14513 Teltow, Germany

2 Institute of Chemistry and Biochemistry, Free University of Berlin, 14195 Berlin, Germany

3 Institute of Chemistry, University of Potsdam, 14469 Potsdam, Germany

* To whom correspondence should be addressed: Prof. Dr. Nan Ma, Prof. Dr.

Andreas Lendlein Email: nan.ma@hzg.de, andrease.lendlein@hzg.de

The publication is available at Materials Research Society through https://doi.org/10.1557/adv.2020.235

ABSTRACT

Recruitment of mesenchymal stem cells (MSCs) to damaged tissue is a crucial step to modulate tissue regeneration. Here, the migration of human adipose-derived stem cells (hADSCs) responding to thermal and mechanical stimuli was investigated using programmable shape-memory polymer actuator (SMPA) sheets. Changing the

temperature repetitively between 10 and 37 °C, the SMPA sheets are capable of reversibly changing between two different pre-defined shapes like an artificial muscle. Compared to non-actuating sheets, the cells cultured on the programmed actuating sheets presented a higher migration velocity (0.32 ± 0.1 vs. 0.57 ± 0.2 µm/min). These results could motivate the next scientific steps, for example, to investigate the MSCs pre-loaded in organoids towards their migration potential.

INTRODUCTION

Recruitment of progenitor cells at lesion points is the initial and crucial step for endogenous tissue regeneration. Mesenchymal stem cells (MSCs) represent a promising source for regenerative medicine applications not only owing to the differentiation potential, but also due to their homing capacity[1-3]. However, the major challenge for an effective MSC-based therapy remains the low infiltration of transplanted cells at the injury site [4, 5]. Improving the migration ability by preconditioning the MSCs prior to transplantation could be a strategy to circumvent this limitation.

Growth factors such as bFGF, VEGF, HGF, IGF and TGF- β1 are typical enhancers of MSC migration[6-10]. Increasing of CXC chemokine receptor 4 expression on MSC surface via small molecule stimulation or gene transfection can promote cell recruitment [11-14]. Besides biochemical factors, it has been reported that the cell migration ability can also be modulated by mechanical cues. For instance, the rigidity of extracellular matrix (ECM) can regulate cell migration by actin and microtubule cytoskeleton assembly and remodeling [15-17]. Compared to stiff cell culture substrates (30 and 600 kPa), a higher cell migration speed can be achieved in MSCs from a soft substrate (3 kPa) due to their weaker formation of focal adhesion complexes [18]. Transient calcium influx, which is highly dependent on the activity of a stretch-activated cation channel was observed in migrating keratinocytes and fibroblasts over a decade ago [19, 20]. The application of mechanical strain (ranging from 5 to 10%) on MSCs efficiently promoted stem cell migration in recent studies [21, 22]. The mechanical stimuli can provide a simple, safe, cost effective and well-defined physical approach for the reinforcement of stem cell migration compared to

established strategies relying on small molecule compounds and transgene expression.

Temperature-controlled programmable shape-memory polymer sheet actuators (SMPA) have been applied as a platform to autonomously apply cyclic mechanical strain to MSCs to direct the cell fate [23]. Cells cultured on programed SMPA under cyclic temperature change can sense both the thermal stimulus (ΔT) and the mechanical stimulus ($\Delta\varepsilon$). The 50 × 50 μm grids on the bottom side of the sheet enabled the visualization of SMPA deformation, without influencing the cells on the topside. During SMPA actuation, more than 10% of material elongation could stimulate hADSC response and influence their behavior, such as proliferation and differentiation [23]. Here, we study the influence of this material as well as the thermal and synchronized mechanical stimuli on stem cell migration. SMPA sheets were utilized under three distinct conditions: i) programmed SMPA (p-SMPA) which exerted a 2D actuation when exposed to cyclic temperature changes between 37 °C and 10 °C (SMPA, ΔT $\Delta\varepsilon$); ii) non-programmed (np-SMPA) SMPA with cyclic temperature changes between 37 °C and 10 °C (SMPA, ΔT); iii) non-programmed SMPA at a constant temperature of 37 °C (SMPA, 37 °C). Standard tissue culture plates (TCP) were used as reference material (Fig. 1A). Cell morphology, migration speed, cytoskeleton organization and integrin mediated mechanical transduction signaling of human adipose-derived stem cells (hADSCs) were investigated to explore the potential molecular mechanism responsible for the influence of SMPA on MSC migration.

EXPERIMENTAL DETAILS

Preparation of SMPA sheets

SMPA sheets containing poly (ε-caprolactone) domains as actuating unit were prepared according to our previous report [23]. The sheets were programmed by stretching to a strain (εprog) of 60% at 50 °C before cooling to –20 °C under constant strain. The circular SMPA specimens with a diameter of 10 mm were punched out and put into the 24-well standard tissue culture plate (TCP).

Cyclic temperature change

Computer-controlled thermochambers (Instec, Colordao, USA), supplied with 5 % (v/v) CO2, were used for realizing the cyclic temperature changes between 37 °C and 10 °C [23]. The time for each cycle was set to 60 minutes (8 minutes from 37 °C to 10 °C, 22 minutes at 37 °C, 8 minutes from 10 °C to 37 °C, and 22 minutes at 10 °C).

Cell culture

hADSCs were isolated from human adipose tissue after informed consent (No.: EA2/127/07; Ethics Committee of the Charité – Universitätsmedizin Berlin, approval from 17.10.2008) [24]. The cells were cultured in Dulbecco's Modified Eagle Medium (DMEM, Life Technologies, Germany) containing 10% (v/v) fetal bovine serum (FBS, Sigma-Aldrich, USA), 100 U/ml penicillin and 100 µg/ml streptomycin (Merck Millipore, Germany), and incubated at 37 °C containing 5% (v/v) CO2. The medium was changed every two days.

Cell migration

5×10^3 /cm^2 hADSCs were seeded on SMPA sheets and TCP, followed by 3 days of cultivation under different conditions. The CellMaskTM Deep Red plasma membrane staining kit was applied for visualization of living cells. Cell nuclei were stained using Hoechst 33342 (Thermo Fisher Scientific, Schwerte, Germany). Cells were then transferred into the cage incubator (37 °C, 5% (v/v) CO2) equipped on a time-lapse microscope (Olympus, Hamburg, Germany). The cell movement was recorded for 10 hours with 10 minutes intervals, and the cell migration was analyzed by tracing the cell nuclei. Data analysis was performed using ImageJ software (NIH, USA) suppled with the plugins of Manual Tracking (Fabrice Cordelieres, Institut Curie, Orsay, France) and Chemotaxis tool (ibidi GmbH, Gräfelfing, Germany).

Cell staining

For immunocytochemical staining, samples were washed with PBS and fixed with 4% (w/v) paraformaldehyde (Sigma-Aldrich, Hamburg, Germany), permeabilized with 0.25% (v/v) Triton X-100 (Sigma-Aldrich, Hamburg, Germany), and blocked with 5% (v/v) normal goat serum (Thermo Fisher Scientific, Schwerte, Germany). The samples were

then incubated with primary antibodies overnight at 4 °C and treated with secondary antibodies (Thermo Fisher Scientific, Schwerte, Germany) for 1 hour at room temperature. The following primary antibodies were used: β-Tubulin (mouse, Thermo Fisher Scientific, Schwerte, Germany), phospho-Myosin Light Chain 2 (Ser19) (mouse, Cell Signaling Technology, Frankfurt am Main, Germany), AlexaFluor® 647 conjugated anti-Integrin β1 (activated, clone HUTS-4, Merck, Darmstadt, Germany). Cell nuclei and F-actin were stained with Hoechst 33342 and ActinRedTM 555 ReadyProbes (Thermo Fisher Scientific, Schwerte, Germany), respectively. The images were taken using a laser scanning confocal microscope (LSM780, Carl Zeiss, Jena, Germany) and analyzed with ImageJ software (NIH, USA).

Statistics

All data were from at least three independent experiments and presented as mean ± standard deviation. Statistical analysis was performed using one-way ANOVA with post-hoc Tukey test, and a p-value < 0.05 was considered statistically significant.

RESULTS AND DISCUSSION

SMPA deformation and hADSC morphology

In a previous report, we have demonstrated the great compatibility of SMPA for hADSCs at the changed temperature from 37 °C to 10 °C, as evidenced by a high cell survive rate after a long term cultivation [23]. Here, we studied the cell morphology at different stimuli and included standard TCP as a reference material. No obvious morphology change was observed in hADSCs cultured in different conditions for 3 days (Fig. 1B). The cells on SMPA sheets exhibited typical spindle-shaped morphology, which was similar to those on standard TCP. Cyclic temperature changes did not affect the cell morphology on both TCP and SMPA sheets. Comparison between the cells on p-SMPA and np-SMPA under the changed temperature suggested that the SMPA actuation had no visible effect on cell morphology.

However, compared to the cells on TCP, the cells on SMPA sheets were less spreaded. This result suggested that the cells might form a looser attachment on SMPA than on

TCP, which could be attributed to the difference of chemical and physical properties between these two surfaces. In addition, the stretching force during SMPA actuation might also contribute to low cell anchoring from the material surface. Since the migration of anchorage-dependent cells are highly dependent on the cell attachment and spreading, one could expect that hADSCs may exhibit different migration capacities on SMPA and TCP [18, 25].

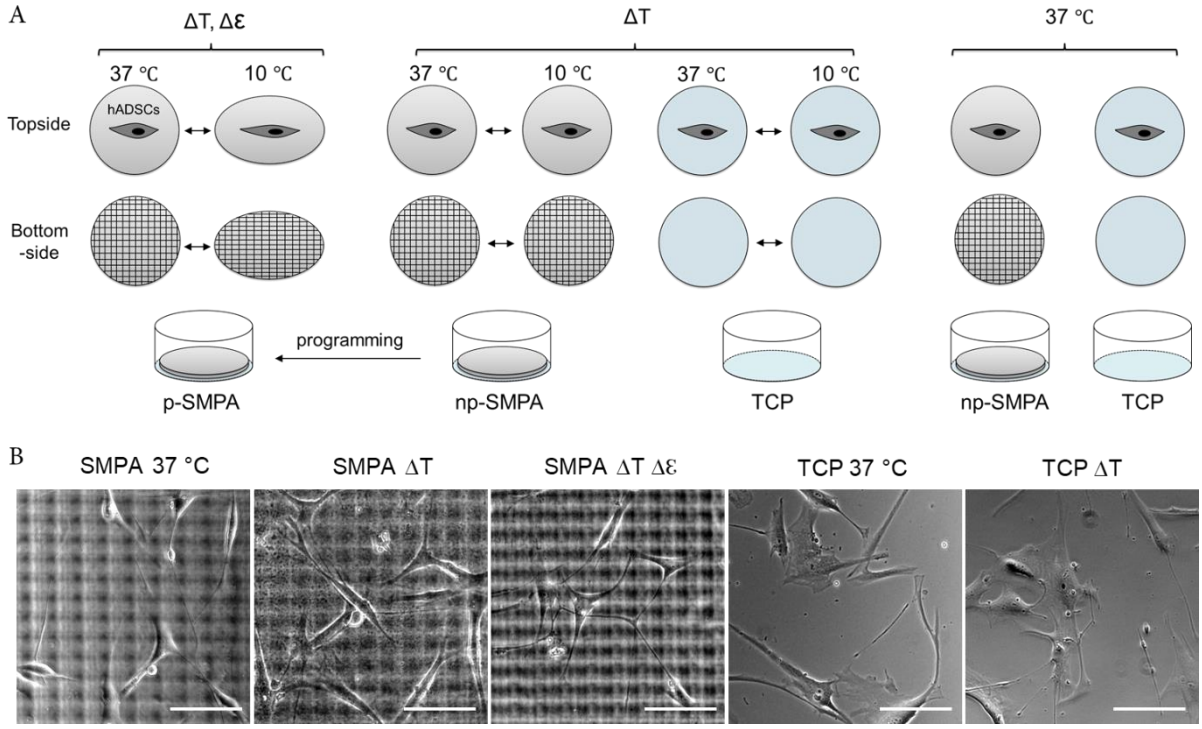

Fig. 1. (A) Schematic illustration of applying different stimuli on hADSCs. When changing the temperature, thermal and mechanical stimuli were generated by using p-SMPA, while only a thermal stimulus was apparent when using np-SMPA sheet or TCP. Neither thermal nor mechanical stimuli were present at 37 °C. (B) Morphology of hADSCs cultured on SMPA sheets and TCP under different stimuli for 3 days. Scale bar = 100 µm.

SMPA actuation promotes hADSC migration

In order to evaluate the migration of hADSCs, the cells were cultured under different conditions and then were observed with a time-lapse microscope to record their

movement for 10 hours. The cells exhibited a faster migration velocity on SMPA sheets than on TCP (Fig. 2), which could be attributed to the relatively looser attachment and less spreading on SMPA as discussed above. The cyclic temperature change resulted in the significant decrease of cell migration velocity on SMPA sheets. However, such an effect was not observed on TCP, suggesting the influence of temperature change on hADSC migration was depent on the materials. The temperature change in this study (60 min for each cycle) might be too fast for cells, cultured on TCP with relatively tighter attachment, to response and alter their migration behavior. Interestingly, hADSC migration was significantly promoted by SMPA actuation. Compared to the cells on SMPA with single thermal stimulus (0.32 ± 0.14 μm/min), the cells exposed to thermal and mechanical dual stimuli showed almost doubled migration velocity (0.57 ± 0.2 μm/min) (Fig. 2B).

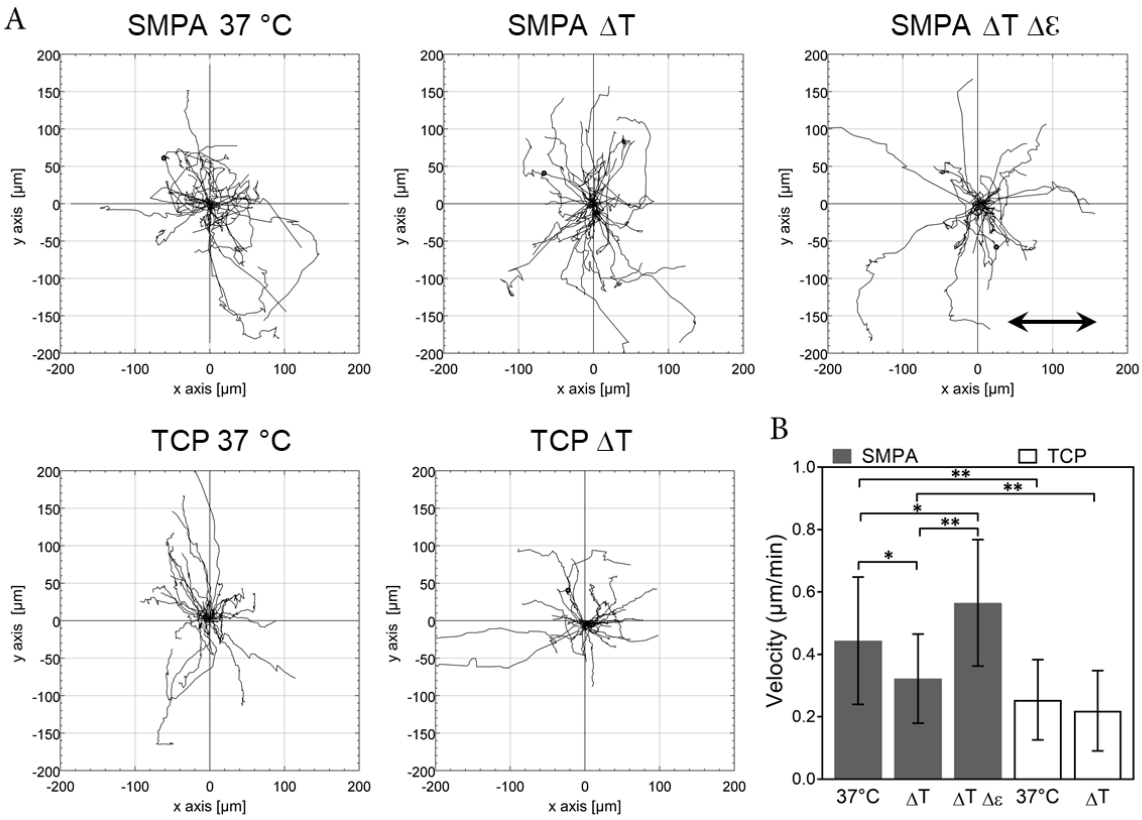

Fig. 2. Migration of hADSCs on SMPA sheets and TCP under different stimuli. The cells were cultured on the material surfaces for 3 days and the migration was recorded for 10 hours using a time-lapse microscope to generate the trajectories of hADSCs (A) and calculate the migration velocity (B, n ⩾ 26 cells for each group, **p* < 0.05 and ***p*

< 0.01). The black arrow in (A) indicates the direction of p-SMPA elongation during temperature change.

Thermal and mechanical stimuli regulate cytoskeleton and cell adhesion

The migration of anchorage-dependent cells is a complex process, which is regulated by the dynamics of cytoskeleton organization and the transduction of spatial and temporal signals [26]. During cell migration, the protrusive and contractile force is generated from actin cytoskeleton, while the formation of the polarized network allowing organelle and protein movement is relying on the microtubules [27]. Crosstalk between the actin cytoskeleton and microtubules are essential for cell migration [28]. In order to investigate the mechanism, through which cells respond to the external stimuli, we cultured the cells under different conditions for 3 days and then performed immunostaining of the key components for regulating cell migration.

Cells exposed only to thermal stimulus presented decreased tubulin and enhanced F-actin compared to the cells without stimuli (SMPA, 37 °C). Exposure of cells to dual stimuli increased the F-actin level but had no obvious effect on tubulin level. SMPA actuation could enhance the tubulin level, as shown by the higher fluorescence intensity in the group with dual stimuli than that with single thermal stimulus (Fig. 3). These results suggested that both thermal and mechanical stimuli could regulate the cytoskeleton organization.

Integrin is a transmembrane receptor and primary mechanosensor of cells, which plays a critical role to mediate signal transduction in response to various mechanical stimuli. Upon external stimulation, integrins can be activated by changing their conformation and affinity, which allows the recruitment of several cytoplasmic proteins including focal adhesions and their variants mediating cell-ECM adhesion and cell migration [29, 30]. As one of the downstream molecules of integrin signalling and a motor protein, myosin can bind to actin filaments to regulate actin movement to generate contractile force. The activity of myosin was found to be highly dependent on its light chain phosphorylation [31, 32].

After 3 days of cultivation on different conditions, increase of pMLC and decrease of integrin activation were observed in cells with only thermal stimulus (SMPA, ΔT), in comparison to cells without stimulus (SMPA, 37 °C). In contrast, the cells exposed to thermal and mechanical dual stimuli (SMPA, ΔT Δε) showed the similar level of activated integrin and enhanced MLC phosphorylation. Higher levels of activated integrin and pMLC were found in cells with dual stimuli compared to the cells on SMPA with single thermal stimulus (Fig. 4). These data indicated that the mechanical cue could be sensed by cells and transduced intracellularly, inducing integrin activation and MLC phosphorylation to mediate cell migration. In summary, thermal and mechanical stimuli could affect cell migration through the regulation of cytoskeleton organization and cell adhesion.

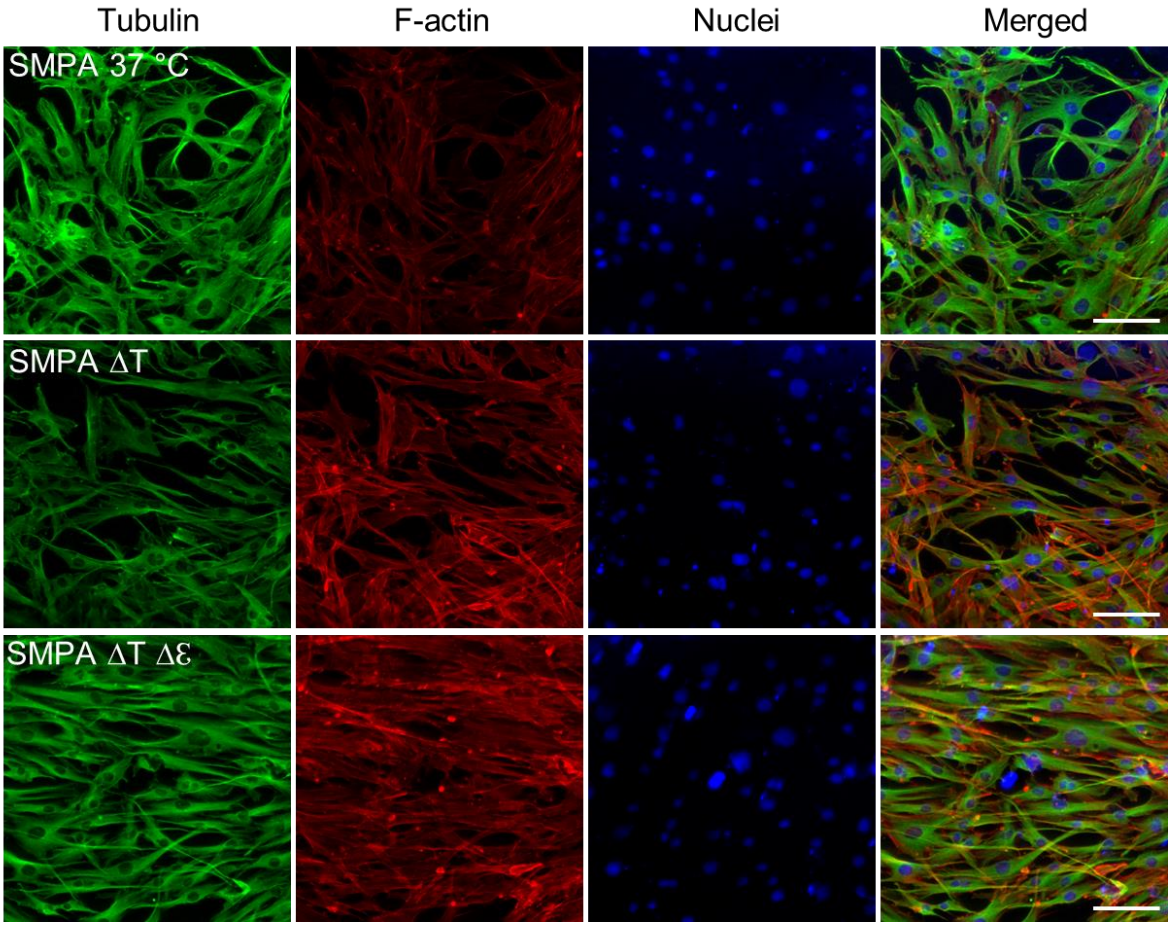

Fig. 3. Representative images of Tubulin (green) and F-actin (red) of hADSCs cultured on SMPA sheets for 3 days under indicated stimuli. Cell nuclei were stained with Hoechst 33342. Scale bar = 100 μm.

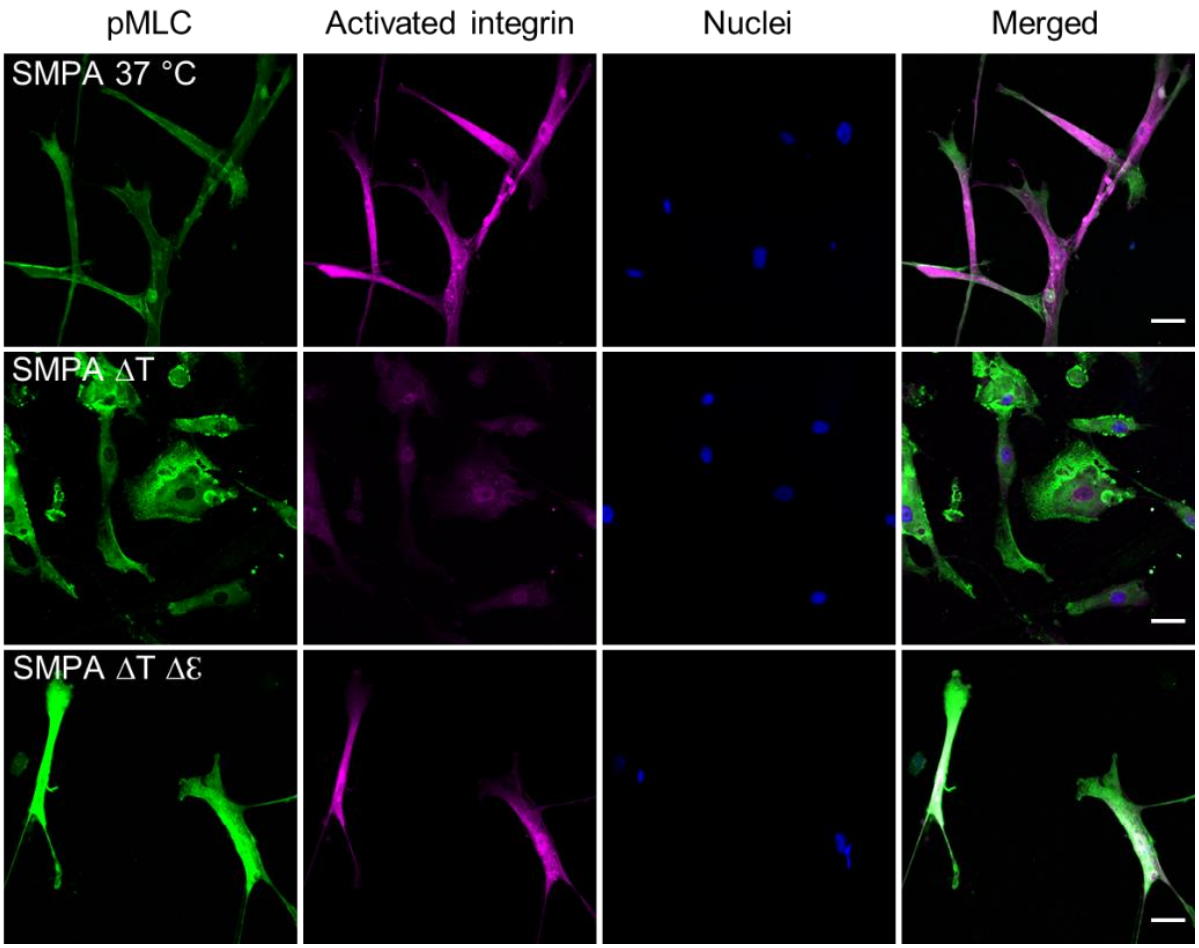

Fig. 4. Representative images of pMLC (green) and activated integrin (purple) of hADSCs. The cells were cultured on SMPA sheets for 3 days under different stimuli. Cell nuclei were stained with Hoechst 33342. Scale bar = 50 μm.

CONCLUSIONS

The influence of thermal and mechanical stimuli on hADSCs migration was investigated using the SMPA sheets in comparison to TCP. The cells on SMPA sheets exhibited faster migration velocity than on TCP. The mechanical stimulus from the actuation of SMPA sheets could significantly enhance cell migration capacity. Both thermal and mechanical stimuli could regulate the cytoskeleton organization and cell adhesion. This study demonstrated the interplay of different external stimuli for

regulating stem cell migration, and provided a noval approach for improving MSCs homing capacity by a pretreatment with physical cues.

ACKNOWLEDGMENTS

We acknowledge Nicole Schneider, Daniela Radzik and Patrick Budach for preparing the SMPA sheets. This work was financially supported by the Helmholtz Association of German Research Centers (through program-oriented funding, Helmholtz Cross Program Initiative "Technology and Medicine - Adaptive Systems", Helmholtz Virtual Institute, Multifunctional Biomaterials for Medicine (grant no. VH-VI-423)), and the Federal Ministry of Education and Research, Germany, through the Program Health Research (Grant 13GW0098, and Project 0315696A “Poly4BioBB”).

References

1. E. J. Oh, H. W. Lee, S. Kalimuthu, T. J. Kim, H. M. Kim, S. H. Baek, L. Zhu, J. M. Oh, S. H. Son, H. Y. Chung and B. C. Ahn, J Control Release 279, 79-88 (2018).
2. W. Lin, L. Xu, S. Zwingenberger, E. Gibon, S. B. Goodman and G. Li, J Orthop Translat 9, 19-27 (2017).
3. X. Fu, G. Liu, A. Halim, Y. Ju, Q. Luo and A. G. Song, Cells 8 (8) 784 (2019).
4. E. Eggenhofer, V. Benseler, A. Kroemer, F. C. Popp, E. K. Geissler, H. J. Schlitt, C. C. Baan, M. H. Dahlke and M. J. Hoogduijn, Front Immunol 3, 297 (2012).
5. I. M. Barbash, P. Chouraqui, J. Baron, M. S. Feinberg, S. Etzion, A. Tessone, L. Miller, E. Guetta, D. Zipori, L. H. Kedes, R. A. Kloner and J. Leor, Circulation 108 (7), 863-868 (2003).
6. A. Schmidt, D. Ladage, T. Schinkothe, U. Klausmann, C. Ulrichs, F. J. Klinz, K. Brixius, S. Arnhold, B. Desai, U. Mehlhorn, R. H. Schwinger, P. Staib, K. Addicks and W. Bloch, Stem Cells 24 (7), 1750-1758 (2006).
7. S. G. Ball, C. A. Shuttleworth and C. M. Kielty, J Cell Biol 177 (3), 489-500 (2007).
8. G. Forte, M. Minieri, P. Cossa, D. Antenucci, M. Sala, V. Gnocchi, R. Fiaccavento, F. Carotenuto, P. De Vito, P. M. Baldini, M. Prat and P. Di Nardo, Stem Cells 24 (1), 23-33 (2006).
9. Y. Li, X. Yu, S. Lin, X. Li, S. Zhang and Y. H. Song, Biochem Biophys Res Commun 356 (3), 780-784 (2007).

10. M. J. Dubon, J. Yu, S. Choi and K. S. Park, J Cell Physiol 233 (1), 201-213 (2018).
11. Q. J. Deng, X. F. Xu and J. Ren, Cell Mol Neurobiol 38 (2), 467-477 (2018).
12. K. Xiao Ling, L. Peng, Z. Jian Feng, C. Wei, Y. Wei Yan, S. Nan, G. Cheng Qi and W. Zhi Wei, Stem Cells Int 2016, 8906945 (2016).
13. A. T. Askari, S. Unzek, Z. B. Popovic, C. K. Goldman, F. Forudi, M. Kiedrowski, A. Rovner, S. G. Ellis, J. D. Thomas, P. E. DiCorleto, E. J. Topol and M. S. Penn, Lancet 362 (9385), 697-703 (2003).
14. X. Liu, B. Duan, Z. Cheng, X. Jia, L. Mao, H. Fu, Y. Che, L. Ou, L. Liu and D. Kong, Protein Cell 2 (10), 845-854 (2011).
15. M. Raab and D. E. Discher, Cytoskeleton (Hoboken) 74 (3), 114-124 (2017).
16. M. Raab, J. Swift, P. C. Dingal, P. Shah, J. W. Shin and D. E. Discher, J Cell Biol 199 (4), 669-683 (2012).
17. L. G. Vincent, Y. S. Choi, B. Alonso-Latorre, J. C. del Alamo and A. J. Engler, Biotechnol J 8 (4), 472-484 (2013).
18. N. Saxena, P. Mogha, S. Dash, A. Majumder, S. Jadhav and S. Sen, J Cell Sci 131 (7) (2018).
19. J. Lee, A. Ishihara, G. Oxford, B. Johnson and K. Jacobson, Nature 400 (6742), 382-386 (1999).
20. C. Wei, X. Wang, M. Chen, K. Ouyang, L. S. Song and H. Cheng, Nature 457 (7231), 901-905 (2009).
21. B. Zhang, Q. Luo, Z. Chen, J. Sun, B. Xu, Y. Ju and G. Song, Stem Cell Res 14 (2), 155-164 (2015).
22. X. Liang, X. Huang, Y. Zhou, R. Jin and Q. Li, Stem Cells Transl Med 5 (7), 960-969 (2016).
23. Z. Deng, W. Wang, X. Xu, O. E. C. Gould, K. Kratz, N. Ma and A. Lendlein, Proc Natl Acad Sci U S A, 117 (4) 1895-1901 (2020).
24. X. Xu, W. Wang, K. Kratz, L. Fang, Z. Li, A. Kurtz, N. Ma and A. Lendlein, Adv Healthc Mater 3 (12), 1991-2003 (2014).
25. K. Webb, V. Hlady and P. A. Tresco, J Biomed Mater Res 49 (3), 362-368 (2000).
26. A. J. Ridley, M. A. Schwartz, K. Burridge, R. A. Firtel, M. H. Ginsberg, G. Borisy, J. T. Parsons and A. R. Horwitz, Science 302 (5651), 1704-1709 (2003).
27. S. Etienne-Manneville, Traffic 5 (7), 470-477 (2004).
28. T. K. Akhshi, D. Wernike and A. Piekny, Cytoskeleton 71 (1), 1-23 (2014).
29. A. Arjonen, J. Alanko, S. Veltel and J. Ivaska, Traffic 13 (4), 610-625 (2012).

30. M. Vicente-Manzanares, C. K. Choi and A. R. Horwitz, J Cell Sci 122 (Pt 2), 199-206 (2009).
31. M. L. Walker, S. A. Burgess, J. R. Sellers, F. Wang, J. A. Hammer, 3rd, J. Trinick and P. J. Knight, Nature 405 (6788), 804-807 (2000).
32. C. Chen, T. Tao, C. Wen, W. Q. He, Y. N. Qiao, Y. Q. Gao, X. Chen, P. Wang, C. P. Chen, W. Zhao, H. Q. Chen, A. P. Ye, Y. J. Peng and M. S. Zhu, J Biol Chem 289 (41), 28478-28488 (2014).

Appendix III

Dedifferentiation of mature adipocytes with periodic exposure to cold

Zijun Deng [a, b], Jie Zou [a, b], Weiwei Wang [a], Yan Nie [a], Wing-Tai Tung [a, c], Nan Ma [a, b, d, *] and Andreas Lendlein [a, b, c, d *]

[a] Institute of Biomaterial Science and Berlin-Brandenburg Center for Regenerative Therapies, Helmholtz-Zentrum Geesthacht, Teltow, Germany
[b] Institute of Chemistry and Biochemistry, Freie Universit¨at Berlin, Berlin, Germany
[c] Institute of Biochemistry and Biology, University of Potsdam, Potsdam, Germany
[d] Helmholtz Virtual Institute – Multifunctional Biomaterials for Medicine, Berlin and Teltow, Germany
Corresponding Authors: nan.ma@hzg.de; andreas.lendlein@hzg.de

Reprinted from Clin Hemorheol Microcirc, 71, Zijun Deng, Jie Zou, Weiwei Wang, Yan Nie, Wing-Tai Tung, Nan Ma, Andreas Lendlein, Dedifferentiation of mature adipocytes with periodic exposure to cold, 415-424. Copyright (2019), with permission from IOS Press.
The publication is available at IOS Press through https://doi.org/10.3233/CH-199005

Abstract:

Lipid-containing adipocytes can dedifferentiate into fibroblast-like cells under appropriate culture conditions, which are known as dedifferentiated fat (DFAT) cells. However, the relative low dedifferentiation efficiency with the established protocols limit their widespread applications. In this study, we found that adipocyte dedifferentiation could be promoted via periodic exposure to cold (10 °C) in vitro. The lipid droplets in mature adipocytes were reduced by culturing the cells in periodic cooling/heating cycles (10 – 37 °C) for one week. The periodic temperature change led to the down-regulation of the adipogenic genes (FABP4, Leptin) and up-regulation of the mitochondrial uncoupling related genes (UCP1, PGC-1α, and PRDM16). In addition, the enhanced expression of the cell proliferation marker Ki67 was observed

in the dedifferentiated fibroblast-like cells after periodic exposure to cold, as compared to the cells cultured in 37 °C. Our in vitro model provides a simple and effective approach to promote lipolysis and can be used to improve the dedifferentiation efficiency of adipocytes towards multipotent DFAT cells.

KEYWORDS: Adipocyte, dedifferentiation, cold, lipid

1. Introduction

Dedifferentiated fat (DFAT) cells have become a promising cell source in stem cell therapy. They could be obtained via the process of dedifferentiation of mature adipocytes. DFAT cells express embryonic stem cell markers [1, 2] and show the multilineage differentiation potential [3-7]. The osteogenic and adipogenic potential of human DFAT cells was even higher than that of adipose tissue-derived MSCs [8] and similar to bone marrow-derived MSCs [9]. Notably, DFAT cells showed absence of cell senescence and low risk of tumor formation in vivo [10]. Given the abundance of adipose tissue in human body, DFAT cells may represent a great potential in clinical applications. However, there is currently no highly efficient method to promote lipid loss and adipocyte dedifferentiation in vitro, which limites the application of DFAT cells.

Adipocytes in fat tissue can regulate energy balance by storing and hydrolyzing lipids. The loss of lipids in mature adipocytes in vivo could lead to their transformation into beige adipocytes or dedifferentiation into fibroblast-like cells [11, 12]. It has been also demonstrated that dedifferentiation of mature adipocytes in vitro was accompanied by the loss of lipid [13]. Cumulative In vivo evidences have suggested that periodic exposure to cold could induce lipid loss and white adipocytes transformation into brown adipocytes [14, 15]. The decrease of white adipocytes and increase of brown or beige adipocytes have been observed in mice after exposure to a cold environment [16]. In addition, in vivo studies have shown that the occurrence of brown adipocytes in white adipose tissue during cold exposure was associated with mitochondrial activity to promote lipolysis [17, 18]. In vitro study has also demonstrated that mitochondrial uncoupling could promote lipid loss in adipocytes, and consequently induce adipocyte dedifferentiation [19]. This process involved the regulation of peroxisome proliferator-activated receptor gamma coactivator 1-alpha (PGC-1 α) and uncoupling protein 1 (UCP1) [20]. However, the effect of cold exposure on lipolysis and adipocyte

dedifferentiation in vitro as well as the underlying mechanism are still unclear, which hided the large-scale production of DFAT cells.

In this study, we hypothesized that the periodic exposure to cold in vitro might be an effective approach to promote the lipolysis and dedifferentiation of the adipocytes. We investigated the lipolysis in mature adipocytes and the proliferation of the dedifferentiated fibroblast-like cells after periodic exposure to cold. The mechanism of the promoted lipolysis and dedifferentiation after exposure to cold was studied.

2. Materials and methods

2.1 Preadipocytes cultivation and adipogenic induction

The human adipose derived stromal cells were isolated from patients adipose tissue as described previously [21]. For cells maintenance, the isolated cells were cultured with Dulbecco's Modified Eagle Medium (DMEM, Life Technologies, Germany) containing 10% (v/v) fetal bovine serum (FBS, Sigma-Aldrich, USA) and 100 U/ml penicillin-streptomycin (Merck Millipore, Germany), and incubated at 37 °C containing 5 % (v/v) CO2. The medium was changed every 2 days. For adipogenesis induction, the cells were cultured with adipogenesis differentiation medium (StemPro® Adipogenesis Differentiation Kit, Life Technologies, Germany) for 2 weeks and the medium was changed every 3 days.

2.2 Adipocytes exposed to cold

To test the influence of periodic cooling on adipocyte dedifferentiation, the adipocytes obtained from ADSC adipogenesis were cultured in a thermal chamber (Instec, USA) providing periodic cooling/heating for 7 days. The temperature in the chamber was cyclic changed from 37 °C to 10 °C, and the changing frequence was 1 times per hour with lasting for 30 minutes at 10 °C and 30 minutes at 37 °C. Cells cultured in 37 °C were used as control group.

2.3 Oil Red O staining

Samples were washed with PBS and fixed in 4% (w/v) paraformaldehyde (Sigma-Aldrich, USA). After washing with PBS and water, the cells were stained with 0.1% (w/v) Oil Red O (Sigma-Aldrich, USA) in 60% (v/v) isopropanol for 15 minutes. The

staining solution was removed and the samples were washed with water. The stained lipids in adipocytes were extracted using isopropanol and quantified by measuring the absorbance at 490 nm with a microplate reader (Infinite200 Pro, Tecan Group Ltd, Switzerland).

2.4 Free fatty acid assay

The supernatant of the cell cultures was collected. The free fatty acid released into the conditioned medium by lipolysis was quantified using a free fatty acid assay kit (Abcam, UK). In brief, 50 µl of standard palmitic acid and 50 µl of supernatant were added in 96 well plate. Then Acyl-CoA synthetase was added and incubated at 37 °C for 30 minutes. Finally the enzyme mix was added and incubated at 37 °C for 30 minutes. The optical density at 570 nm was measured using the microplate reader (Infinite200 Pro, Tecan Group Ltd, Switzerland).

2.5 Immunocytochemistry

The samples were washed with PBS and fixed with 4% (v/v) paraformaldehyde (Sigma-Aldrich, USA), permeabilized with 0.25% (v/v) Triton X-100 (Sigma-Aldrich, USA), and blocked using 5% (v/v) normal goat serum (Life Technologies, Germany). Samples were incubated with the primary antibodies overnight at 4 °C and then incubated with the secondary antibodies (Life Technologies, Germany) for 1 hour at room temperature. The nuclei were stained with 4,6-diamidino-2- phenylindole (DAPI; Sigma-Aldrich, USA). The images were taken using confocal microscopy (LSM780, Carl Zeiss, Germany). The following primary antibodies were used: Ki67 (rat, Cell Signaling Technology, Germany), FABP4 (rabbit, Life Technologies, Germany), Perilipin-1 (goat, Life Technologies, Germany).

2.6 mRNA expression analysis

The mRNA level was quantified by qRT-PCR. The total RNA was isolated using the PureLink RNA Mini Kit (Life Technologies, Germany) according to the manufacturer's protocol. The concentration of the total RNA was measured using the microplate reader (Infinite200 Pro, Tecan Group Ltd, Switzerland) with a NanoQuant Plate (Tecan Group Ltd, Switzerland). The cDNA was synthesized using the RT2 First Strand kit (Qiagen, Germany). Real-time PCR was performed using the StepOnePlus real-time

PCR System (Applied Biosystems, USA), and RT2 SYSB Green ROX qPCR Mastermix (Qiagen, Germany) was used in the amplification. The GAPDH was used as a housekeeping gene. The primers in the following were used for each gene.

Primer	Forward	Reverse
FABP4	GCTTTGCCACCAGGAAAGTG	ATGGACGCATTCCACCACCA
Leptin	TTTGGCCCTATCTTTTCTATGTCC	TGGAGGAGACTGACTGCGTG
PPARγ	GATACACTGTCTGCAAACATATCACAA	CCACGGAGCTGATCCCAA
C/EBPα	GCAAGAGCCGCGACAAG	GGCTCGGGCAGCTGCTT
UCP1	CTGGAATAGCGGCGTGCTT	AATAACACTGGACGTCGGGC
PGC-1α	GCCAAACCAACAACTTTATCTCTTC	CACACTTAAGGTGCGTTCAATAGTC
PRDM16	GAGGAGGACGATGAGGACAG	CGGCTCCAAAGCTAACAGAC
GAPDH	ATGGGGAAGGTGAAGGTCG	GGGGTCATTGATGGCAACAATA

2.7 Statistics

Statistical analysis and plotting were performed using GraphPad Prism (Version 7.0) software. The results are presented as mean ± standard deviation (SD). More than three independent experiments were used in the study. Statistical analysis was performed using independent-samples t-test (*p <0.05, ** p <0.01.).

3. Results

3.1 Periodic exposure to cold decreased the lipid droplets in adipocytes

To examine the relationship between periodic exposure to cold and lipid loss in vitro, we evaluated the lipid droplet formation in adipocytes. Bright field images indicated that the volume of the lipid in adipocytes was significantly decreased after periodic exposure to cold (Fig.1. A). Oil Red O (ORO) staining further showed that large lipid droplets were replaced by small lipid droplets, and more cells lost their lipids completely and turned into fibroblast-like cells after periodic exposure to cold, compared to adipocytes cultured in 37 °C (Fig.1. B). Compared to cells maintained at 37 °C, the extracted ORO reduced approximately 59% in adipocytes after periodic exposure to cold (Fig.1. C). The results suggested that the periodic exposure to cold promotes lipid loss in adipocytes in vitro.

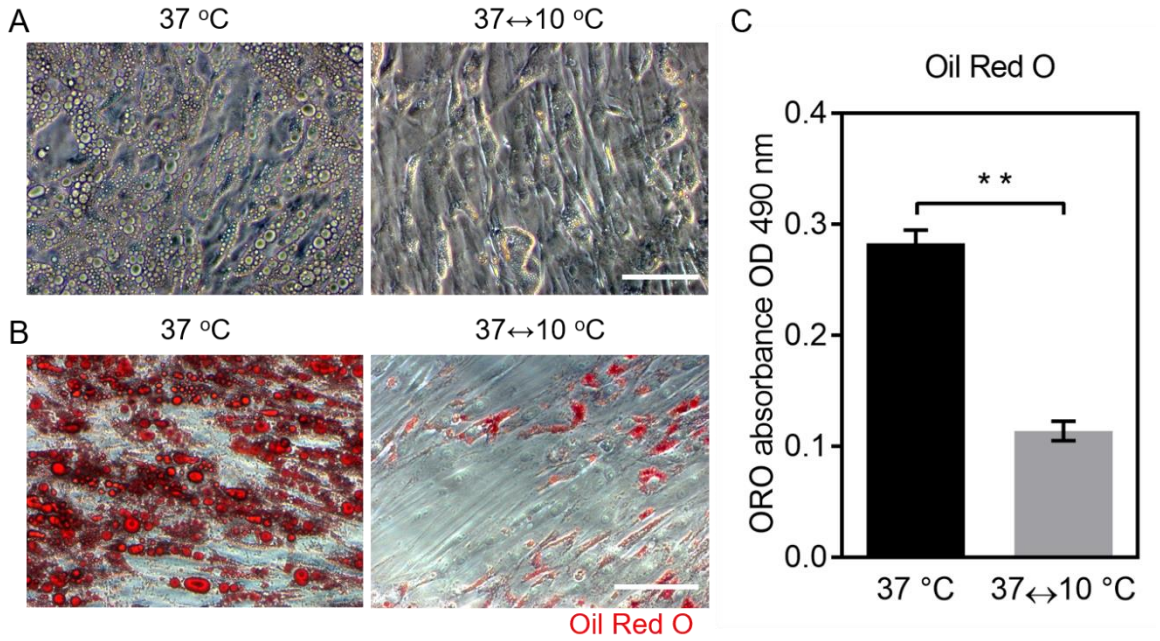

Fig.1. Decreased lipids in adipocytes after periodic exposure to cold. A. Bright field microscopy images of cells on TCP after periodic exposure to cold and to 37 °C for one week, scale bar = 100 µm. B. Oil Red O staining for lipids in adipocytes after periodic exposure to cold and to 37 °C for one week, scale bar = 100 µm. C. Quantification of Oil Red O (n=6; mean ± SD; $p < 0.01$).

3.2 Increased lipolysis with periodic exposure to cold in adipocytes

In order to understand the lipid metabolism after periodic exposure to cold, we determined the amount of the lipid storage protein perilipin-1 and hydrolysis of triglycerides. After periodic exposure to cold, the perilipin-1 expression was decreased in adipocytes, and the lipid droplets were smaller compared with the adipocytes maintained at 37 °C (Fig. 2. A). Lipolysis induces the lipid droplets hydrolysis into glycerol and free fatty acids, which is important for adipocytes dedifferentiation. Therefore, the amount of free fatty acids in the culture medium was evaluated. The result showed that the amount of free fatty acids in the medium was almost doubled after the periodic exposure to cold (37↔10 °C: 78.94 ±16.26 µM), as compared to the control group (37 °C: 38.12 ±5.21 µM) (Fig. 2. B). These results suggested that the periodic exposure to cold promoted the lipolysis, which led to a decrease of lipids in adipocytes.

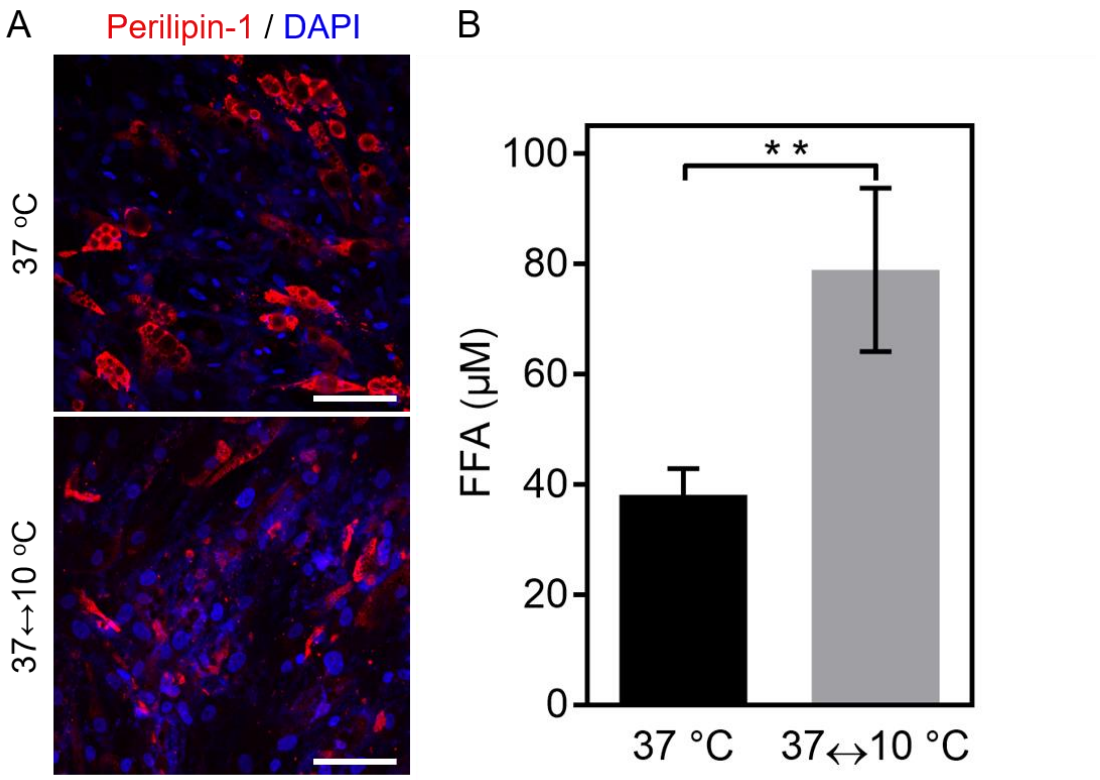

Fig. 2. Periodic exposure to cold improved lipolysis in cells. A. Perilipin-1 immunostaining after periodic exposure to cold and to 37 °C for one week, scale bar = 100 µm. B. Quantification of free fatty acid in culture medium after one week periodic exposure to cold and to 37 °C (n=7; mean ± SD; p <0.01).

3.3 Periodic exposure to cold altered adipogenic gene expression

To confirm adipocyte dedifferentiation, the mRNA expression level of mature white adipocyte related genes (fatty acid-binding protein 4 (FABP4) and Leptin) were determined. It was found that FABP4 and Leptin were down-regulated significantly in the adipocytes with periodic exposure to cold for 1 week, compared to the adipocytes maintained at 37 °C (Fig. 3). The mRNA expression levels of the transcription factors PPARγ and C/EBPα did not showed significant differences between these two groups (Fig. 3).

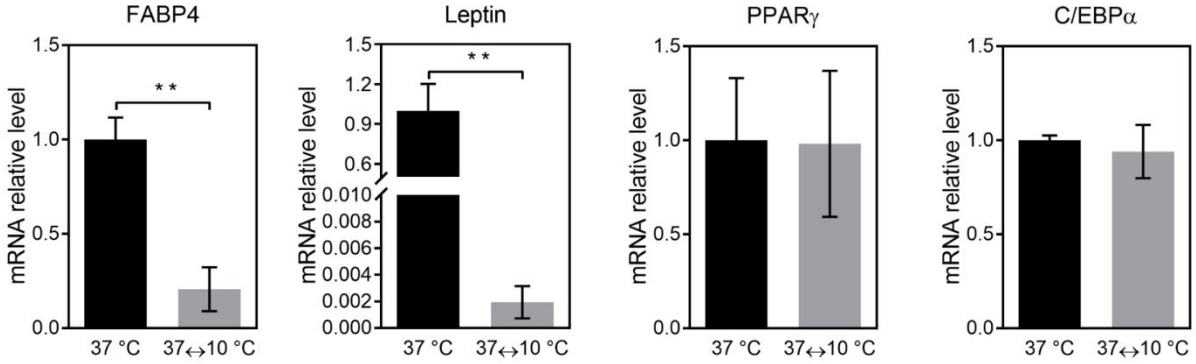

Fig.3. Expression of adipogenic genes after one week of culture in 37 °C and periodic exposure to cold (n=6; mean ± SD; **p <0.01).

3.4 Mitochondrial activation after periodic exposure to cold in adipocytes

In order to explore the relationship between increased lipolysis, decreased mature adipocytes population, and periodic exposure to cold, we examined the mitochondrial activity, which plays a central role in heat production in order to overcome periodic exposure to cold. The mRNA expression of UCP1 and PGC-1α were up-regulated significantly after periodic exposure to cold for one week, compared with adipocytes maintained at 37 °C. In addition, the treatment of periodic exposure to cold enhanced the mRNA expression of PR domain containing 16 (PRDM16) (Fig. 4). The high expression of PRDM16 accelerated the lipids loss and promoted the mature white adipocyte transformation into brown adipocyte. The up-regulation of UCP1, PGC-1α

and PRDM16 after periodic exposure to cold could enhance the lipolysis in adipocyte via mitochondrial uncoupling, which further improved the dedifferentiation process.

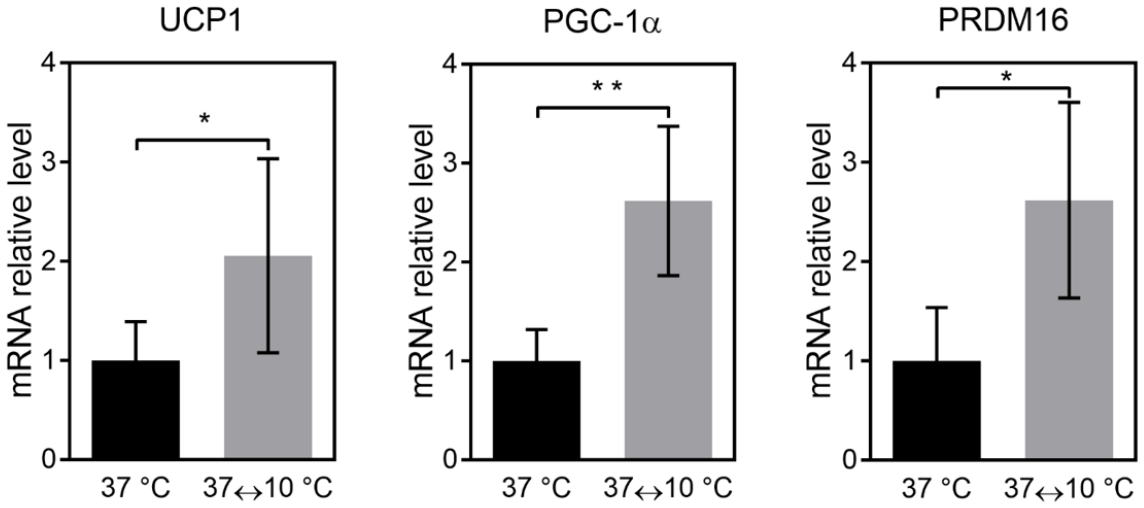

Fig.4. Expression of mitochondrial uncoupling and brown adipocyte transformation genes was up-regulated after periodic exposure to cold for one week (n=6; mean ± SD; *p <0.05, **p <0.01).

3.5 Periodic exposure to cold increased proliferation potential of dedifferentiated adipocytes

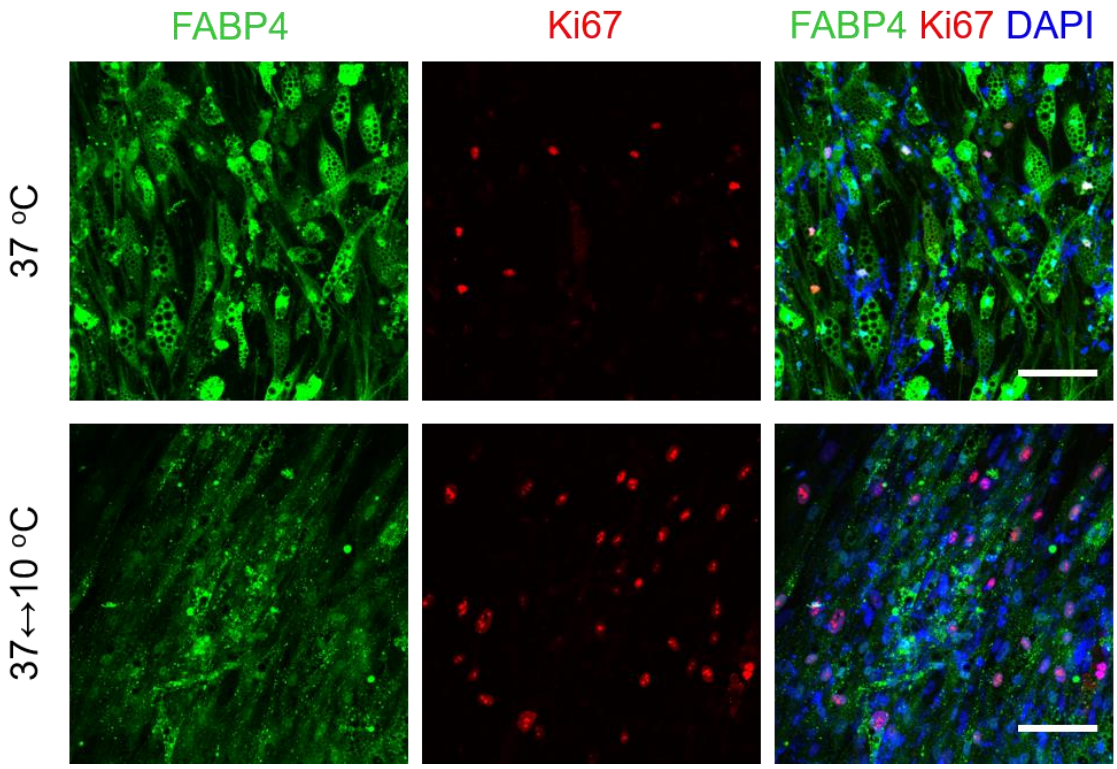

Fig.5. Periodic exposure to cold for one week decreased expression of mature adipocyte marker and increased cell proliferation activity. Cells were immunostained to visulize adipocyte marker FABP4 (green), proliferation marker Ki67 (red) and DAPI (blue). Scale bar = 100 μm.

To evaluate the proliferation activity of dedifferentiated cells from mature adipocytes, the expression of proliferation marker Ki67 and adipocyte marker FABP4 were studied. The immunostaining images displayed more Ki67 positive cells after periodic exposure to cold, compared to cells maintained at 37 °C (Fig. 5). The Ki67 high-expressing cells showed the low expression of FABP4. These results suggested that the mature adipocytes dedifferentiated with a higher proliferation potential after exposure to cold.

4. Discussion

Adipocytes can dedifferentiate both in vitro and in vivo, while the underlying mechanism is still unclear. In vivo studies suggested that exposure to cold could reduce mature white adipocytes, and β-adrenergic receptor played an important role in lipid loss and brown adipogenesis in white adipose tissue during cold [14, 22]. It is found that cold, rather than sympathomimetics, is the major factor to activate mature white adipocyte transformation into brown adipocyte in vivo [23]. Nevertheless, the in vivo system relying on animals is different from humans, and it is hard to clarify the molecular mechanism at single cell level. In this study, we investigated the periodic cooling effects on adipocyte dedifferentiation in vitro. The results provided an evidence that the periodic exposure to cold could induce lipolysis in adipocyte and promote mature adipocytes dedifferentiation. The cell model in vitro used here excluded the influences of neuroendocrine system.

Mitochondria uncoupling plays a key role in the process of lipid metabolism and adipocyte dedifferentiation [19]. UCP1 and PGC-1α are genes related to lipid consumption by mitochondrial uncoupling [24, 25]. We found that the periodic exposure to cold up-regulated the UCP1 and PGC-1α mRNA levels and improved the loss of lipids, which was consistent with the previous work [26]. FABP4 and Leptin are significantly expressed in mature white adipocyte [27, 28]. The down-regulation of FABP4 and Leptin and the up-regulation of PRDM16 suggested the transformation of mature adipocytes into brown adipocytes. Our results confirmed that the periodic cooling could enhance the mitochondrial activity, which was highly related to the dedifferentiation process. The transcriptional factors PPARγ and C/EBPα involved in adipogenesis as well as the process of transformation or dedifferentiation of white adipocyte. The PPARγ could regulate the white and brown adipogenesis, the transformation from white to brown adipocyte, and lipolysis [29-31]. C/EBPα played a central role in white adipose development, but its function in brown adipocyte transformation is still controversial [32-35]. In our study, the mRNA levels of PPARγ and C/EBPα did not show significant difference between the dedifferentiated and non-dedifferentiated groups, suggesting that their expression levels were not closely assoiated with the dedifferentiation process.

Accumulation and consumption of lipids are important for adipocyte differentiation and dedifferentiation. The lipids in mature adipocyte become unstable in the

dedifferentiation process. The surface of the lipid droplets was coated by perilipin-1 protein in adipocyte, which is important to regulate the lipid accumulation [36]. In this study, the perilipin-1 expression was decreased with the increase of lipolysis after periodic exposure to cold. Previous studies using perilipin-null mice [37, 38] and gene transfection technique [39] have shown that high expression of perilipin can inhibit lipolysis during white adipocyte differentiation, which was consistent with our results. However, it is still unclear how the periodic cooling could affect the activity of perilipin. Previous studies proposed that phosphorylation of perilipin could induce lipolysis via PKA pathway [40, 41]. Therefore, further study focusing on the phosphorylation of perilipin in periodic cooling condition might be helpful to address this question.

In this study, the adipocytes differentiated from ADSCs were used as a cell model to test the effects of periodic cooling on adipocyte dedifferentiation. Further studies should be performed with freshly isolated mature adipocytes to verify the effects of periodic cooling on adipocyte dedifferentiation. This might provide an innovative methodology to improve the production of DFAT cells from fat tissue.

5. Conclusion

Periodic exposure to cold promoted lipolysis and mature adipocytes dedifferentiation into fibroblast-like cells with high proliferation potential. This approach could be applied as a potential strategy to increase the efficiency of dedifferentiation from mature adipocytes. The DFAT cells generated from human fat tissue with high-efficiency may serve as a new cell source in stem cell therapy and regenerative medicine.

Acknowledgements

This work was financially supported by the Helmholtz Association through Helmholtz Graduate School for Macromolecular Bioscience (MacroBio, VH-GS-503), Helmholtz Cross Programme Initiative “Technology and Medicine - Adaptive Systems”, Helmholtz Virtual Institute “Multifunctional Biomaterials for Medicine (VH-VI-423), and programme-oriented funding.

This communication was presented at the Joint Meeting of the European Society for Clinical Hemorheology and Microcirculation, the International Society for Clinical Hemorheology, and the International Society of Biorheology, 2-6 July 2018, Krakow, Poland.

References

[1] M. Jumabay, R. Abdmaulen, A. Ly, M.R. Cubberly, L.J. Shahmirian, S. Heydarkhan-Hagvall, D.A. Dumesic, Y. Yao, K.I. Bostrom, Pluripotent stem cells derived from mouse and human white mature adipocytes, Stem Cells Transl Med, 3 (2014) 161-171.

[2] D. Murata, A. Yamasaki, S. Matsuzaki, T. Sunaga, M. Fujiki, S. Tokunaga, K. Misumi, Characteristics and multipotency of equine dedifferentiated fat cells, J Equine Sci, 27 (2016) 57-65.

[3] H. Yamada, D. Ito, Y. Oki, M. Kitagawa, T. Matsumoto, T. Watari, K. Kano, Transplantation of mature adipocyte-derived dedifferentiated fat cells promotes locomotor functional recovery by remyelination and glial scar reduction after spinal cord injury in mice, Biochem Biophys Res Commun, 454 (2014) 341-346.

[4] T. Kazama, M. Fujie, T. Endo, K. Kano, Mature adipocyte-derived dedifferentiated fat cells can transdifferentiate into skeletal myocytes in vitro, Biochem Biophys Res Commun, 377 (2008) 780-785.

[5] H. Nobusue, K. Kano, Establishment and characteristics of porcine preadipocyte cell lines derived from mature adipocytes, J Cell Biochem, 109 (2010) 542-552.

[6] S. Kikuta, N. Tanaka, T. Kazama, M. Kazama, K. Kano, J. Ryu, Y. Tokuhashi, T. Matsumoto, Osteogenic effects of dedifferentiated fat cell transplantation in rabbit models of bone defect and ovariectomy-induced osteoporosis, Tissue Eng Part A, 19 (2013) 1792-1802.

[7] Y. Oki, S. Watanabe, T. Endo, K. Kano, Mature adipocyte-derived dedifferentiated fat cells can trans-differentiate into osteoblasts in vitro and in vivo only by all-trans retinoic acid, Cell Struct Funct, 33 (2008) 211-222.

[8] N. Kishimoto, Y. Momota, Y. Hashimoto, S. Tatsumi, K. Ando, T. Omasa, J. Kotani, The osteoblastic differentiation ability of human dedifferentiated fat cells is higher

than that of adipose stem cells from the buccal fat pad, Clin Oral Investig, 18 (2014) 1893-1901.

[9] A. Poloni, G. Maurizi, P. Leoni, F. Serrani, S. Mancini, A. Frontini, M.C. Zingaretti, W. Siquini, R. Sarzani, S. Cinti, Human dedifferentiated adipocytes show similar properties to bone marrow-derived mesenchymal stem cells, Stem Cells, 30 (2012) 965-974.

[10] A. Poloni, G. Maurizi, D. Mattiucci, E. Busilacchi, S. Mancini, G. Discepoli, A. Amici, M. Falconi, S. Cinti, P. Leoni, Biosafety evidence for human dedifferentiated adipocytes, Journal of cellular physiology, 230 (2015) 1525-1533.

[11] Y. Liao, Z. Zeng, F. Lu, Z. Dong, Q. Chang, J. Gao, In vivo dedifferentiation of adult adipose cells, PLoS One, 10 (2015) e0125254.

[12] A. Bartelt, J. Heeren, Adipose tissue browning and metabolic health, Nat Rev Endocrinol, 10 (2014) 24-36.

[13] T. Matsumoto, K. Kano, D. Kondo, N. Fukuda, Y. Iribe, N. Tanaka, Y. Matsubara, T. Sakuma, A. Satomi, M. Otaki, J. Ryu, H. Mugishima, Mature adipocyte-derived dedifferentiated fat cells exhibit multilineage potential, J Cell Physiol, 215 (2008) 210-222.

[14] G. Barbatelli, I. Murano, L. Madsen, Q. Hao, M. Jimenez, K. Kristiansen, J.P. Giacobino, R. De Matteis, S. Cinti, The emergence of cold-induced brown adipocytes in mouse white fat depots is determined predominantly by white to brown adipocyte transdifferentiation, Am J Physiol Endocrinol Metab, 298 (2010) E1244-1253.

[15] J. Himms-Hagen, A. Melnyk, M.C. Zingaretti, E. Ceresi, G. Barbatelli, S. Cinti, Multilocular fat cells in WAT of CL-316243-treated rats derive directly from white adipocytes, Am J Physiol Cell Physiol, 279 (2000) C670-681.

[16] J. Sanchez-Gurmaches, C.M. Hung, D.A. Guertin, Emerging Complexities in Adipocyte Origins and Identity, Trends Cell Biol, 26 (2016) 313-326.

[17] A.M. Cypess, A.P. White, C. Vernochet, T.J. Schulz, R. Xue, C.A. Sass, T.L. Huang, C. Roberts-Toler, L.S. Weiner, C. Sze, A.T. Chacko, L.N. Deschamps, L.M. Herder, N. Truchan, A.L. Glasgow, A.R. Holman, A. Gavrila, P.O. Hasselgren, M.A. Mori, M. Molla, Y.H. Tseng, Anatomical localization, gene expression profiling and functional characterization of adult human neck brown fat, Nat Med, 19 (2013) 635-639.

[18] C. Tao, S. Huang, Y. Wang, G. Wei, Y. Zhang, D. Qi, Y. Wang, K. Li, Changes in white and brown adipose tissue microRNA expression in cold-induced mice, Biochem Biophys Res Commun, 463 (2015) 193-199.

[19] S. Tejerina, A. De Pauw, S. Vankoningsloo, A. Houbion, P. Renard, F. De Longueville, M. Raes, T. Arnould, Mild mitochondrial uncoupling induces 3T3-L1 adipocyte de-differentiation by a PPARgamma-independent mechanism, whereas TNFalpha-induced de-differentiation is PPARgamma dependent, J Cell Sci, 122 (2009) 145-155.

[20] A. De Pauw, S. Tejerina, M. Raes, J. Keijer, T. Arnould, Mitochondrial (dys)function in adipocyte (de)differentiation and systemic metabolic alterations, Am J Pathol, 175 (2009) 927-939.

[21] X. Xu, W. Wang, K. Kratz, L. Fang, Z. Li, A. Kurtz, N. Ma, A. Lendlein, Controlling major cellular processes of human mesenchymal stem cells using microwell structures, Adv Healthc Mater, 3 (2014) 1991-2003.

[22] A. Frontini, S. Cinti, Distribution and development of brown adipocytes in the murine and human adipose organ, Cell Metab, 11 (2010) 253-256.

[23] A.M. Cypess, Y.C. Chen, C. Sze, K. Wang, J. English, O. Chan, A.R. Holman, I. Tal, M.R. Palmer, G.M. Kolodny, C.R. Kahn, Cold but not sympathomimetics activates human brown adipose tissue in vivo, Proc Natl Acad Sci U S A, 109 (2012) 10001-10005.

[24] L. Madsen, L.M. Pedersen, H.H. Lillefosse, E. Fjaere, I. Bronstad, Q. Hao, R.K. Petersen, P. Hallenborg, T. Ma, R. De Matteis, P. Araujo, J. Mercader, M.L. Bonet, J.B. Hansen, B. Cannon, J. Nedergaard, J. Wang, S. Cinti, P. Voshol, S.O. Doskeland, K. Kristiansen, UCP1 induction during recruitment of brown adipocytes in white adipose tissue is dependent on cyclooxygenase activity, PLoS One, 5 (2010) e11391.

[25] B.K. Sharma, M. Patil, A. Satyanarayana, Negative regulators of brown adipose tissue (BAT)-mediated thermogenesis, J Cell Physiol, 229 (2014) 1901-1907.

[26] L. Ye, J. Wu, P. Cohen, L. Kazak, M.J. Khandekar, M.P. Jedrychowski, X. Zeng, S.P. Gygi, B.M. Spiegelman, Fat cells directly sense temperature to activate thermogenesis, Proc Natl Acad Sci U S A, 110 (2013) 12480-12485.

[27] A. Baessler, V. Lamounier-Zepter, S. Fenk, C. Strack, C. Lahmann, T. Loew, G. Schmitz, M. Bluher, S.R. Bornstein, M. Fischer, Adipocyte fatty acid-binding

protein levels are associated with left ventricular diastolic dysfunction in morbidly obese subjects, Nutr Diabetes, 4 (2014) e106.

[28] P.G. Cammisotto, L.J. Bukowiecki, Mechanisms of leptin secretion from white adipocytes, Am J Physiol Cell Physiol, 283 (2002) C244-250.

[29] W.T. Festuccia, M. Laplante, M. Berthiaume, Y. Gelinas, Y. Deshaies, PPARgamma agonism increases rat adipose tissue lipolysis, expression of glyceride lipases, and the response of lipolysis to hormonal control, Diabetologia, 49 (2006) 2427-2436.

[30] Q.Q. Tang, M.D. Lane, Adipogenesis: from stem cell to adipocyte, Annu Rev Biochem, 81 (2012) 715-736.

[31] M. Harms, P. Seale, Brown and beige fat: development, function and therapeutic potential, Nat Med, 19 (2013) 1252-1263.

[32] M.C. Carmona, R. Iglesias, M.J. Obregon, G.J. Darlington, F. Villarroya, M. Giralt, Mitochondrial biogenesis and thyroid status maturation in brown fat require CCAAT/enhancer-binding protein alpha, J Biol Chem, 277 (2002) 21489-21498.

[33] H.G. Linhart, K. Ishimura-Oka, F. DeMayo, T. Kibe, D. Repka, B. Poindexter, R.J. Bick, G.J. Darlington, C/EBPalpha is required for differentiation of white, but not brown, adipose tissue, Proc Natl Acad Sci U S A, 98 (2001) 12532-12537.

[34] Q. Jin, F. Zhang, T. Yan, Z. Liu, C. Wang, X. Ge, Q. Zhai, C/EBPalpha regulates SIRT1 expression during adipogenesis, Cell Res, 20 (2010) 470-479.

[35] E. Wei, R. Lehner, D.E. Vance, C/EBPalpha activates the transcription of triacylglycerol hydrolase in 3T3-L1 adipocytes, Biochem J, 388 (2005) 959-966.

[36] A.S. Greenberg, J.J. Egan, S.A. Wek, N.B. Garty, E.J. Blanchette-Mackie, C. Londos, Perilipin, a major hormonally regulated adipocyte-specific phosphoprotein associated with the periphery of lipid storage droplets, J Biol Chem, 266 (1991) 11341-11346.

[37] J. Martinez-Botas, J.B. Anderson, D. Tessier, A. Lapillonne, B.H. Chang, M.J. Quast, D. Gorenstein, K.H. Chen, L. Chan, Absence of perilipin results in leanness and reverses obesity in Lepr(db/db) mice, Nat Genet, 26 (2000) 474-479.

[38] J.T. Tansey, C. Sztalryd, J. Gruia-Gray, D.L. Roush, J.V. Zee, O. Gavrilova, M.L. Reitman, C.X. Deng, C. Li, A.R. Kimmel, C. Londos, Perilipin ablation results in a lean mouse with aberrant adipocyte lipolysis, enhanced leptin production, and resistance to diet-induced obesity, Proc Natl Acad Sci U S A, 98 (2001) 6494-6499.

[39] D.L. Brasaemle, B. Rubin, I.A. Harten, J. Gruia-Gray, A.R. Kimmel, C. Londos, Perilipin A increases triacylglycerol storage by decreasing the rate of triacylglycerol hydrolysis, J Biol Chem, 275 (2000) 38486-38493.

[40] J.T. Tansey, A.M. Huml, R. Vogt, K.E. Davis, J.M. Jones, K.A. Fraser, D.L. Brasaemle, A.R. Kimmel, C. Londos, Functional studies on native and mutated forms of perilipins. A role in protein kinase A-mediated lipolysis of triacylglycerols, J Biol Chem, 278 (2003) 8401-8406.

[41] H. Miyoshi, S.C. Souza, H.H. Zhang, K.J. Strissel, M.A. Christoffolete, J. Kovsan, A. Rudich, F.B. Kraemer, A.C. Bianco, M.S. Obin, A.S. Greenberg, Perilipin promotes hormone-sensitive lipase-mediated adipocyte lipolysis via phosphorylation-dependent and -independent mechanisms, J Biol Chem, 281 (2006) 15837-15844.